nature COMMUNICATIONS

ARTICLE

https://doi.org/10.1038/s41467-021-24053-4 OPEN

Mating can initiate stable RNA silencing that overcomes epigenetic recovery

Sindhuja Devanapally[1,2], Pravrutha Raman[1,2], Mary Chey[1], Samual Allgood[1], Farida Ettefa[1], Maïgane Diop[1], Yixin Lin[1], Yongyi E. Cho[1] & Antony M. Jose[1✉]

Stable epigenetic changes appear uncommon, suggesting that changes typically dissipate or are repaired. Changes that stably alter gene expression across generations presumably require particular conditions that are currently unknown. Here we report that a minimal combination of *cis*-regulatory sequences can support permanent RNA silencing of a single-copy transgene and its derivatives in *C. elegans* simply upon mating. Mating disrupts competing RNA-based mechanisms to initiate silencing that can last for >300 generations. This stable silencing requires components of the small RNA pathway and can silence homologous sequences in *trans*. While animals do not recover from mating-induced silencing, they often recover from and become resistant to *trans* silencing. Recovery is also observed in most cases when double-stranded RNA is used to silence the same coding sequence in different regulatory contexts that drive germline expression. Therefore, we propose that regulatory features can evolve to oppose permanent and potentially maladaptive responses to transient change.

[1] University of Maryland, College Park, MD, USA. [2] These authors contributed equally: Sindhuja Devanapally, Pravrutha Raman. ✉email: amjose@umd.edu

When organisms reproduce by building a near copy of themselves, they recreate the information needed for making another copy. This heritable information is stored as the genome sequence and as particular spatial arrangements of regulators within each new generation[1–3]. Rare mutations in genome sequence that result from failed DNA repair are transmitted across generations through DNA replication during each cell division. Unlike such genetic changes, epigenetic changes, which do not alter genome sequence, can result in three possible outcomes: passive dilution, active repair through negative feedback, or active maintenance through positive feedback. Therefore, both the mechanisms that detect change and the associated regulatory contexts are relevant for the persistence of epigenetic changes.

Stable epigenetic changes that last for hundreds of generations have been observed in a variety of systems. In every case, they are characterized by mechanisms that include positive feedback for copying or amplifying the change. For example, in *Paramecium aurelia*, where changes in the cortical arrangement of cilia can be stable, new rows of cilia are made using previous rows as templates[4]. In wild *Saccharomyces*, where changes in protein folding can persist for many generations, the folded structures of prion proteins template the folding of newly made proteins[5]. In *Cryptococcus neoformans*, where changes in ancestral DNA methylation can potentially persist for millions of years, methyltransferases copy methylation patterns upon DNA replication[6]. In every case, positive feedback ensures that ancestral epigenetic changes are not diluted across generations as cells divide.

Positive feedback alone, however, does not guarantee the stability of an epigenetic change across generations. For example, although the presence of RNA amplification correlates with reported cases of persistent RNA silencing, most induced silencing dissipates within a few generations (reviewed in ref.[7]). In *Caenorhabditis elegans*, RNA-dependent RNA polymerases (RdRPs) are used for the small RNA-guided production of additional small RNAs[8] that are complementary to terminally modified mRNA fragments[9]. This cycle of small RNA production can act across generations, leading to effects that last for varying numbers of generations (Supplementary Table 1). However, the mere presence of small RNAs (Supplementary Table 1) or terminally modified mRNA fragments[9] does not result in indefinite RNA silencing. Changes lasting for a few generations that cannot be explained by direct parental effects have been considered transgenerational[10]. Such temporary transgenerational changes could be qualitatively distinct from induced changes that are stable for hundreds of generations. These considerations suggest that other currently unknown factors that recruit or enhance positive feedback mechanisms are crucial for stable epigenetic changes.

Here we introduce mating as a simple approach to reproducibly initiate RNA silencing of a single-copy transgene that can last for hundreds of generations. A minimal combination of *cis*-regulatory sequences from this transgene can support such stable change within the *C. elegans* germline. Genes that share subsets of these regulatory sequences can be silenced for a few generations, but subsequently recover from and even become resistant to some forms of RNA silencing. Thus, our results establish a paradigm for analyzing the regulatory differences that determine persistent epigenetic change versus epigenetic recovery.

Results

Mating can disrupt gene expression by initiating piRNA-mediated silencing. We serendipitously discovered that a previously generated two-gene operon (the single-copy transgene *oxSi487*, ref.[11] Fig. 1a and Supplementary Fig. 1a) has an exceptional capacity for retaining changes in gene expression for many generations. This transgene referred to here as *T* encodes a bicistronic operon that expresses *mCherry* and *gfp* in the germline, presumably as one pre-mRNA transcript before being spliced into mature mRNAs (Fig. 1b and Supplementary Fig. 1b). While progeny that inherit *T* maternally showed uniform mCherry and GFP expression, progeny that inherit *T* paternally showed loss of expression (Fig. 1c, d, left), despite stable expression of *T* within the male parents (Fig. 1a). Mating alone is not sufficient to cause silencing because when both parents expressed *T*, all descendants showed stable expression (Fig. 1d, left, Supplementary Fig. 1c). Hemizygosity alone is not sufficient to cause silencing because all hemizygous descendants generated from a cross of wild-type males with hermaphrodites that express *T* showed stable expression (Supplementary Fig. 1d). Hermaphrodite sperm were not necessary for this phenomenon because cross progeny of feminized animals, which cannot self-fertilize, mated with transgenic males showed silencing (Supplementary Fig. 1e). We refer to this silencing that is initiated upon mating males with *T* to hermaphrodites or females without *T* as mating-induced silencing because it appears to be distinct from previously reported epigenetic silencing phenomena (Supplementary Table 2). Although the extent of the observed mating-induced silencing was variable in progeny, it was initiated in every cross where *T* was inherited only paternally (Fig. 1d, right). Initiation was extremely reliable because it was observed in >1500 animals from each one of >140 independent crosses in wild-type, *dpy-* or *unc*-marked genetic backgrounds. In every comparison, precisely the same markers were used to control for genetic background of animals being compared. The extent of mating-induced silencing ('dim' and 'off' animals), however, varied from 68 to 100% of cross progeny scored depending on the context of different genetic markers. Since the reasons for this variability are currently unclear, we did not make strong inferences from small variations in this study. Mating-induced silencing was not observed with other genes, including those sharing extensive sequence identity with *T* (Supplementary Fig. 2a, b). We also did not detect any significant differences in abundance or subcellular localization of RNA transcripts of *T* and susceptible variants of *T* (Supplementary Fig. 3a) compared to those of genes not susceptible to mating-induced silencing (Supplementary Fig. 2c–e). Thus, mating-induced silencing can be initiated reproducibly at the population level and the susceptibility of *T* to silencing without the addition of external triggers provides a reliable paradigm for inducing and analyzing the stability of epigenetic change.

To discover the parts of *T* that are required for its susceptibility to mating-induced silencing, we systematically modified sequence features of *T* (Supplementary Fig. 3a). All tested variants of *T* were susceptible to mating-induced silencing (Fig. 1e and Supplementary Fig. 1f–h), including *Tcherry*, a minimal variant comprising *Pmex-5* promoter driving expression of *mCherry* with a *cye-1* 3′ UTR (Fig. 1e and Supplementary Fig. 3a). Therefore, operon structure, histone sequences, co-transformation marker (*C. briggsae unc-119(+)*), and the method of genomic integration are not sufficient to explain susceptibility to mating-induced silencing. Germline gene expression in *C. elegans* can depend on 3′ UTRs[12,13] and genomic position[14]. Neither altering the 3′ UTR nor changing the genomic position eliminated susceptibility of *Tcherry* to mating-induced silencing (Fig. 1e, Supplementary Figs. 1i and 3a). However, when *mCherry* sequence from *Tcherry* was fused to the endogenous *mex-5* gene within the context of native regulatory features, *mCherry* became resistant to mating-induced silencing (Fig. 1a, e). Resistance to silencing cannot be attributed merely to presence of endogenous sequences because *T* was susceptible despite the presence of histone *h2b* coding

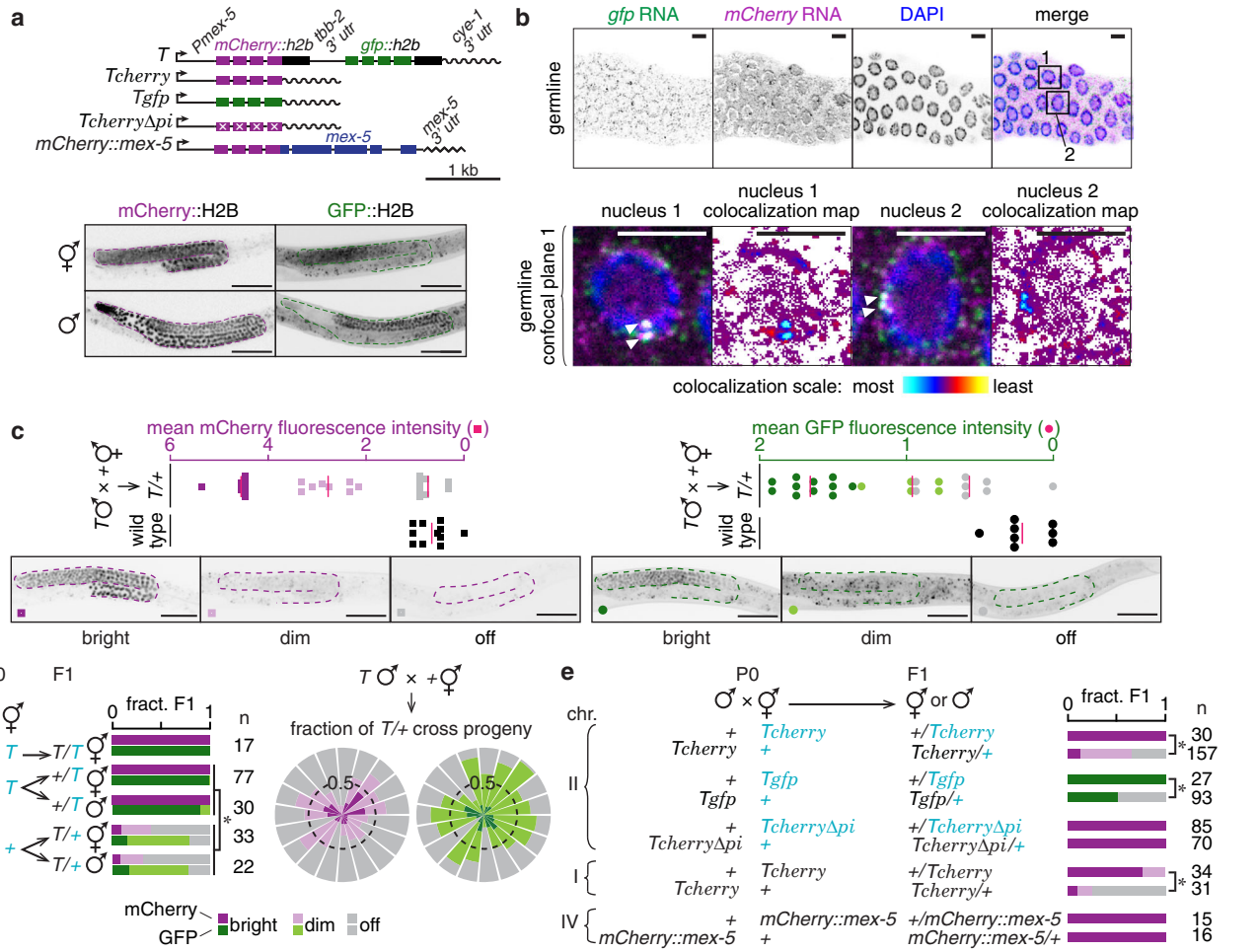

Fig. 1 Mating can disrupt gene expression by initiating RNA silencing. a Schematics of the single-copy transgene *Pmex-5::mCherry::h2b::tbb-2 3′utr::gpd-2 operon::gfp::h2b::cye-1 3′ utr* referred to as *T*, of independently generated minimal variants expressing only *mCherry* (*Tcherry*), *gfp* (*Tgfp*) or *mCherry* lacking piRNA-binding sites (*TcherryΔpi*) and of *mCherry* fused to endogenous *mex-5* coding sequence (*mCherry::mex-5*) are depicted (top). Germlines (dotted outline) of representative L4-staged hermaphrodites and males showing mCherry (magenta) or GFP (green) expression from *T* are indicated (bottom). **b** Single-molecule fluorescence in situ hybridization (smFISH) of *mCherry* and *gfp* in dissected gonads of animals expressing *T* reveals that *mCherry* RNA and *gfp* RNA colocalize as one or two spots (white arrowheads) within nuclei. Representative confocal plane (germline) imaged from a dissected gonad. Additional images are in Supplementary Fig. 1b. Colocalization heat map represents the extent of overlap between pixels corresponding to *mCherry* RNA and *gfp* RNA. **c** Quantification (top) and representative images (bottom) of the germline (magenta outline and green outline) of hemizygous animals (*T*/+) scored as having bright, dim, or not detectable (off) mCherry (left) or GFP (right) fluorescence. Average normalized fluorescence (red bar) within the germline was calculated for 11 bright, 5–8 dim, 8 off (gray), and 7 wild-type (black) L4-staged hermaphrodites. **d** Cross progeny males and hermaphrodites that inherited *T* from one or both parents were scored for expression of mCherry and GFP from *T* (left). Rose plot of independent repeats of mating-induced silencing of *T* (right). Each segment (mCherry, left and GFP, right) represents independent trials of one to four biological replicates and includes data from experiments depicted in other figures within the manuscript (total $n = 561$ animals). Dashed circles indicate half the fraction of animals scored. **e** Animals expressing *T*, *Tcherry*, *Tgfp*, *TcherryΔpi* or *mCherry* fused to the endogenous *mex-5* coding sequence (*mCherry::mex-5*) were mated with non-transgenic animals and resulting cross progeny were scored as having bright (magenta or green), dim (pink or light green), or not detectable (off, gray) levels of mCherry or GFP fluorescence. Number next to curly brackets refers to the chromosome on which each gene is present. All scored cross progeny were hermaphrodites except in the case of animals with *Tcherry* on chromosome I, where males were scored to ensure that cross-progeny were scored. In all figures, homozygous genotypes are indicated as a single character for simplicity—for example, '*T*' represents homozygous *T*/*T* animals, '+' represents non-transgenic or wild-type (+/+) animals etc. Also see Supplementary Figs. 1–7. Asterisks indicate $P < 0.05$ using χ^2 test. Chromosomes with a *dpy* marker (blue font) and numbers of animals scored (*n*) are indicated. Scale bars, 50 μm (**a**, **c**) and 5 μm (**b**). Source data are provided as a Source Data file.

regions. Lastly, other transgenes with homologous intron sequences (*Dendra2::H2B* in Supplementary Fig. 2a) or *mex-5* promoter (*mCherry*^{var2}*::mex-5* in Supplementary Fig. 2a) were not susceptible to mating-induced silencing. Thus, regulatory features that contribute to *Tcherry* expression (*cis*-regulatory sequences, intranuclear localization of DNA, chromatin neighborhood, etc.) are sufficient to support change in gene expression upon mating.

To examine if unequal partitioning of parental factors could cause preferential mating-induced silencing in early progeny as observed during RNA interference (RNAi)[15,16], we separately measured silencing in four successive cohorts of progeny (Supplementary Fig. 1j). Proportions of animals that showed silencing were comparable in each cohort, ruling out such systematic bias. The variation in mCherry and GFP fluorescence was correlated in most individual F1 animals (Supplementary Fig. 1k), suggesting that silencing occurs either on unspliced pre-

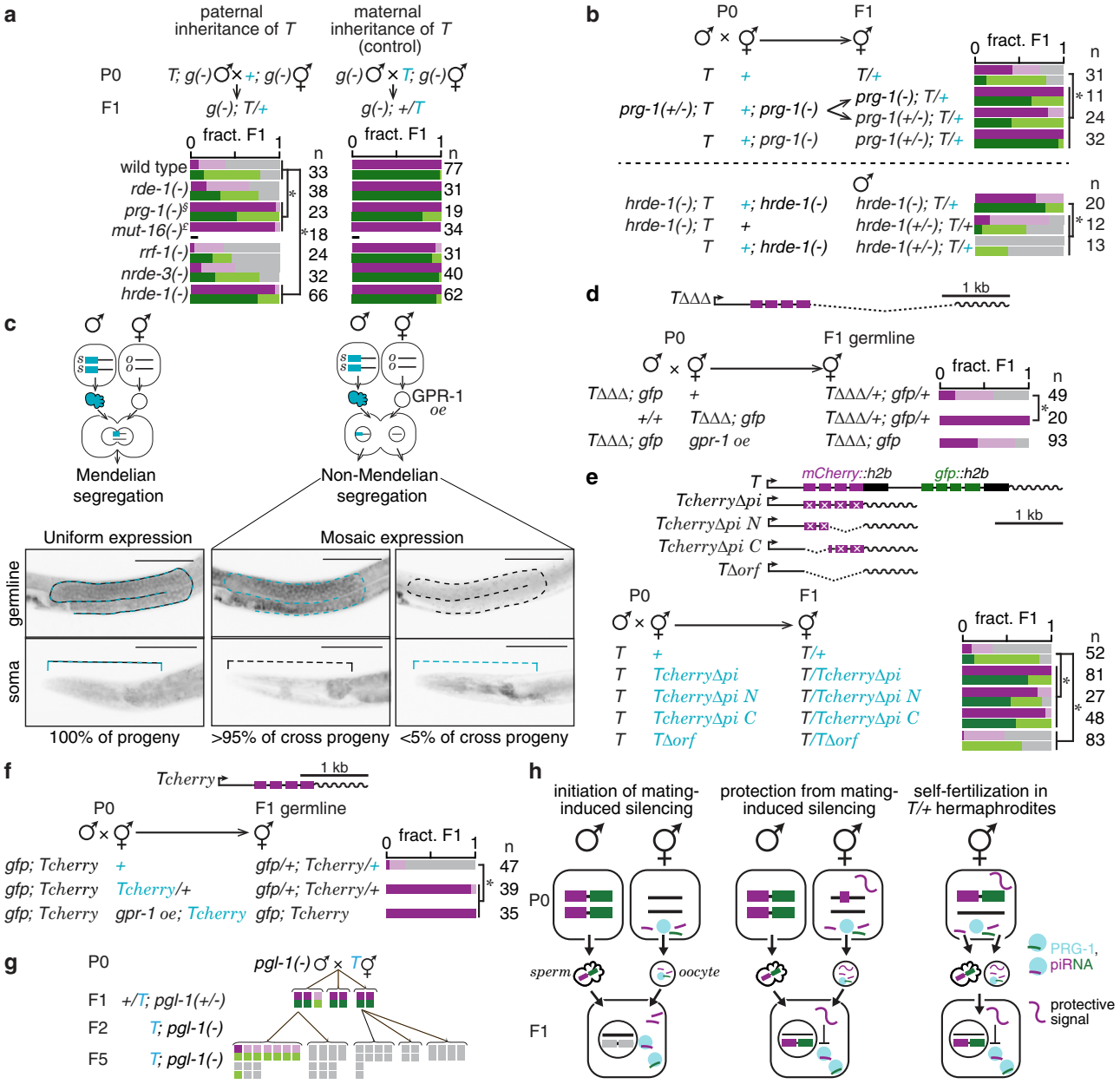

mRNA or simultaneously on both *mCherry* and *gfp* mRNA during or after pre-mRNA splicing.

Examining known RNA silencing factors (Supplementary Fig. 3b; refs. [9,17].) revealed that mating-induced silencing required the primary Argonaute PRG-1, mutator protein MUT-16, and the secondary Argonaute HRDE-1 (Fig. 2a), distinguishing it from silencing by feeding RNAi, which was PRG-1-independent (Supplementary Fig. 3c). Four observations support an inter-generational mechanism for the initiation of mating-induced silencing using PRG-1-bound small RNAs called piRNAs. One, reduction in protein fluorescence from *T* was accompanied by reduction in RNA levels in silenced progeny (Supplementary Fig. 4a, b). Two, removal of predicted piRNA sites[18] in *mCherry* (*TcherryΔpi*) eliminated mating-induced silencing (Fig. 1e and Supplementary Fig. 3d). Three, maternal absence of PRG-1 and zygotic absence of HRDE-1 prevented initiation of silencing (Fig. 2b). Four, preventing pronuclear fusion in progeny using maternal overexpression of the G-protein regulator GPR-1 (Fig. 2c, d; refs.[19,20]; see Methods) still resulted in silencing, indicating that initiation is independent of maternal chromatin in the germline of progeny. Because PRG-1 loss abolished mating-induced silencing of *gfp* in *T* (Fig. 2a, b) and because *Tgfp* (*Pmex-5::gfp::cye-1 3′ UTR*) was also silenced by mating, there is a potential for endogenous piRNAs complementary to *gfp*[18] to trigger mating-induced silencing of *gfp* independent of *mCherry*. Together, these results suggest that maternal PRG-1-bound piRNAs trigger production of secondary small RNAs using transcripts from *T* (Fig. 2h, left) and MUT-16-dependent perinuclear mutator foci[21], which then bind HRDE-1 and cause silencing in progeny.

In summary, mating can disrupt the expression of a set of single-copy transgenes and cause transgenerational RNA silencing. This stable RNA silencing could result from the activation/gain of mechanisms that promote silencing or the repression/loss of mechanisms that prevent silencing, or both.

Homologous maternal transcripts protect against initiation of mating-induced silencing. Initiation of mating-induced silencing of paternally inherited *T* could be prevented by maternal

Fig. 2 Requirements for initiation of and protection from mating-induced silencing. a Mating-induced silencing was initiated as in Fig. 1d in a wild-type or in different mutant (*g(-)*) backgrounds (left) and silencing in resulting cross progeny were compared with that of the same genotypes from control crosses (right). Wild-type crosses shown here are the same as in Fig. 1d. An additional wild-type cross with a different visible marker (not depicted, but showed mating-induced silencing—mCherry: bright = 5, dim = 6, off = 25 and GFP: bright = 7, dim = 12, off = 17 in F1 progeny) was performed for comparison with the *rde-1(-)* cross on the right. Use of *prg-1(−/+)* parent males owing to the poor mating by *prg-1(-)* parent males is indicated (§). Requirement of *mut-16* in initiation of silencing was examined by scoring only mCherry fluorescence, but not GFP fluorescence, in male cross progeny (£). **b** Requirement of *prg-1* and *hrde-1* in initiation was tested by mating parents mutant for either of these genes and scoring cross progeny. **c** Scheme to test effect of *gpr-1* overexpression: *gtbp-1::gfp* (blue) males mated with wild-type hermaphrodites (left) or with hermaphrodites overexpressing *gpr-1* in the germline (*gpr-1 oe,* right). *s* and *o* label DNA inherited through sperm and oocyte respectively. Representative images show differences in segregation of *gtbp-1::gfp* in the germline (top) and the head (soma, bottom) in cross progeny. Colored outlines and brackets show the parental origin of germline or pharynx. **d** Animals expressing *TΔΔΔ* and *Pgtbp-1::gtbp-1::gfp* marker *(gfp)* were mated with either non-transgenic animals or animals overexpressing *gpr-1* (*gpr-1 oe*). Fluorescence from mCherry in the germline of cross progeny was scored. Gene structures are also depicted here (top) and in other panels. **e** *T* males were mated with hermaphrodites expressing variants of *TcherryΔpi* and progeny with paternally inherited *T* were scored. **f** Males expressing *Pgtbp-1::gtbp-1::gfp* marker (*gfp*) and *Tcherry* were mated with hermaphrodites that expressed *Tcherry* in a wild-type or *gpr-1* overexpression (*gpr-1 oe*) background and fluorescence of paternally inherited *Tcherry* was scored in cross progeny. **g** *T* animals were mated with *pgl-1* mutants and expression of *T* was assessed in hemizygous cross progeny and in homozygous descendants. Each vertical pair of boxes represents fluorescence intensity of mCherry and GFP within the same animal. **h** Schematics depict inferences from mating-induced silencing: left, when *T* males are mated with hermaphrodites lacking *T*, cross progeny are silenced by PRG-1 inherited through the oocyte using piRNAs targeting *mCherry* and *gfp* in *T*; middle, when *T* males are mated with hermaphrodites expressing a fragment of *T*, even with piRNA target sites mutated (e.g. *TcherryΔpi N*), cross progeny are protected from silencing initiated by PRG-1 inherited through the oocyte; right, when hemizygous hermaphrodites self-fertilize using transgenic sperm carrying *T* and oocytes that lack *T* but carry piRNAs targeting *T*, self-progeny remain unsilenced possibly due to a protective signal, likely RNAs, derived from parental *T* transmitted through the oocyte into progeny. Chromosomes with a *dpy* marker (blue font), number (*n*) of animals scored (**a**, **b**, **d**–**g**) and scale bars, 50 µm, (**c**) are indicated. Scoring of fluorescence is as in Fig. 1. Also see Supplementary Figs. 1, 3, 4. Asterisks indicate $P < 0.05$ using χ^2 test. Also see 'Genetic Crosses' under Methods. Source data are provided as a Source Data file.

expression of *T* (Fig. 2e), suggesting that a signal derived from maternal *T* can protect paternal *T* from silencing. Consistently, the protective signal mapped to a ~3.2 Mb region that includes *T* (Supplementary Fig. 5a). This ability to protect was also largely retained by variants of *T* containing *mCherry* (Fig. 2e, Supplementary Figs. 3a and 5b, c). Maternal presence of *mCherry*, even as a hemizygous single copy could protect both *mCherry* and *gfp* in more progeny compared to maternal presence of two copies of *gfp* (Supplementary Fig. 5b, c). This protective signal could explain why hemizygous self-progeny of hemizygous hermaphrodites showed stable expression of *T* for multiple generations even if *T* inherited through self-sperm is capable of being silenced (Fig. 2h, right, Supplementary Fig. 1d). In each generation of hemizygous hermaphrodites, the transgene is expected to be inherited through self-sperm 50% of the time (Supplementary Fig. 1d) and a maternal protective signal could be required for expression of *T* inherited through self-sperm. Therefore, either a protective signal inherited through oocytes licenses expression of *T* inherited through self-sperm in each generation or *T* inherited through self-sperm is not susceptible regardless of whether there is a protective signal inherited through the oocytes. Once paternally inherited *T* was protected, expression of *T* was stably maintained in descendants generated by self-fertilization (Supplementary Fig. 5d). Nevertheless, protected cross progeny remained susceptible to initiation similar to unsilenced progeny that escaped initiation of mating-induced silencing (Supplementary Fig. 5e, f). Because maternally expressed variants of *T* could confer protection despite nonsense mutations or deletions that disrupted the coding sequence (Supplementary Figs. 3a and 5b), the protective signal could be derived from parts of *T*. Consistently, *TcherryΔpi* sequences showed the strongest level of protection despite the inability of their transcripts to bind piRNAs, even when the N- or C-terminal sections of *TcherryΔpi* coding sequence were deleted (Fig. 2e, *TcherryΔpi N*/C). Therefore, protection cannot be explained by a simple model whereby complementary maternal *mCherry* sequences compete away maternal piRNAs. Protection was weak when only the last exon of *TcherryΔpi* was used (Supplementary Fig. 5b, *TcherryΔpi exon 4*) and was completely abolished when the entire open reading frame was deleted (Fig. 2e, *TΔorf*). Other genes that share the same *mCherry* protein sequence or additional DNA sequences identical to regions of *T* could not protect *T* (Supplementary Fig. 5g, h). The protective signal did not require interactions between homologous chromosomes because *TcherryΔpi* on chromosome II could protect *Tcherry* on chromosome I from mating-induced silencing (Supplementary Fig. 5i). Lastly, preventing fusion of zygotic pronuclei still resulted in protection of paternal *T* (Fig. 2f). Collectively, these observations suggest that protection relies on a diffusible sequence-specific signal, likely maternally inherited transcript(s).

We noted that different *TcherryΔpi* variants appeared to protect in proportion to their coding-sequence lengths regardless of the number of mutated piRNA target sites (Supplementary Fig. 5j; also see Fig. 2e and Supplementary Fig. 5b). This observation suggests that either variants of *T* produce different amounts of the protective signal or that maternally inherited transcripts themselves protect by titrating away silencing small RNAs made against *T* triggered downstream of piRNA-binding in progeny (Supplementary Fig. 5j, k). The Argonaute CSR-1 has been proposed to play a role in promoting the expression of germline genes[22,23] and in the prevention or reversal of transgene silencing in the germline[24,25]. CSR-1 has also been proposed to regulate spermiogenesis and oogenesis[23], to silence sperm-specific transcripts in coordination with germ granules[26], and to tune the levels of germline transcripts[27]. These diverse roles make effects caused by the loss of CSR-1 difficult to interpret. Furthermore, the embryonic lethality caused by chromosome segregation defects in *csr-1* mutants[28] makes rigorous analyses across generations challenging. Nevertheless, we examined a component of the CSR-1 pathway that interacts with these small RNAs but lacks the confounding developmental defects. Unlike CSR-1, removal of the uridylyltransferase CDE-1 that uridylates CSR-1-associated small RNAs causes fewer pleiotropic effects[28,29]. CDE-1 loss did not abolish protection (Supplementary Fig. 5l). Although additional experiments are needed to identify the molecular machinery that mediates protection from mating-induced silencing, the ability of *TcherryΔpi* variants to protect both mRNAs from *T* suggests that the derived maternal signals

from *T* engage more complex mechanisms that license expression within the germline[30]. Protection of germline transcripts from piRNA-mediated silencing can occur within phase-separated condensates called P granules, which when disrupted can cause mis-regulation and aberrant distribution of some endogenous transcripts[31,32]. We tested for potentially similar mis-regulation of transcripts from *T* and observed complete silencing in some animals upon loss of the P granule component PGL-1 without the need for mating (Fig. 2g). This observation suggests that stable transgenerational expression of *T* likely reflects reliable recognition of transcripts from *T* within P granules as part of 'self' in every generation, according to some current models.

Thus, mating disrupts competing RNA-based mechanisms that regulate expression to initiate silencing (Fig. 2h) and maternal transcripts with partial homology are sufficient to oppose silencing by piRNAs. Protection by maternal transcripts explains the directionality of mating required for silencing and, in hindsight, also suggests explanations for the situations where we did not observe silencing (Supplementary Fig. 1l).

Silencing induced by mating is actively maintained for >300 generations. Once the expression state of *T* was established in cross progeny after mating, the expression state remained similar in subsequent generations (Fig. 3a and Supplementary Fig. 5m). Descendants of silenced F2 animals stayed silenced in 100% of animals in each tested generation for more than 300 generations without additional selection (Fig. 3b, c, Supplementary Figs. 5n and 6a, b). We refer to animals carrying a stably silenced copy of the transgene or its variants obtained by mating-induced silencing with an *i* (e.g. *iT*, where *i* stands for inactive) in the remainder of the paper. Consistent with transgenerational RNA silencing, *iT* animals showed a ~30- to 37-fold decrease in mRNA and ~4- to 6-fold decrease in pre-mRNA (Supplementary Fig. 6c). Transgenerational silencing could be detected even with variants of *T* that include a minimal coding sequence (Supplementary Fig. 5o, p), suggesting that additional sequence features are not needed for stable heritable silencing. Silencing triggered by piRNAs can last for many generations and be associated with repressive chromatin modifications[22,33–36]. Among RNA silencing and chromatin factors (Supplementary Fig. 3b), transgenerational stability of mating-induced silencing required the nuclear Argonaute HRDE-1, the nucleotidyltransferase RDE-3/MUT-2, and the intrinsically disordered protein MUT-16 even after 250 generations of silencing (Fig. 3c and Supplementary Fig. 6d). MUT-16 and RDE-3/MUT-2 are present in perinuclear foci where they promote the production of secondary small RNAs by RdRPs RRF-1 and EGO-1[21]. We examined animals that lack RRF-1 alone and animals that in addition lack zygotic EGO-1 (because animals that lack both maternal and zygotic EGO-1 are sterile[37,38]). Despite the potential for maternal rescue of *ego-1*, there was recovery of weak mCherry and GFP expression in *rrf-1 (-) ego-1(-)* double mutants but not in *rrf-1(-)* single mutants (Fig. 3c), implicating these RdRPs in maintaining silencing in every generation. Similarly, only some *hrde-1(-)* progeny of *hrde-1(+/−)* animals showed expression, potentially due to maternal rescue, but all *hrde-1(-)* progeny in the next generation showed expression (Supplementary Fig. 6d). Thus, transgenerational silencing of *T* reflects active establishment of silencing by secondary small RNAs in every generation for hundreds of generations rather than passive loss of gene expression through DNA mutation (e.g., as occurs during repeat-induced point mutation in *Neurospora*[39]). Once expression was recovered in *hrde-1* mutants, restoring wild-type HRDE-1 did not re-establish silencing (Supplementary Fig. 6e), indicating permanent loss of silencing signals. HRDE-1-bound small RNAs can recognize nascent transcripts and recruit chromatin modifiers to establish repressive histone modifications (e.g., H3K9me3) at target genes[22,40]. Neither the histone methyltransferases MET-2[41,42] or SET-32[42,43] nor the chromodomain protein HERI-1[44] was required for silencing (Fig. 3c). Descendants from a lineage that experienced >250 generations of silencing showed no significant changes in H3K9 methylation (Supplementary Fig. 6f, g). While transgenerational epigenetic inheritance (TEI) induced upon mating may be associated with additional unexamined molecular changes, reduction in RNA levels without any associated chromatin modifications is sufficient to explain maintenance (Fig. 3c, model).

A signal associated with stable RNA silencing can enable *trans* silencing of homologous sequences. Continued requirement of HRDE-1 to maintain stable silencing indicates that RNA silencing is likely associated with production of new small RNAs in every generation driven by small RNAs and/or template RNAs inherited from the previous generation. This positive feedback acting across generations could affect the expression of homologous genes because small RNAs can diffuse and encounter other complementary sequences, potentially initiating silencing at these new targets (Fig. 4a). To test this possibility, we examined whether stable silencing of *iT* has any *trans* effects on other homologous genes. We found that *iT* transmitted through one gamete could silence *T* inherited from the other gamete, regardless of the number of generations for which *iT* remained inactive (Fig. 4b and Supplementary Fig. 7a). Furthermore, presence of *iT* in any one parent was sufficient to cause significant silencing in progeny that inherited *T* only from the other, unsilenced parent (Fig. 4c). This *trans* silencing signal either is or relies on HRDE-1-dependent small RNAs because it is mostly eliminated upon loss of zygotic HRDE-1 (Fig. 4d). While meiosis is completed in sperm before fertilization, it is stalled at prophase I in oocytes until fertilization[45]. Nevertheless, oocyte meiosis is completed early in the one-cell zygote such that only a haploid genome is present in the oocyte pronucleus when it meets the sperm pronucleus. By preventing fusion of the haploid nuclei, we observed that direct interaction between parental chromatin was dispensable for *trans* silencing to occur (Fig. 4e), suggesting that *trans* silencing relies on a signal that is separable from DNA. This DNA-independent signal when transmitted through sperm must have separated from DNA in the male germline but when transmitted through oocytes can separate from DNA either in the hermaphrodite germline or in the embryo. Yet, this separable signal was not detectably inherited for more than one generation independent of *iT*, suggesting that it requires parental presence of *iT* for production (Supplementary Fig. 7b). Once *T* was silenced in *trans* by *iT*, the newly silenced copy of *T* remained silenced across generations, even when propagated by selfing without a copy of the ancestral *iT* (Fig. 4f and Supplementary Fig. 7c). Thus, silencing relies on a signal that is maternally deposited in every generation. This heritable silencing signal could be either HRDE-1-dependent small RNAs or downstream effectors made zygotically in response to a different intergenerational signal.

We examined the potential spread of a silencing signal associated with *iT* to sequences at other genomic positions. Genes sharing coding sequence identity, but not genes with only intronic or protein sequence identity, were silenced within the germline by *iT* in *trans* (Fig. 4g and Supplementary Fig. 7d). *Trans* silencing could only be detected with a stably established *iT* but not simultaneously with initiation of mating-induced silencing of *T* (Supplementary Fig. 7e), suggesting that initiation and maintenance of mating-induced silencing are either quantitatively distinct (e.g., different amounts of small RNAs) or

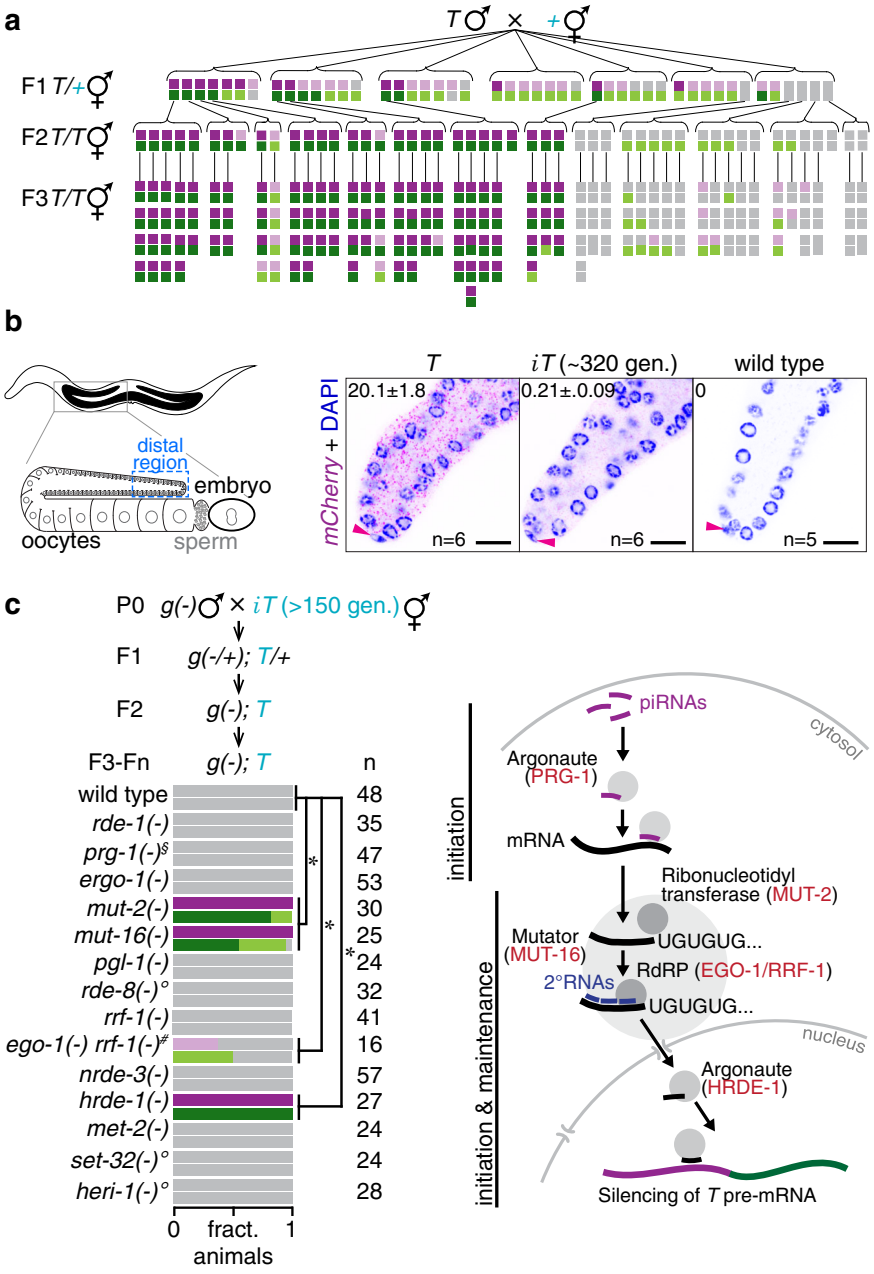

Fig. 3 Mating-induced silencing is actively maintained for >300 generations. a Mating-induced silencing was initiated and silencing was scored in cross progeny and their descendants. Each vertical pair of boxes represents fluorescence intensity of mCherry and GFP within the same animal (bright, dim, and off, as in Fig. 1c). **b** Maintenance of mating-induced silencing was measured by smFISH against *mCherry* exonic RNA in indicated distal region of dissected gonads of adult *T*, *iT* (silenced for ~320 generations) or wild-type animals. Pink arrowheads indicate the nucleus of the distal tip cell. Animals with median values of fluorescence or RNA signal in the distal region are shown in representative images. smFISH probes used are depicted in Supplementary Fig. 2d. Merged (DAPI + *mCherry* RNA smFISH) images shown here are also shown in Supplementary Fig. 6a as separate channels with remaining images from the same animals. Numbers within images indicate number of RNAs per 100 μm^2 with standard error of the mean. **c** Left, *iT* hermaphrodites that showed 150–250 generations of continued silencing were crossed with males mutant for RNAi genes (*g(-)*) and resulting descendants homozygous for the mutant allele of the gene were scored at F3 (*rde-1(-), prg-1(-), rrf-1(-), ego-1(-) rrf-1(-), nrde-3(-), hrde-1(-)*), F4 (*ergo-1(-), heri-1(-)*), F5 (*pgl-1(-), rde-3/mut-2(-), mut-16(-), set-32(-)*), ~F15 (*rde-8(-)*) generations, or scored at F4/F6/F8 and pooled (*met-2(-)*). Use of *prg-1(−/+)* parent males owing to the poor mating by *prg-1(-)* parent males is indicated (§). Use of fertile *ego-1(−/+) rrf-1(−/−)* parent hermaphrodites, rather than sterile *ego-1(-) rrf-1(-)* parent hermaphrodites, mated to *iT* males is indicated (#). Use of Cas9-mediated genome editing rather than genetic cross to introduce mutation is indicated (°). Right, Model of piRNA-mediated RNA silencing (see text for details). Scoring of silencing (**a**, **c**) is as in Fig. 1c. Chromosomes with a *dpy* marker (blue font), number (*n*) of animals scored (**c**) or imaged by confocal microscopy (**b**) and scale bar (10 μm) are indicated. Also see Supplementary Figs. 5 and 6. Asterisks indicate $P < 0.05$ using χ^2 test (**c**). Also see 'Genetic Crosses' under Methods. Source data are provided as a Source Data file.

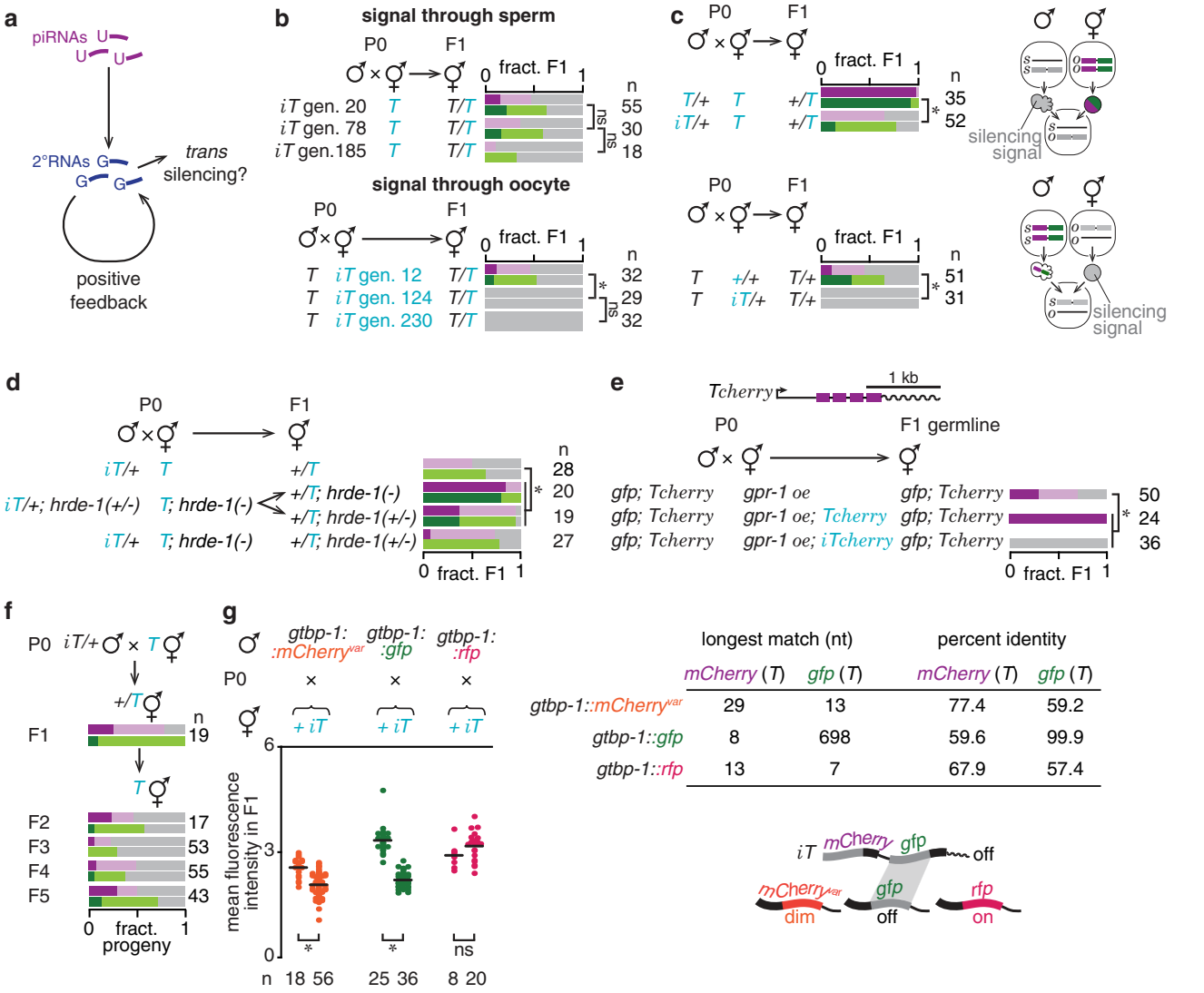

Fig. 4 Stable silencing after mating is associated with heritable silencing signals that can act in *trans*. **a** Schematic showing piRNA-mediated activation of a positive feedback for production of secondary small RNAs (2° RNAs) upon mating-induced silencing. The secondary small RNAs made at one gene could potentially act on other homologous genes (*trans* silencing). **b** Animals expressing *T* were mated with *iT* animals that remained silenced for many generations (*iT* gen. number), and cross progeny were scored. The combined data from each cross is shown in Supplementary Fig. 7a. **c** *T* animals were mated with non-transgenic or hemizygous *iT* animals and cross progeny that inherited only *T* were scored. Schematic: parental presence of *iT* can be sufficient to silence *T* inherited through the other gamete, indicating the inheritance of a separable silencing signal (gray filling). **d** Requirement of *hrde-1* for the activity of the silencing signal was tested by parental, maternal, and/or zygotic loss of HRDE-1. **e** *Tcherry* animals silenced for more than five generations upon initiation of mating-induced silencing were designated as *iTcherry* here. Males expressing *Tcherry* and *Pgtbp-1::gtbp-1::gfp* marker (*gfp*) were mated with *iTcherry* or *Tcherry* hermaphrodites overexpressing *gpr-1* (*gpr-1 oe*). Expression of paternally inherited *Tcherry* in the germline was scored in cross progeny. **f** Silencing of *T* by the separable silencing signal or in *trans* by *iT* was assessed across generations. The remaining results of this cross showing the effect of *trans* silencing are shown in Supplementary Fig. 7c. **g** Males that express homologous (*gfp*) or non-homologous (*mCherry*^{var}, a synonymous *mCherry* variant or *rfp*) sequences fused to endogenous *gtbp-1* expressed ubiquitously were mated with non-transgenic or *iT* hermaphrodites and fluorescence of GTBP-1::GFP, GTBP-1::mCherry^{var} or GTBP-1::RFP was quantified in cross progeny (left). Percentage of nucleotide identity and length of the longest continuous match shared by different fluorescent protein coding sequences in pairwise alignment using the Needleman–Wunsch algorithm (penalties for mismatch = 0.1, gap = −1, and gap extension = −0.2) with the *mCherry* or *gfp* sequence of *T* as reference are shown (right top). Schematic summary of homology-dependent *trans* silencing (right bottom). See Supplementary Data files 1–6 for each pairwise sequence alignment. Scoring of silencing (**b**–**f**) is as in Fig. 1c. Chromosomes with a *dpy* marker (blue font) and number of animals scored (*n*) are indicated. Asterisks indicate $P < 0.05$ using χ^2 test (**b**–**d**), Wilson's estimates for proportions (**e**) or two-sided Student's *t*-test (**g**), and ns indicates $P > 0.05$ using the same tests. Also see Supplementary Fig. 7 and 'Genetic Crosses' under Methods. Source data are provided as a Source Data file.

qualitatively distinct (e.g., different timing of small RNA production or different nature of small RNAs). Consistent with *trans* silencing being homology-dependent, *iTΔ* established by mating-induced silencing after deleting *gfp* from *T* did not silence other *gfp* genes in *trans* (Supplementary Fig. 7f). In all cases, silencing (in *trans* or by the separable silencing signal) was restricted to the germline. Furthermore, maternal but not paternal transmission of the silencing signal affected expression of homologous genes (Supplementary Fig. 7g). This difference in efficacy and/or transmission of the silencing signal could reflect differences in the intracellular environment in the two gametes and/or differences in the nature or

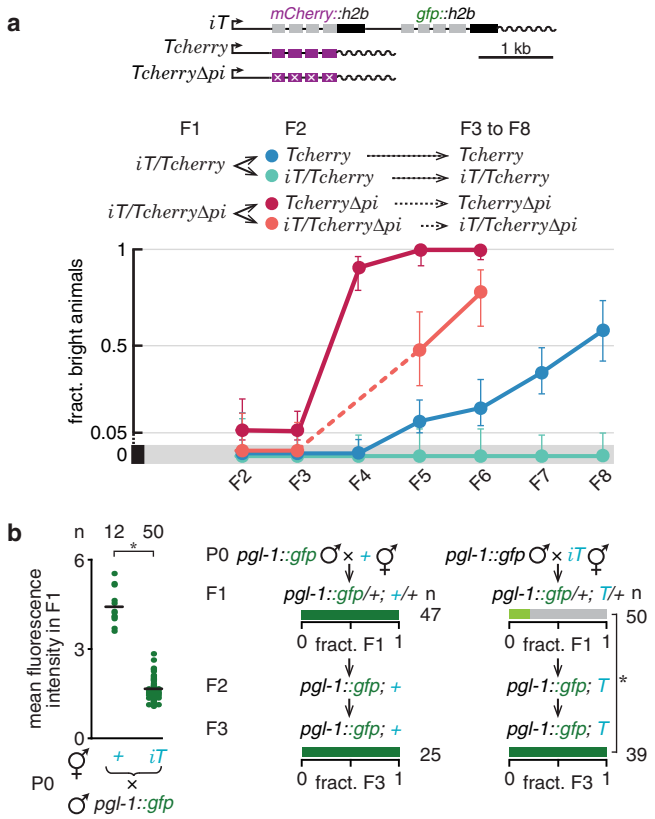

Fig. 5 *Trans* silencing within the germline can be followed by recovery of gene expression and resistance to subsequent silencing within a few generations. a *Tcherry* or *TcherryΔpi* animals were mated with *iT* stably silenced for >150 generations and fractions of animals with bright *Tcherry* or *TcherryΔpi* expression were scored in resulting cross progeny (F1) and their descendants (F2 through ≤F8). Error bars indicate 95% confidence intervals. Schematics of transgenes used are indicated above the graphs. See Supplementary Fig. 7j, k for number of animals analyzed in each generation for each genotype and for pedigree. Fractions of bright animals are plotted and error bars indicate 95% CI. **b** *pgl-1::gfp* animals were mated with non-transgenic or *iT* animals and fluorescence of PGL-1::GFP was quantified in cross progeny (left) or scored as in Fig. 1c in cross progeny and their descendants (middle and right). Chromosomes with a recessive *dpy* marker (blue font) and number of animals scored (*n*) are indicated. Also see Supplementary Fig. 7. Asterisks indicate $P < 0.05$ using two-tailed Student's *t*-test (b, left) or χ^2 test (**b**, right). Source data are provided as a Source Data file.

levels of silencing signal inherited through the two gametes[17,46].

Genes can recover from silencing and become resistant to *trans* silencing. Sensitivity of *T* to TEI was previously observed when ancestral exposure to neuronal double-stranded RNA (dsRNA) resulted in >25 generations of silencing[47]. To explore whether changes that alter expression of *T* always result in permanent silencing, we used *trans* silencing as an alternative method to initiate silencing and examined the frequency with which recovery of gene expression can occur in the germline. Interaction of *T* with *iT* resulted in strong *trans* silencing of *T* as expected but also weak reactivation of expression from descendants of *iT* (Supplementary Fig. 7h). This reactivation could be mediated by the activity of protective signals opposing silencing signals (Supplementary Fig. 7i), leading to a small fraction of the descendants of *iT* animals showing expression in every generation (Supplementary Fig. 7h). However, the *trans* silencing effect of *iT* on both *Tcherry* and *TcherryΔpi* (Fig. 5a and Supplementary Fig. 7j, k) was less robust. One generation of exposure to *iT* resulted in silencing even in the absence of *iT* in descendants with homozygous *Tcherry* and *TcherryΔpi*, but expression recovered within a few generations. About 60% of *Tcherry* animals and almost 100% of *TcherryΔpi* animals recovered within seven generations (Fig. 5a). Intriguingly, *TcherryΔpi* became resistant to *trans* silencing despite the continued presence of the silenced *iT* (compare *iT/Tcherry* vs. *iT/TcherryΔpi* in Fig. 5a). The continued silencing of *iT* was indicated by the absence of nuclear-localized GFP and mCherry. These observations suggests that piRNAs binding to a target transcript (*Tcherry*) or perfect homology to *iT* promotes its continued susceptibility to *trans* silencing by small RNAs made from *iT*. Since endogenous genes expressed within the germline are thought to have 'licensing' features that antagonize silencing by piRNAs (e.g., PATC sequences[14], CSR-1 targeting[24]), we examined *trans* silencing of an endogenous gene tagged with *gfp*. The *pgl-1::gfp* gene exhibited a switch from complete *trans* silencing by *iT* in the first generation to undetectable silencing within two generations (Fig. 5b). These results provide two surprising insights into RNAs associated with stable silencing: (1) they are not sufficient for inducing stable silencing at homologous genes even after successful silencing of these genes for a few generations; (2) their activity can be opposed by signals derived from recently active homologous genes despite initial silencing.

Persistence of silencing by dsRNA depends on the regulatory context of the target gene. Several studies have reported TEI under diverse conditions, but variations between studies preclude a consistent explanation for susceptibility to TEI (Supplementary Table 1). We therefore simultaneously used identical experimental conditions of feeding RNAi[48] to target identical *gfp* sequences expressed as part of low or single-copy germline genes in parent animals and examined silencing in their untreated descendants (F1–F5). Because parental dsRNA can be deposited into progeny[15,16], only silencing that persists beyond the F2 generation can be unambiguously considered as transgenerational. Out of six target genes tested, two genes showed silencing up to F2 progeny, but only *T* showed silencing beyond F2 (Fig. 6a and Supplementary Fig. 8a–f). Therefore, transgenerational silencing is variable even when targeting the same coding sequence expressed within the same tissue under different regulatory contexts. Even for *T*, while silencing could be maintained upon unbiased propagation, some animals could recover from silencing in later generations (Fig. 6b). Similar to recovery from *trans* silencing (Fig. 5), descendants showed recovery despite silencing in parents (Fig. 6a). The reason for persistent RNA silencing versus recovery from RNA silencing cannot be attributed solely to HRDE-1[40] because silencing was not stable at all target genes despite being HRDE-1-dependent (Supplementary Fig. 8g). We investigated if enhancing silencing by dsRNA could overcome recovery to increase the duration of TEI. Removal of three proteins shown to oppose silencing, the endonuclease ERI-1[49], HERI-1[44], or MET-2[50], enhanced persistence of silencing (Fig. 6c, d and Supplementary Fig. 8h), albeit to a much lesser extent than previously reported for other target genes[44,50]. Thus, *T* and its variants are genes with rare regulatory contexts that enable coding sequences to overcome recovery and retain changes in expression for many generations.

Collectively, we propose that our observations on the response to induced RNA silencing reveal two types of regulatory contexts that drive expression within the *C. elegans* germline (Fig. 7): type I are vulnerable to permanent change in response to transient perturbations and type II are either resistant to perturbations or

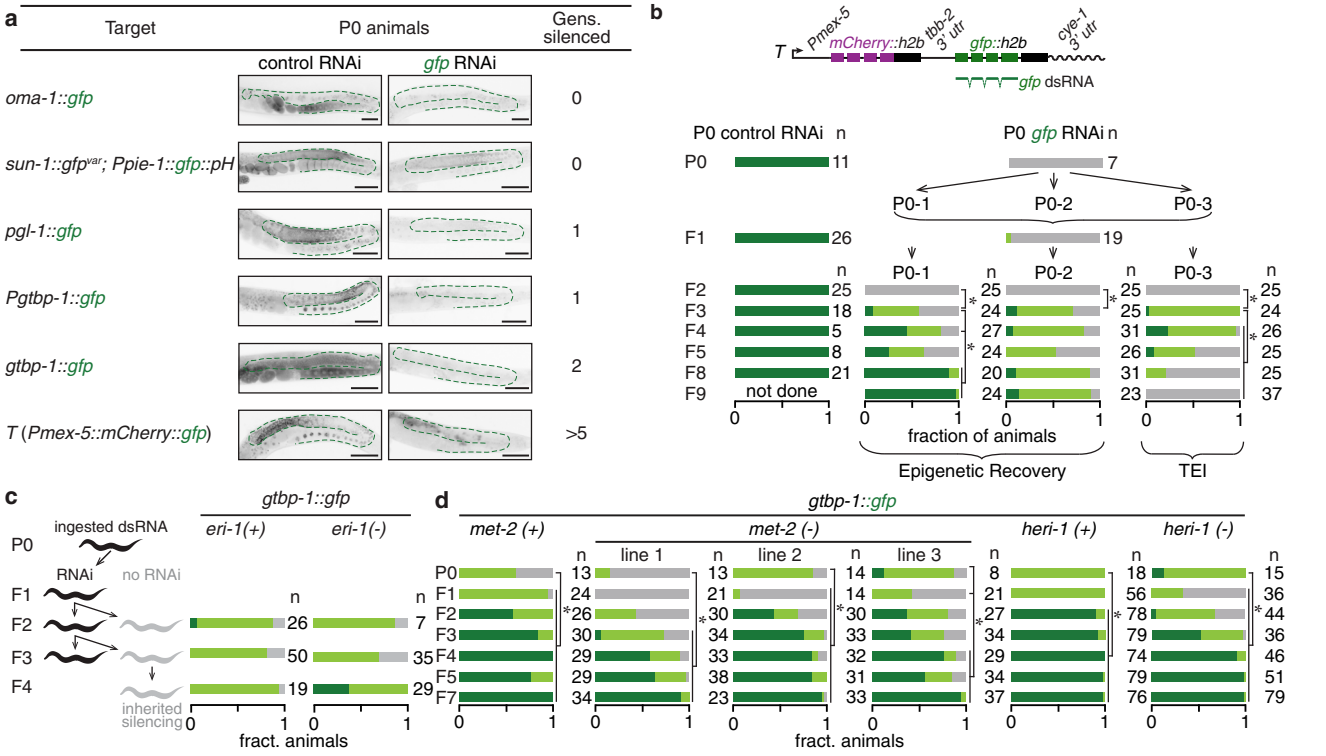

Fig. 6 Genes silenced by dsRNA in parents commonly recover from silencing in descendants. a Six target genes containing the same *gfp* sequence were exposed to the same sources of control RNAi or *gfp* RNAi. P0 animals were fed dsRNA for 24 h, and the P0 animals and their untreated descendants for up to five generations (F1–F5) were analysed. Representative images highlight the germline (green outline) of P0 animals. Numbers of descendant generations that show silencing are indicated. Note that *sun-1::gfp*^{var} is also present in the animal with *PH::gfp*, but is not silenced because its *gfp*^{var} sequence only has <14-nt of continuous homology with the *gfp*-dsRNA used for feeding RNAi. Scale bars indicate 50 µm. **b** P0 animals expressing *T* were exposed to control RNAi (P0 control RNAi) or *gfp*-dsRNA (P0 *gfp* RNAi) for 24 h and silencing was analysed in P0 animals and in their untreated descendants. Upon *gfp* RNAi, P0 and F1 animals were each pooled for imaging but subsequent generations each descending from one P0 ancestor (P0-1, P0-2, or P0-3) were imaged as individual isolates. All generations shown were scored by imaging except F2s, which were scored by eye. While one isolate showed TEI, the other two isolates recovered expression (epigenetic recovery). As indicated with a schematic, the sequence of *gfp* dsRNA matches the exons of *gfp* coding sequence. **c** *gtbp-1::gfp* animals were fed *gfp*-dsRNA (black) for one, two or three consecutive generations and their untreated progeny (gray) in a wild-type (*eri-1(+)*) or *eri-1(−)* background were scored for expression of GFP. **d** *gtbp-1::gfp* hermaphrodites in wild-type (*met-2(+)* and *heri-1(+)*), *met-2(−)* or *heri-1(−)* backgrounds were fed *gfp*-dsRNA for 24 h and untreated descendants in subsequent generations (F1–F7) were scored as in Supplementary Fig. 8c. Feeding RNAi of other strains was performed concurrently, thus data for *gtbp-1::gfp* here is the same as in Supplementary Fig. 8c. In *heri-1(-)* animals, the statistical difference between P0 and F1–F2 is due to increased silencing, but that between P0 and F3–F7 is due to decreased silencing. Most animals fed control RNAi and descendants showed bright expression of GFP (except 2 out of 45 F5 descendants and 1 out of 37 F7 descendants of *heri-1(-)* animals that showed dim expression). Number of animals scored (*n*) are indicated. Asterisks indicate $P < 0.05$ using χ^2 test. Also see Supplementary Fig. 8. Source data are provided as a Source Data file.

can recover from them within a few generations. Additional work is needed to discover the particular regulatory molecules and their arrangements that distinguish type I genes from type II genes.

Discussion

The hallmarks of mating-induced silencing are: (1) silencing is initiated upon inheritance only through the male sperm; (2) once initiated, silencing is stable for many generations; (3) transgenerational silencing is associated with a DNA-independent silencing signal that is made in every generation, can be inherited for one generation, and can silence homologous sequences; and (4) maternal exonic sequences can prevent initiation of silencing. While to our knowledge no other known phenomenon shares all of these hallmarks (Supplementary Table 2), phenomena that share some of these features (elaborated in Supplementary Discussion) can inform future mechanistic studies.

Our analysis of the bicistronic operon *T* and its derivatives suggests that competing maternal signals establish gene expression in progeny. While maternally inherited PRG-1 and piRNAs mediate mating-induced silencing of the paternally inherited copy of *T* in progeny (Fig. 2), silencing is opposed whenever a maternal protective signal is present (Fig. 2f). This protective signal can act away from the maternal genome, and although its identity is currently unclear, two observations constrain possibilities. One, the maternal presence of part of the *mCherry* coding region from *T* can protect both *mCherry* and *gfp* expression (Fig. 2e), suggesting sequence-dependent recognition of unspliced pre-mRNA or DNA as the target to protect in cross progeny. Two, active *T* continues to be susceptible to mating-induced silencing regardless of protection or escape from silencing in previous generations (Supplementary Fig. 5e, f), suggesting that cross progeny need to inherit the maternal protective signal for consistent gene expression in every generation.

This work reveals that the direction of a genetic cross can strongly influence the phenotype of cross progeny (Fig. 1). Additionally, because not every sibling from a cross has the same phenotype, the choice of the sibling selected for further manipulation can have a profound effect. Subsequent transgenerational persistence of silencing can make phenotype independent of genotype, resulting in erroneous conclusions. Thus, when using

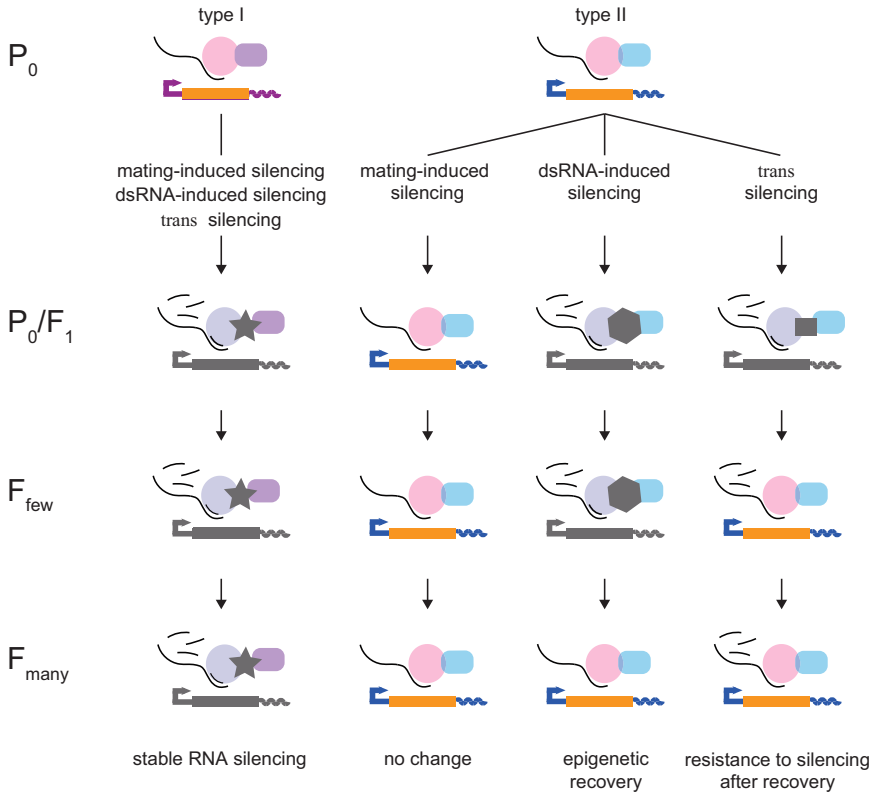

Fig. 7 Model depicting two types of genes with distinct transgenerational regulation. Type I genes stably express a recombinant sequence (*T, Tcherry, Tgfp*, etc. described in this study) and yet can undergo permanent heritable change upon RNA silencing initiated using one of multiple methods (left column). Type II genes stably express a recombinant sequence (*gtbp-1::gfp, mCherry::mex-5*, etc. described in this study) and show (1) no change when subject to mating-induced silencing, (2) show silencing for a few generations followed by epigenetic recovery when subjected to dsRNA silencing, (3) show recovery from silencing followed by resistance when subject to *trans* silencing by another silenced gene. We propose that differential recruitment of regulators to the same coding sequence during the P0/F1 generation could explain cases of permanent heritable change versus recovery from change.

genetic crosses to generate strains, both the direction of the genetic cross and choice of the individual cross progeny selected for propagation needs to be controlled for—especially when evaluating epigenetic phenomena. For example, we ensured that every cross was performed with the transgene present in the hermaphrodite to avoid initiating mating-induced silencing in our previous study examining silencing by dsRNA from neurons[47].

The transgenerational stability of mating-induced silencing with potential for recovery of expression even after hundreds of generations (Fig. 3) suggests that this mechanism could be important on an evolutionary time scale. Genes subject to such silencing could survive selection against their expression and yet be expressed in descendants as a result of either environmental changes that alter epigenetic silencing or mutations in the silencing machinery (e.g. in *hrde-1*). This mechanism thus buffers detrimental genes from selective pressures akin to how chaperones buffer defective proteins from selective pressures[51]. Many endogenous genes in *C. elegans* are silenced by HRDE-1[22,40,52,53], some of which could have been acquired when a male with the gene mated with a hermaphrodite without the gene.

There is considerable excitement in the possibility of mechanisms that perpetuate acquired changes and accelerate adaptive evolution[10,54,55]. Our analysis using RNA silencing as an example of induced epigenetic change suggests that the stability of acquired changes is likely to be limited at most genes and that particular regulatory contexts are needed to promote stable epigenetic change. By comparing two different transgenes expressed within the germline, it was proposed that the duration of transgenerational silencing depends on stochastic 'states' adopted by individual organisms[56]. However, examining the same coding sequences with different regulatory contexts (Fig. 6 and Supplementary Fig. 2) suggests that the extent of silencing is not a cell or organism level property, but rather a gene level property. Indeed, different genes within the same tissue can have different genetic requirements for RNA silencing (e.g., *bli-1* silencing but not *dpy-7* silencing requires the nuclear Argonaute NRDE-3[57]). This need for additional regulatory context for the persistence of induced changes is supported by the analysis of RNA-mediated epigenetic changes in yeast[58–60]. Thus, stable epigenetic change requires both a mechanism to copy or amplify induced changes and gene-specific regulatory contexts that recruit or activate this mechanism.

Methods

Summary. All *C. elegans* strains were generated and maintained by using standard methods[61]. Strains were grown at 20 °C, with the exception of some strains with mutations in *prg-1(-)* and *mut-16(-)*, which were grown at 15 °C (see Supplementary Table 3 for full list of strains and Supplementary Table 4 for oligonucleotides used). In all cases, matching control crosses were performed at the same temperature as test crosses. The transgene *T* (*oxSi487*) was introduced into mutant genetic backgrounds through genetic crosses using transgenic hermaphrodites and mutant males to avoid initiation of mating-induced silencing. In all crosses, transgenic genotypes are represented without repetition for simplicity (e.g. '*T*', '*Tcherry*' to refer to homozygous animals *T/T*, *Tcherry/Tcherry*, respectively). Genotypes represented as '+' are non-transgenic animals with marker mutation(s) (+/+ in colored font) or wild-type animals (+/+ or +). Cross progeny from genetic crosses were identified by balancing or marking *oxSi487* with recessive mutations in *dpy-2(e8) unc-4(e120)*, *unc-4(e120)*, *dpy-2(e8)*, *unc-8(e49) dpy-20 (e1282)* and CRISPR-Cas9 generated alleles of *dpy-10*. In some crosses, cross progeny were identified by genotyping for *oxSi487* transgene using PCR. Genome

editing was performed using Cas9 protein and sgRNAs[62] in most cases (Supplementary Table 5). Silencing of all transgenic strains was measured by imaging under identical non-saturating conditions using a Nikon AZ100 microscope. Quantification of images was performed using NIS Elements (Nikon) and ImageJ (NIH).

Nomenclature of transgenes. The letter *T* is used to specify the transgene *oxSi487* in all genetic crosses. The active or expressing allele of *oxSi487* is named as *T* and the inactive or the silenced allele of *oxSi487* is named as *iT* in parents. Genotypes that additionally include a recessive marker (*dpy* or *dpy unc*) are in blue or pink font. See Supplementary Fig. 3 for all variants of *T* and 'Genetic Crosses' for details on recessive mutations used.

Feeding RNAi and scoring associated defects. RNAi experiments were performed at 20 °C on nematode growth media plates supplemented with 1 mM IPTG (Omega Bio-Tek) and 25 µg/ml Carbenicillin (MP Biochemicals) (RNAi plates). In all cases genotype- and age-matched animals were fed control RNAi (L4440) and scored alongside as a control.

Single generation (P0 feeding RNAi). This assay was performed as described previously[15] and was used in all figures with feeding RNAi except Fig. 6c (see 'Multiple Generations' below). Briefly, L4 animals were fed dsRNA against target genes for 24 h. Some P0 animals were scored for expression while remaining were washed four times in M9 buffer and then allowed to crawl on unseeded plates for an hour to get rid of residual RNAi food. Animals were then singly placed on OP50 and 6–12 L4 animals were blindly passaged every 3–4 days to prevent starvation and to keep track of the generations post feeding. L4 animals were scored in each generation by imaging and L4 siblings were passaged to obtain progeny for the next generation. In feeds performed in Supplementary Fig. 8d and Fig. 6b, F2 animals were scored by eye.

Multiple generations (P0-F2 feeding RNAi). Multiple generations of animals (P0-F2) were subjected to feeding RNAi. F1 and F2 animals were scored at L4 stage to assess the potency of the RNAi food and L4 stage siblings were transferred to a new plate with RNAi food to prevent starvation. Similar to the P0 Feeding RNAi protocol, adults (24 h post L4) were washed four times with M9 buffer to remove residual dsRNA and transferred to a plate with OP50. Untreated progeny were then scored for inherited silencing effects. This assay was used in Fig. 6c.

Expression of dsRNA. To study inherited silencing, we expressed dsRNA from an extrachromosomal array that is mitotically unstable. Animals that express the array will have both progeny that inherit the array and those that do not. We used an array expressing dsRNA in neurons and DsRed in the pharynx from *jamEx140 [Prgef-1::gfp-dsRNA::unc-54 3′UTR* and *Pmyo-2::DsRed::unc-54 3′UTR]*[47]. Progeny that lack the array were evaluated to measure inherited silencing since parents were exposed to dsRNA from the array but progeny were not. This assay was used in Supplementary Fig. 8h.

Stages of worms that were imaged using Nikon AZ100 microscope. Fluorescence intensity of mCherry or GFP was scored after imaging L4-staged animals in all feeding RNAi experiments except in P0 RNAi fed animals and animals expressing *oma-1::gfp* or *Ppie-1::gfp::PH* (Fig. 6a and Supplementary Fig. 8a–f). Fluorescence intensity of mCherry or GFP was scored after imaging L4-staged animals represented in Figs. 1a, c–e, 2a, b, d–g, 3a, c, 4b, c (signal through sperm), d–g, 5, 6 and Supplementary Figs. 1c–k, 2a, b, 3c, 4a, 5a–i, l, n–p, 6d, e, 7a–k, 8a–h (except P0 animals). Fluorescence intensity of mCherry or GFP was scored in adults at 24 h post L4 stage in only P0 animals represented in Fig. 6a, d and in animals represented in Figs. 1e, 2a (*mut-16(-)* animals), g, 4b, c (signal through oocyte), 6b (P0 and F2), Supplementary Figs. 1a, i, 5g, i, m, 6d, 7b, c (F2 through F5), h and i. Fluorescence intensity of mCherry or GFP was scored in adults at 48 h post L4 stage represented in Fig. 4e and Supplementary Fig. 7c (F1s only).

Genetic crosses. Three L4 hermaphrodites and 7–13 males were placed on the same plate and allowed to mate in each cross plate. Cross progeny were analyzed 3–5 days after the cross plate was set up. At least two independent matings were set up for each cross. For crosses in Fig. 4f (F1s only), Supplementary Figs. 5a, c (cross with *Mos1*/+ only), h, m, n, 7c (F1s only), the required genotypes were determined by PCR (primers P1, P2, and P3) after scoring all animals and only the data from animals with the correct genotypes were plotted. In Figs. 1c–e, 2a, b, g, 3c, 4b–d, 5b and Supplementary Figs. 1c, d, j, k, 2a, 5a, d–g, 6d, e, 7a, b, d–i, *dpy-2(e8)* (~3 cM from *oxSi487*) was used as a linked marker or balancer to determine the genotype of *T*. In Figs. 1e, 2a, f, 3a, 4e, f, 5b and Supplementary Figs. 1f–h, 3d, 5a–d, i, o, p, 7c, j, k, *dpy-10(-)* (~7 cM from *oxSi487*) was used as a linked marker or balancer to determine the genotype of *T*. In Supplementary Figs. 2a, 5d, e, h, *unc-8(e49) dpy-20 (e1282)* was used as a linked marker or balancer to determine the genotype of *ax2053*. In Supplementary Fig. 5a, *unc-4(e120)* (~1.5 cM from *oxSi487*) was used as a linked marker or balancer to determine the genotype of *T*. In Fig. 2a right (control for *rde-1(-)*), *dpy-17(e164) unc-32(e189)* were used as markers to facilitate identification of cross progeny. Some crosses additionally required identification of cross progeny by genotyping of single worms, including those from Figs. 2b, g, 3c (for *ego-1(-) rrf-1(-)*), 4d, Supplementary Figs. 5a, c (*Mos1*/+ only), h, l, 6d, e, 7c, f, g. Animals from crosses with *T; prg-1(+/−)* males in Fig. 2b top or 3c were also genotyped to identify *T/+; prg-1(−/−)* or *T; prg-1(−/−)* cross progeny, respectively. In crosses from Supplementary Figs. 5f, h, 7f, i (control cross), cross progeny of the required genotype was identified by the absence or presence of pharyngeal mCherry or GFP[47], respectively. All strains analyzed for initiation (Fig. 2) and maintenance (Fig. 3) requirements had been mutant for at least two generations, except when testing the requirement for *prg-1(-)* in initiation, which was done using *prg-1(-)* animals that were mutant for one generation or *ego-1(-)* in maintenance, which was done using *ego-1(+/−)* parents.

Genetic crosses with mut-16 mutants to test for initiation of mating-induced silencing. In Fig. 2a, L4 male cross progeny were scored for only mCherry fluorescence because GFP fluorescence was difficult to assess in the single gonad arm of the L4 male germline due to gut autofluorescence.

Genetic crosses to determine if recovery of expression upon removal of wild-type hrde-1 is lost upon re-introduction of wild-type hrde-1. In Supplementary Fig. 6e, *hrde-1(-)* mutant males were mated with *iT* hermaphrodites that remained silenced for ~270 generations, resulting in cross progeny (F1) that were allowed to produce self-progeny of varying genotypes (F2) from which animals homozygous for *T* and for the wild-type or the mutant allele of *hrde-1* were assessed across generations by passaging self-progeny (F3 through F7). In addition, every generation of *hrde-1(-); T* hermaphrodites produced by self-fertilization (F2 through F6) was mated with either wild-type (+/+) or *hrde-1(-)* males to examine the possibility of re-initiation of transgenerational silencing. mCherry and GFP fluorescence was scored in heterozygous F1 cross progeny (*hrde-1(−/+)*) and in F3 or later descendants of genotypes depicted. Cross progeny (gray text) of F2 *hrde-1(-); T* hermaphrodites mated with wild-type males were not obtained despite multiple biological repeats due to experimental design. Specifically, the mating was set up in replicates between a single *hrde-1(-); T* hermaphrodite with three wild-type males at every generation, beginning from the F2 generation onwards. The selection of hermaphrodites of *hrde-1(-); T* genotype was successful only from F3 generation, because homozygous *hrde-1(-); T* could only be set up from the F2 generation, which is the very first generation the genotype of descendants can become *hrde-1 (-); T* after the cross set up at P0. As a result, F2 *hrde-1(-); T* hermaphrodites were needed for crosses, but they could not be distinguished from their *hrde-1(+); T* or *hrde-1(+/−); T* siblings on the F1 > F2 plate. The only way to determine the genotype of the hermaphrodite used was by first mating a single random hermaphrodite of unknown *hrde-1* genotype with three wild-type males, and then allowing for the F3 progeny to be laid for 3 days before sacrificing the F2 hermaphrodite for genotyping. However, by this point, the F2 hermaphrodite would be harboring wild-type sperm in its spermatheca, which could potentially confound the genotyping PCR.

Genetic crosses using animals overexpressing gpr-1. To analyze DNA-independent signals we used a recently developed tool that prevents paternal and maternal pronuclei from fusing within the zygote[19,20]. A G protein regulator, GPR-1, when overexpressed maternally, increases forces that pull on spindle poles and prevents the maternal and paternal nuclei from fusing. This allows the contents of the paternal nucleus to be inherited only into cells of the P lineage and the contents of the maternal nucleus to be inherited only into the AB lineage. By way of such non-Mendelian segregation in most cross progeny, paternal DNA is inherited into all germline cells and select somatic cells (such as the intestine and body-wall muscles) and maternal DNA is only inherited into the somatic cells (Fig. 2d). A smaller fraction of progeny either have maternal DNA in the germline and some soma, and paternal DNA in most somatic cells (Fig. 2d), or undergo Mendelian segregation with paternal and maternal DNA in all cells (data not shown). To analyze the robustness of this tool in our hands, we tested the segregation of paternal and maternal DNA using *gtbp-1::gfp*, which expressed cytoplasmic GFP in all tissues (Fig. 2d). When hermaphrodites overexpressing *gpr-1* (*gpr-1 oe*) were crossed with males carrying *gtbp-1::gfp*, >95% of cross progeny showed non-Mendelian segregation with paternal DNA inherited into cells of the P lineage (based on presence of GFP in the germline) and maternal DNA into cells of the AB lineage (based on absence of GFP in some pharyngeal cells and neurons). A much smaller population of cross progeny (<5%) showed either the inverse pattern of segregation or Mendelian segregation. We used *gtbp-1::gfp* as the marker to identify non-Mendelian cross progeny in further crosses with *gpr-1 oe*. To analyze effects of parental signals on *T* in the germline, we had to ensure that *T* (and the accompanying marker gene, *gtbp-1::gfp*) was always inherited from the male because the majority of non-Mendelian cross progeny would inherit paternal DNA into the germline. Since the transgene expressing *gpr-1* also expressed a synonymous variant of *gfp*, we used a variant of *T* i.e., either *TΔΔΔ* or *Tcherry* for further analyses to avoid GFP fluorescence from two different sources, confounding interpretation.

Genetic crosses with *Pmex-5::Tcherry::mex-5 3′utr* and *Pmex-5::Tcherry::tbb-2 3′ utr*. Integration of *Pmex-5::Tcherry::mex-5 3′utr* and *Pmex-5::Tcherry::tbb-2 3′utr* by MosSCI into the genome resulted in spontaneous silencing of the transgenes[22],

whose expression could be revived by mutation of *hrde-1*. Because parental *hrde-1* was dispensable and zygotic *hrde-1* was sufficient for initiation of mating-induced silencing (Fig. 2b), we used *Pmex-5::Tcherry::mex-5 3′utr; hrde-1(-)* or *Pmex-5::Tcherry::tbb-2 3′utr; hrde-1(-)* parent animals in reciprocal crosses to test for mating-induced silencing (Supplementary Fig. 1i). These crosses resulted in cross progeny of genotypes *Pmex-5::Tcherry::mex-5 3′utr; hrde-1(+/−)* or *Pmex-5::Tcherry::tbb-2 3′utr; hrde-1(+/−)*, respectively, which were then scored for mating-induced silencing.

Generation and maintenance of *iT* and *iT*Δ strains. To make hermaphrodites with *iT* linked to a *dpy* marker, AMJ581 hermaphrodites were mated with N2 males to generate cross progeny males that all show bright mCherry fluorescence from *oxSi487*. These males were then mated with N2 hermaphrodites to give cross progeny (F1) with undetectable mCherry fluorescence. F1 animals were allowed to give progeny (F2) that were homozygous for *oxSi487* as determined by the homozygosity of a linked *dpy-2(e8)* mutation. One such F2 animal was isolated to be propagated as the *iT* strain (AMJ692).

To make males with *iT*, *dpy-17(e164) unc-32(e189)* hermaphrodites were mated with EG6787 males to generate cross progeny (F1) hermaphrodites with undetectable mCherry fluorescence. These cross progeny were allowed to have self-progeny (F2) that are homozygous for *oxSi487*. Two such F2s were isolated to be propagated as two different *iT* lines. One of these was designated as AMJ724 and used for further experiments. These strains maintained the silencing of *oxSi487* and were heat-shocked to produce males. Genotypes of *iT* strains were verified using PCR.

To make hermaphrodites with *iTΔ* linked to a *dpy* marker, AMJ767 hermaphrodites were mated with N2 males to generate cross progeny males with bright mCherry fluorescence. These males were then mated with GE1708 hermaphrodites to give cross progeny (F1) with undetectable mCherry fluorescence. F1 animals were allowed to give descendants that are homozygous for *TΔ* as determined by genotyping for *jamSi20*. A homozygous descendant was isolated to be propagated as the *iTΔ* strain (AMJ917). Genotypes of *iTΔ* strains were verified using PCR.

AMJ692 was used to test for recovery of gene expression ~150 generations after it was made. This generation time was estimated as follows: worms were passaged every 3.5 days for 143 generations over a period of 556 days, except for three intervals when they were allowed to starve and larvae were recovered after starvation. These intervals with recovery from starvation spanned a total of ~6 generations over 49 days. Thus, the total number of generations = 143 + ~6 = ~150 generations. The generation times for other *iT* strains, AMJ724, AMJ552, and AMJ844, were similarly estimated. *iT* strain silenced for >150 generations was used to test the requirements for RNAi factors in the maintenance of transgenerational silencing.

CRISPR-Cas9 mediated editing of *oxSi487*. To generate edits in *oxSi487*, Cas9-based genome editing with a co-conversion strategy[62] was used. Guide RNAs were amplified from pYC13 using primers listed in Supplementary Table 5. The amplified guides were purified (PCR Purification Kit, Qiagen) and tested in vitro for cutting efficiency (Cas9, New England Biolabs catalog no. M0386S). For most edits, homology template for repair (repair template) was made from gDNA using Phusion High Fidelity polymerase (New England Biolabs catalog no. M0530S) and gene-specific primers to separately amplify regions precisely upstream and downstream of the site to be edited. The two PCR products were used as templates to generate the entire repair template using Phusion High Fidelity Polymerase and the fused product was purified using NucleoSpin Gel and PCR Clean-up (Macherey-Nagel, catalog no. 740609.250). Homology templates to generate *TΔΔ* and *dpy-10(-)* were single-stranded DNA oligos. Wild-type animals were injected with 0.12–12.9 pmol/µl of guide RNAs, 0.08–1.53 pmol/µl of homology repair template to make edits in *T* and in *dpy-10* and 1.6 pmol/µl of Cas9 protein (PNA Bio catalog no. CP01). In animals with *TΔΔ* edit, *Punc-119* deletion resulted in Unc animals due to the *unc-119(ed3)* mutation in the background of EG6787, suggesting that a functional transcript was not made from the remaining part of the rescuing *Punc-119::unc-119::unc-119 3′utr* insertion at *ttTi5605*. Edits were verified using PCR and Sanger sequencing. For additional details on specific reagents, see Supplementary Table 5.

CRISPR-Cas9 mediated insertion. To generate large insertions, the Cas9-based editing protocol was adapted from ref. [63]. The following mix was injected into HT1593 animals: 42–55 ng/µl plasmid expressing Cas9 protein and sgRNA sequence specific to chromosome II site near *ttTi5605* (pDD122) or chromosome I site near *ttTi4348* (pSD18), 105 ng/µl of pMA122 (*Phsp-16.41::peel-1::tbb-2utr*), 42–55 ng/µl of repair plasmid for insertion of *Tcherry*^{Crispr} (*jamSi38, jamSi40, jamSi41*) or *Tcherry* I (*jamSi56*). Following injection, animals were singled out and the plate was allowed to crowd until starvation. Starved plates were heat-shocked at 34 °C for 2.5–4 h and heat-shocked animals were allowed to recover overnight. Non-Unc animals that survived the heat shock were singled out, propagated and screened for the edit using PCR. Single-copy insertions were then verified in isolates that screened positive for the edit after extraction of genomic DNA.

Mos-mediated single-copy insertion (MosSCI). To generate large insertions, the MosSCI protocol was adapted from ref. [11]. The following mix was injected into EG4322 animals: 50–55 ng/µl plasmid expressing Mos1 transposase (pCFJ601: *Peft-3::mos1 transposase::tbb-2utr*), 105 ng/µl of pMA122 (*Phsp-16.41::peel-1::tbb-2utr*), 50–55 ng/µl of repair plasmid for insertion of *Tcherry*, *Tgfp*, *TcherryΔpi*, *Tcherry::tbb-2 3′ utr* or *Tcherry::mex-5 3′ utr* into chromosome II near *ttTi5605* insertion site. Following injection, animals were singled out and the plate was allowed to crowd until starvation. Starved plates were heat-shocked at 34 °C for 2.5–4 h and heat-shocked animals were allowed to recover overnight. Non-Unc animals that survived the heat shock were singled out, propagated and screened for the edit using PCR. Single-copy insertions were then verified in isolates that screened positive for the edit after extraction of genomic DNA.

Quantitative RT-PCR (RT-qPCR). Total RNA was isolated using TRIzol (Fisher Scientific) from 50 to 100 µl pellets of mixed-stage animals. Three biological replicates were isolated by pelleting animals from three different plates of the same strain. RNA was extracted by chloroform extraction, precipitated using isopropanol, washed with ethanol and resuspended in 20–30 µl of nuclease-free water. 2–5 µl of resuspended RNA was set aside to run on a gel and the remaining was DNase-treated in DNase buffer (100 mM Tris-HCl, pH 8.5, 5 mM $CaCl_2$, 25 mM $MgCl_2$), and incubated with 0.25 µl DNase I (New England Biolabs, 2 units/µl) at 37 °C for 60 min followed by heat inactivation at 75 °C for 10 min. Pre- and post-DNase treated RNA were run on a 1% agarose gel to check for the presence of rRNA bands. RNA concentration was measured and equal amounts (500–5000 ng) of RNA were converted to cDNA using SuperScript III Reverse Transcriptase (Invitrogen catalog no. 18080044) with two-fold reduced quantities compared to manufacturer's recommendations. For cDNA conversion, 3–5 technical replicates were done for each biological replicate of each sample and RT primer P82 was used for *R11A8.1*, P176 for *tbb-2* pre-mRNA, P177 *for tbb-2* mRNA, P83 for *mCherry* pre-mRNA P84 for *mCherry* mRNA, P78 for *gfp* pre-mRNA, and P85 for *gfp* mRNA. PCR was performed with the cDNA as template and using LightCycler 480 SYBR Green I Mastermix (Roche catalog no. 4707516001) guidelines according to the manufacturer's recommendations. For analysis of pre-mRNA, primers P86 and P87 were used for *R11A8.1*, P88 and P89 were used for *tbb-2*, P93 and P179 were used for *mCherry*, and P96 and P97 were used for *gfp*. For analysis of mRNA, primers P94 and P95 were used for *tbb-2*, P90 and P91 were used for *mCherry*, and P98 and P99 were used for *gfp*. Fold change was calculated using 2^{-Ct} values and samples were normalized to total RNA.

Three (Supplementary Fig. 2c) to six (Supplementary Fig. 6c) independent biological replicates were typically measured, with each biological replicate being the median of three to five technical replicates. A scaled scatter plot was used to depict the relative abundance of pre-mRNA and mRNA for each biological replicate. RNA abundance was estimated as proportional to 2^{-Ct} and target transcripts were normalized to total RNA to obtain relative abundance.

Chromatin immunoprecipitation-qPCR (ChIP-qPCR). This protocol was adapted from ref. [64] 300–500 µl of frozen mixed-stage worm pellets were used for each ChIP experiment. Three biological replicates were done for every strain and worms from each sample were split into 100 µl pellets. Frozen pellets were crushed by grinding with a mortar and pestle. Crushed pellets were resuspended in 1 ml buffer A (15 mM HEPES-Na, pH 7.5, 60 mM KCl, 15 mM NaCl, 0.15 mM beta-mercaptoethanol (CALBIOCHEM catalog no. 444203), 0.15 mM spermine (Sigma-Aldrich catalog no. S3256-1G), 0.15 mM spermidine (Sigma-Aldrich catalog no. S2626-1G), 0.34 M sucrose, 1X HALT protease (ThermoScientific catalog no. 78440) and phosphatase inhibitor cocktail (ThermoScientific catalog no. 78440)). To crosslink, formaldehyde was added to a final concentration of 2%, and incubated at room temperature for 15 min. The formaldehyde was quenched by adding 0.1 ml 1 M Tris HCl (pH 8.0). The lysate was spun at 15,000 × *g* for 1 min at 4 °C. The resulting pellets were washed twice with ice-cold buffer A by centrifuging between washes. The pellets were resuspended in 0.3 ml buffer A with 2 mM $CaCl_2$. Micrococcal nuclease (Roche catalog no. M0247S) was added to a final concentration of 0.3 U/µl and incubated for 5 min at 37 °C (the tubes were inverted several times per minute). EGTA to a final concentration of 20 mM was added to stop the digestion reaction and samples were centrifuged at 15,000 × *g* for 1 min at 4 °C, followed by washing the resulting pellets with 300 µl of ice-cold RIPA buffer (1X PBS, 1% NP40 (Spectrum catalog no. T1279), 0.5% sodium deoxycholate (Sigma-Aldrich catalog no. D6750-10G), 0.1% SDS, 1X HALT protease and phosphatase inhibitor and 2 mM EGTA (Sigma-Aldrich catalog no. E3889-10G)). Samples were centrifuged at 15,000 × *g* for 1 min at 4 °C. The pellet was resuspended after washes in 0.8 ml ice-cold RIPA buffer, and solubilized by shearing using the Covaris[65]. Samples were kept on ice at all times except during shearing. All sheared lysates for each biological replicate were pooled and split equally to precipitate for all chromatin marks being measured. Sheared lysates were centrifuged at 15,000 × *g* for 2 min. 80 µl of the supernatant was set aside at −20 °C for "input" libraries and the remaining supernatant was used for IP. Antibodies were chosen based on their efficiency in *C. elegans*[66]. One of 2 µg of anti-H3 antibody (Abcam, ab1791), 3 µg of anti-H3K9me1 antibody (Abcam, ab8896), 3 µg of anti-H3K9me2 antibody (Abcam, ab1220) or 2 µg of anti-H3K9me3 antibody (Abcam, ab8898) was added and agitated gently at 4 °C overnight. 50 µl of protein A Dynabeads (10% slurry in 1x PBS buffer) was added and mixed by shaking for 2 h

at 4 °C. The beads were then washed four times (4 min/wash) with ice-cold 600 µl LiCl washing buffer (100 mM Tris HCl, pH 8, 500 mM LiCl, 1% NP-40, 1% Sodium deoxycholate). A magnetic stand (DynaMag-2 Magnet, Thermo Scientific) was used to pellet beads and the supernatant was discarded after every wash. Beads and input were incubated with 450 µl worm lysis buffer (0.1 M Tris HCl, pH 8, 100 mM NaCl, 1% SDS) containing 200 µg/ml proteinase K at 65 °C for 4 h with agitation every 30 min to elute the immunoprecipitated nucleosome and reverse crosslinks. DNA was isolated by organic extraction and precipitation. DNA obtained was measured by qPCR using LightCycler 480 SYBR Green I Mastermix according to the manufacturer's recommendations (see PCR portion of qRT-PCR method for details and pre-mRNA, or equivalently DNA, primers for *R11A8.1, mCherry* and *gfp*). Fold change was calculated using $2^{-\Delta\Delta Ct}$ method and samples were normalized to co-immunoprecipitated control gene, *R11A8.1*.

Single-molecule fluorescence in situ hybridization (smFISH). Custom Stellaris FISH probes were designed against only exons of *mCherry* and *gfp* sequence from *oxSi487* using the web-based Stellaris FISH Probe Designer from Biosearch Technologies (www.biosearchtech.com/stellarisdesigner). Any probe design expected to span exon-exon junctions was avoided to allow for the equivalent detection of both mature and nascent transcripts. Standard *C. elegans* smFISH protocol followed by 4′,6-diamidino-2-phenylindole (DAPI) staining was used as described[67,68]. The probe blend to detect *mCherry* includes 25 exon-specific probes (P112 through P136) each tagged with Quasar 670 dye and antisense to *mCherry* RNA. The probe blend to detect *gfp* includes 26 exon-specific probes (P137 through P162) each tagged with Quasar 670 dye and antisense to *gfp* RNA. The adapted smFISH protocol is as follows: 50–100 L4 animals or adult animals ~24 h post L4 (Fig. 3b, Supplementary Figs. 2e, 4b, 6a) were paralyzed in 400 µl 1X Phosphate Buffered Saline 0.1% Tween-20 (PBST, Amresco, catalog number C999G23 K875-500ML) containing 0.25 mM levamisole for dissection or whole animals younger than L4 (Supplementary Fig. 4b) were washed in 1X PBST and fixed in 1 ml fix solution (3.7% formaldehyde (Amresco, catalog number 0493-500 ML) in 1X PBST) on a nutator at room temperature. Fixation time ranged between 15 and 45 min across different trials. Samples were washed in 1X PBST, incubated for 10 min in permeabilizing solution (0.1% Triton X-100 in 1 ml of 1X Gibco PBS pH 7.4 (Thermofisher Scientific, catalog number 10010023)), washed twice in PBST and resuspended in 1 ml 70% ethanol and incubated between 1 and 7 days at 4 °C. Fixed animals were then equilibrated and washed with wash buffer (2X Sodium Saline Citrate (SSC, Sigma Aldrich, catalog number 11666681001), 10% formamide (Millipore Sigma, catalog number 4650-500 ML or Amresco, catalog number 0314-500 ML), 0.01% Tween-20 (Fisher Scientific, catalog number BP337-100)) hybridized with 0.025 µM probes diluted in hybridization buffer (10% dextran sulfate (Sigma Aldrich, catalog number D8906-5G), 2X SSC, 10% formamide) for 48 h in a 37 °C rotator in the dark. Hybridized animals were then washed in wash buffer, incubated with DAPI solution (1 µg/ml DAPI in wash buffer) for 30–120 min protected from light, washed twice in wash buffer for 5 min each in a rotator and used for mounting. Worms were resuspended and incubated for 5 min at room temperature or up to 6 h at 4 °C in a GLOX buffer without enzymes (2X SSC, 1% glucose (Fisher Scientific, catalog number D16-500), 0.1 M Tris pH 8.0 (Thermofisher Scientific, catalog number AM9855G) in RNase-free water), treated with freshly made GLOX-enzyme buffer (100 µl GLOX buffer, 1 µl glucose oxidase (MP Biomedicals/Fisher Scientific, catalog number 0219519610), 3.7 mg/ml, 1 µl catalase (Fisher Scientific, catalog number S25239A), 1 µl 200 mM Trolox (Acros Organics/Fisher Scientific, catalog number 218940050)) and prepared for imaging by dropping the sample on a coverslip followed by placing and sealing on a microscope slide with a mix of Vaseline, lanoline, and paraffin. All samples within a single experimental set included control strains and were subjected to identical conditions (e.g. incubation times) to minimize variability within the experiment. RNase-free conditions were used in all smFISH experiments.

AMJ1259, AMJ1260, and AMJ1261 females were mated with AMJ1045 or EG6787 males and extruded gonads of cross progeny hermaphrodites staged at ~24 h post L4 were subjected to smFISH protocol using *mCherry* probes (Supplementary Fig. 4b). For Supplementary Fig. 6a, b, extruded gonads of EG6787 ("*T*"), AMJ552 ("*iT*"), and N2 ("wild type") adult hermaphrodites staged at ~24 h post L4 were subjected to the smFISH protocol using either *mCherry* or *gfp* probes. For Supplementary Fig. 2e top row, extruded gonads of EG6787, AMJ1170, JH3323, and N2 adult hermaphrodites staged at ~24 h post L4 were subjected to the smFISH protocol using *mCherry* probes alone. For Supplementary Fig. 2e bottom row, extruded gonads of EG6787, AMJ1195, JH3197, and N2 adult hermaphrodites staged at ~24 h post L4 were subjected to the smFISH protocol using *gfp* probes alone.

Confocal microscopy to image single-molecule RNA signals or protein fluorescence. Images were taken using Leica SP5 confocal microscope with the ×63 oil immersion objective at 500% digital zoom for smFISH samples and 400% digital zoom to capture protein fluorescence. A single confocal slice of 0.5 µm thickness was captured at regions corresponding to distal, loop, or proximal regions of the dissected gonad. The Z position was oriented to be the same plane as the nucleus of the distal tip cell for all three regions imaged in most dissected gonads. To image whole worms between L2 and L3 stages for smFISH, a Z stack of a part of the germline that could be accommodated within the field of view at the same magnification as was used for dissected gonads was imaged with a step size of 0.5–1 µm and displayed as a maximum intensity projection. Brightfield and DAPI images were taken using photomultiplier tubes whereas *mCherry* and *gfp* RNA and protein fluorescence images were taken using Hybrid Detector (HyD). For both smFISH and protein fluorescence, the XY laser scan was set to 400 Hz and imaged at a resolution of 1024 × 1024 pixels. Quasar 670 probes were excited using Alexa 633 nm laser (50% White Light Laser) and signal was detected between 650 and 715 nm with the pinhole at 105.05 µm. DAPI was excited using 405 nm (3–30% UV laser) and signal was acquired between 422 and 481 nm with the pinhole at 95.52 µm. For Quasar 670 and mCherry or GFP protein fluorescence, a line average of 6–8 with 1–2 frame accumulation was used. For DAPI, 3–4 line average was used.

Quantification of silencing and measurement of fluorescence intensity. To classify fluorescence intensity after imaging, animals of the L4 stage or 24 h after the L4 stage were mounted on a slide after paralyzing the worm using 3 mM levamisole (Sigma-Aldrich, Cat# 196142), imaged under non-saturating conditions (Nikon AZ100 microscope and Photometrics Cool SNAP HQ^2 camera), and binned into three groups—bright, dim and off. A C-HGFI Intensilight Hg Illuminator was used to excite GFP or Dendra2 (filter cube: 450–490 nm excitation, 495 dichroic, and 500–550 nm emission), or mCherry or RFP (filter cube: 530–560 nm excitation, 570 dichroic, and 590–650 nm emission). Sections of the gonad that are not obscured by autofluorescence from the intestine were examined to classify GFP and mCherry fluorescence from *oxSi487*. Autofluorescence was appreciable when imaging GFP or Dendra2 but not when imaging mCherry.

In some cases, fluorescence intensity within the germline was scored by eye without imaging at L4 stage in Fig. 6c and Supplementary Fig. 8h or at 24 h after the L4 stage in Supplementary Figs. 5e, f (to find bright male F1s), 7b (to find off male F1s) and 8a at fixed magnification and zoom using the Olympus MVX10 fluorescent microscope without imaging.

To quantitatively measure protein fluorescence of mCherry and GFP from *T* imaged using Nikon AZ100 as described above (Fig. 1c) and protein fluorescence from other transgenes (Figs. 4g, 5b left and Supplementary Fig. 8a–f), regions of interest (ROI) were marked using either NIS elements or ImageJ (NIH) and the intensity was measured. Background was subtracted from the measured intensity for each image. For Figs. 1c, 4g, 5b and Supplementary Fig. 8a–f, fluorescence intensity was measured as x − b, where x = mean intensity of ROI and b = mean intensity of background. The obtained intensity values were converted to a $\log_2$ scale and plotted.

In experiments with feeding RNAi, target gene (*gfp*) and control RNAi fed animals for each strain were imaged at the same exposure. Control and experimental animals were all imaged at non-saturating conditions either at a fixed exposure or by setting exposure to their respective controls. Previous reports have suggested that the pharynx, neurons, and vulval muscles can be resistant to silencing by dsRNA[69,70] and hence were not included in our scoring.

All images being compared were adjusted identically using Adobe Photoshop for display.

Quantification of expression from Tgfp. Insertion of *Tgfp* into the genome resulted in variable GFP expression in all animals. However, in the case of mating-induced silencing, silenced animals displayed no detectable silencing of GFP as measured by quantification. To quantitatively measure fluorescence of GFP from *Tgfp* (Supplementary Fig. 1f), ROI of the germline that excluded the intestine was marked using Fiji (NIH) and the intensity was measured. An area outside the worm within the same image was measured for background intensity. The mean fluorescence intensity from *Tgfp* expression was calculated by subtracting the background intensity from measured GFP intensity as described above.

Quantification of smFISH signals. Leica images (.lif format) were opened in Fiji (NIH), display range was adjusted, background was subtracted twice sequentially using a rolling ball radius of 50 pixels (~2.7 µm), threshold was adjusted, and number of RNA dots ≤250 object voxels in size were quantified per unit area. All parameters were adjusted identically among images of strains being compared. All images being compared were adjusted identically using Adobe Photoshop for display.

Colocalization between smFISH signals of *mCherry* and *gfp* transcripts (Fig. 1b and Supplementary Fig. 1b) was done using Colocalization Colormap plugin within Fiji. The plugin finds the correlation between pixel intensities from the same spatial coordinates between two images using the following formula: [(intensity of the pixel in *mCherry* RNA image − average pixel intensity in *mCherry* RNA image) × (intensity of the pixel in *gfp* RNA image − average pixel intensity in *gfp* RNA image)]/[(maximum pixel intensity in *mCherry* RNA image − average pixel intensity in *mCherry* RNA image) × (maximum pixel intensity in *gfp* RNA image − average pixel intensity in *gfp* RNA image)]. The values of the correlation will range between 1(most colocalized) to −1(least colocalized) and is represented by a scale in the figure. The original mCherry images contained fluorescence signal from both mCherry::H2B (which represents nuclear chromatin) and from *mCherry* RNA probed with Quasar 570 probes. These images captured both mCherry protein and RNA signals because of a large overlap between fluorescence spectra from mCherry and Quasar 570. Using these images, we obtained an approximation of *mCherry* RNA signal by subtracting the mCherry::H2B signal using DAPI images whose

signals coincided with mCherry::H2B signals, but not with *mCherry* RNA signals. The resulting subtracted image (mCherry protein + *mCherry* RNA − DAPI) was then used to examine the extent of colocalization between *mCherry* RNA and *gfp* RNA (Fig. 1b and Supplementary Fig. 1b).

Statistical analyses, reproducibility, and plotting. For each figure, χ^2 test was used to compare data as indicated in figure legends except in cases where only one category (bright or silenced) was present in both datasets being compared, in which case Wilson's estimates for proportions was used. All comparisons shown include comparisons between only GFP fluorescence or only mCherry fluorescence within each experiment. Significance for ChIP and qRT-PCR experiments and crosses were compared using Student's *t*-test (Fig. 2a (*Tgfp*), Supplementary Figs. 1f, 2c, 6c, f, g). Matlab, R, and Microsoft Excel were used to plot fluorescence intensity (bar chart, rose plot, box and whisker plot, dot plot, line plot) and qPCR data. Exact *P* values are provided in Source Data. The biological replicates for each experiment are as indicated in figures, figure legends, and methods. Experiments were performed once or the number of times indicated within Source Data as independent cross plates for genetic crosses. Critical experiments were replicated by multiple authors (mating-induced silencing by 8 authors, *pgl-1*-dependent silencing by two authors). In these cases, results were reproducible. Representative images presented were from different imaging sessions, where similar patterns were observed with number of imaging sessions as indicated here: Fig. 1a shows representative images from >10 sessions of >10 animals; Fig. 1c shows representative images from 1 session of 5–11 animals of each category; Fig. 2c mosaic expression from 2 sessions and 92 animals (mosaicism was also tested with *sur-5::gfp*, which showed similar results); Fig. 6a representative RNAi from 1 session and 7 animals; Fig. 1b and Supplementary Fig. 1b representative figure of colocalization from 2 sessions and 6 gonads.

Reporting summary. Further information on research design is available in the Nature Research Reporting Summary linked to this article.

Data availability

All data generated or analyzed during this study are included in this published article (and its Supplementary Information files). More than 10,000 images were generated during this study to document expression levels. These images and other data supporting the finding of this study are available from the authors upon reasonable request. Source data are provided for this paper at https://doi.org/10.6084/m9.figshare.14642820.

Received: 21 December 2020; Accepted: 29 May 2021;
Published online: 09 July 2021

References

1. Jose, A. M. Replicating and cycling stores of information perpetuate life. *BioEssays* **40**, 1700161 (2018).
2. Jose, A. M. A framework for parsing heritable information. *J. R. Soc. Interface* **17**, 20200154 (2020).
3. Jose, A. M. Heritable epigenetic changes alter transgenerational waveforms maintained by cycling stores of information. *BioEssays* **42**, 1900254 (2020).
4. Beisson, J. & Sonneborn, T. M. Cytoplasmic inheritance of the organization of the cell cortex in *Paramecium aurelia*. *Proc. Natl Acad. Sci. USA* **53**, 275–282 (1965).
5. Halfmann, R. et al. Prions are a common mechanism for phenotypic inheritance in wild yeasts. *Nature* **482**, 363–368 (2012).
6. Catania, S. et al. Evolutionary persistence of DNA methylation for millions of years after ancient loss of a de novo methyltransferase. *Cell* **180**, 263–277 (2020).
7. Duempelmann, L., Skribbe, M. & Bühler, M. Small RNAs in the transgenerational inheritance of epigenetic information. *Trends Genet* **36**, 203–214 (2020).
8. Pak, J. & Fire, A. Distinct populations of primary and secondary effectors during RNAi in *C. elegans*. *Science* **315**, 241–244 (2007).
9. Shukla, A. et al. poly(UG)-tailed RNAs in genome protection and epigenetic inheritance. *Nature* **582**, 283–288 (2020).
10. Cavalli, G. & Heard, E. Advances in epigenetics link genetics to the environment and disease. *Nature* **571**, 489–499 (2019).
11. Frøkjær-Jensen, C., Davis, M. W., Ailion, M. & Jorgensen, E. M. Improved Mos1-mediated transgenesis in *C. elegans*. *Nat. Methods* **9**, 117–118 (2012).
12. Diag, A., Schilling, M., Klironomos, F., Ayoub, S. & Rajewsky, N. Spatiotemporal m(i)RNA architecture and 3' UTR regulation in the *C. elegans* germline. *Dev. Cell* **47**, 785–800 (2018).
13. Merritt, C., Rasoloson, D., Ko, D. & Seydoux, G. 3' UTRs are the primary regulators of gene expression in the *C. elegans* germline. *Curr. Biol.* **14**, 1476–1482 (2008).
14. Frøkjær-Jensen, C. et al. An abundant class of non-coding DNA can prevent stochastic gene silencing in the *C. elegans* germline. *Cell* **166**, 343–357 (2016).
15. Marré, J., Traver, E. C. & Jose, A. M. Extracellular RNA is transported from one generation to the next in *Caenorhabditis elegans*. *Proc. Natl Acad. Sci. USA* **113**, 12496–12501 (2016).
16. Wang, E. & Hunter, C. P. SID-1 functions in multiple roles to support parental RNAi in *Caenorhabditis elegans*. *Genetics* **207**, 547–557 (2017).
17. Almeida, M. V., Andrade-Navarro, M. A. & Ketting, R. F. Function and evolution of nematode RNAi pathways. *Noncoding RNA* **5**, 8 (2019).
18. Zhang, D. et al. The piRNA targeting rules and the resistance to piRNA silencing in endogenous genes. *Science* **359**, 587–592 (2018).
19. Besseling, J. & Bringmann, H. Engineered non-Mendelian inheritance of entire parental genomes in *C. elegans*. *Nat. Biotechnol.* **34**, 982–986 (2016).
20. Artiles, K. L., Fire, A. Z. & Frøkjær-Jensen, C. Assessment and maintenance of unigametic germline inheritance for *C. elegans*. *Dev. Cell* **48**, 827–839 (2019).
21. Phillips, C. M., Montgomery, T. A., Breen, P. C. & Ruvkun, G. MUT-16 promotes formation of perinuclear mutator foci required for RNA silencing in the *C. elegans* germline. *Genes Dev.* **26**, 1433–1444 (2012).
22. Shirayama, M. et al. piRNAs initiate an epigenetic memory of nonself RNA in the *C. elegans* germline. *Cell* **150**, 65–77 (2012).
23. Conine, C. C. et al. Argonautes promote male fertility and provide a paternal memory of germline gene expression in *C. elegans*. *Cell* **155**, 1532–1544 (2013).
24. Wedeles, C. J., Wu, M. Z. & Claycomb, J. M. Protection of germline gene expression by the *C. elegans* argonaute CSR-1. *Dev. Cell* **27**, 664–671 (2013).
25. Seth, M. et al. The C. elegans CSR-1 argonaute pathway counteracts epigenetic silencing to promote germline gene expression. *Dev. Cell* **27**, 656–663 (2013).
26. Campbell, A. C. & Updike, D. L. CSR-1 and P granules suppress sperm-specific transcription in the *C. elegans* germline. *Development* **142**, 1745–1755 (2015).
27. Gerson-Gurwitz, A. et al. A small RNA-catalytic argonaute pathway tunes germline transcript levels to ensure embryonic divisions. *Cell* **165**, 396–409 (2016).
28. Claycomb, J. M. et al. The Argonaute CSR-1 and its 22G-RNA cofactors are required for holocentric chromosome segregation. *Cell* **139**, 123–134 (2009).
29. van Wolfswinkel, J. C. et al. CDE-1 affects chromosome segregation through uridylation of CSR-1-bound siRNAs. *Cell* **139**, 135–148 (2009).
30. Johnson, C. L. & Spence, A. M. Epigenetic licensing of germline gene expression by maternal RNA in *C. elegans*. *Science* **333**, 1311–1314 (2011).
31. Ouyang, J. P. T. et al. P granules protect RNA interference genes from silencing by piRNAs. *Dev. Cell* **50**, 716–728 (2019).
32. Dodson, A. E. & Kennedy, S. Germ granules coordinate RNA-Based epigenetic inheritance pathways. *Dev. Cell* **50**, 704–715 (2019).
33. Ashe, A. et al. piRNAs can trigger a multigenerational epigenetic memory in the germline of *C. elegans*. *Cell* **150**, 88–99 (2012).
34. Lee, H. C. et al. C. elegans piRNAs mediate the genome-wide surveillance of germline transcripts. *Cell* **150**, 78–87 (2012).
35. Luteijn, M. J. et al. Extremely stable Piwi-induced gene silencing in *Caenorhabditis elegans*. *EMBO J.* **31**, 3422–3430 (2012).
36. Bagijn, M. P. et al. Function, targets, and evolution of *Caenorhabditis elegans* piRNAs. *Science* **337**, 574–578 (2012).
37. Smardon, A. et al. EGO-1 is related to RNA-directed RNA Polymerase and functions in germ-line development and RNA interference in *C. elegans*. *Curr. Biol.* **10**, 167–178 (2000).
38. Vought, V. E., Ohmachi, M., Lee, M. H. & Maine, E. M. EGO-1, a putative RNA-directed RNA polymerase, promotes germline proliferation in parallel with GLP-1/notch signaling and regulates the spatial organization of nuclear pore complexes and germline P granules in *Caenorhabditis elegans*. *Genetics* **170**, 1121–1132 (2005).
39. Selker, E. U. & Stevens, J. N. DNA methylation at asymmetric sites is associated with numerous transition mutations. *Proc. Natl Acad. Sci. USA* **82**, 8114–8118 (1985).
40. Buckley, B. A. et al. A nuclear Argonaute promotes multigenerational epigenetic inheritance and germline immortality. *Nature* **489**, 447–451 (2012).
41. Towbin, B. D. et al. Step-wise methylation of histone H3K9 positions heterochromatin at the nuclear periphery. *Cell* **150**, 934–947 (2012).
42. Spracklin, G. et al. The RNAi inheritance machinery of *Caenorhabditis elegans*. *Genetics* **206**, 1403–1416 (2017).
43. Schwartz-Orbach, L. et al. *Caenorhabditis elegans* nuclear RNAi factor SET-32 deposits the transgenerational histone modification, H3K23me3. *eLife* **9**, e54309 (2020).
44. Perales, R. et al. Transgenerational epigenetic inheritance is negatively regulated by the HERI-1 chromodomain protein. *Genetics* **210**, 1287–1299 (2018).
45. Greenstein, D. Control of oocyte meiotic maturation and fertilization. WormBook, ed. The *C. elegans* Research Community, WormBook. https://doi.org/10.1895/wormbook.1.53.1, http://www.wormbook.org (2005).

46. Almeida, M. V., de Jesus Domingues, A. M. & Ketting, R. F. Maternal and zygotic gene regulatory effects of endogenous RNAi pathways. *PLoS Genet* **15**, e1007784 (2019).
47. Devanapally, S., Ravikumar, S. & Jose, A. M. Double-stranded RNA made in *C. elegans* neurons can enter the germline and cause transgenerational gene silencing. *Proc. Natl Acad. Sci. USA* **112**, 2133–2138 (2015).
48. Timmons, L. & Fire, A. Specific interference by ingested dsRNA. *Nature* **395**, 854 (1998).
49. Kennedy, S., Wang, D. & Ruvkun, G. A conserved siRNA-degrading RNase negatively regulates RNA interference in *C. elegans*. *Nature* **427**, 645–649 (2004).
50. Lev, I. et al. MET-2-dependent H3K9 methylation suppresses transgenerational small RNA inheritance. *Curr. Biol.* **27**, 1138–1147 (2017).
51. Rutherford, S. L. & Lindquist, S. Hsp90 as a capacitor for morphological evolution. *Nature* **396**, 336–342 (1998).
52. Ni, J. Z. et al. A transgenerational role of the germline nuclear RNAi pathway in repressing heat stress-induced transcriptional activation in *C. elegans*. *Epigenetics Chromatin* **9**, 3 (2016).
53. Akay, A. et al. The helicase Aquarius/EMB-4 is required to overcome intronic barriers to allow nuclear RNAi pathways to heritably silence transcription. *Dev. Cell* **42**, 241–255 (2017).
54. Klosin, A., Casas, E., Hidalgo-Carcedo, C., Vavouri, T. & Lehner, B. Transgenerational transmission of environmental information in *C. elegans*. *Science* **356**, 320–323 (2017).
55. van der Graaf, A. et al. Rate, spectrum, and evolutionary dynamics of spontaneous epimutations. *Proc. Natl Acad. Sci. USA* **112**, 6676–6681 (2015).
56. Houri-Ze'evi, L. et al. A tunable mechanism determines the duration of the transgenerational small RNA inheritance in *C. elegans*. *Cell* **165**, 88–99 (2016).
57. Raman, P., Zaghab, S. M., Traver, E. C. & Jose, A. M. The double-stranded RNA binding protein RDE-4 can act cell autonomously during feeding RNAi in *C. elegans*. *Nucleic Acids Res.* **45**, 8463–8473 (2017).
58. Yu, R., Wang, X. & Moazed, D. Epigenetic inheritance mediated by coupling of RNAi and histone H3K9 methylation. *Nature* **558**, 615–619 (2018).
59. Kowalik, K. M. et al. The Paf1 complex represses small-RNA-mediated epigenetic gene silencing. *Nature* **520**, 248–252 (2015).
60. Duempelmann, L. et al. Inheritance of a phenotypically neutral epimutation evokes gene silencing in later generations. *Mol. Cell* **74**, 534–541 (2019).
61. Brenner, S. The genetics of *Caenorhabditis elegans*. *Genetics* **77**, 71–94 (1974).
62. Arribere, J. A. et al. Efficient marker-free recovery of custom genetic modifications with CRISPR/Cas9 in *Caenorhabditis elegans*. *Genetics* **198**, 837–846 (2014).
63. Dickinson, D. J., Ward, J. D., Reiner, D. J. & Goldstein, B. Engineering the *Caenorhabditis elegans* genome using Cas9-triggered homologous recombination. *Nat. Methods* **10**, 1028–1034 (2013).
64. Guang, S. et al. An Argonaute transports siRNAs from the cytoplasm to the nucleus. *Science* **321**, 537–541 (2008).
65. Gushchanskaia, E. R., Esse, R., Ma, Q., Lau, N. C. & Grishok, A. Interplay between small RNA pathways shapes chromatin landscape in *C. elegans*. *Nucleic Acids Res.* **47**, 5603–5616 (2019).
66. Egelhofer, T. A. et al. An assessment of histone-modification antibody quality. *Nat. Struct. Mol. Biol.* **18**, 91–93 (2011).
67. Lee, C. et al. Single-molecule RNA Fluorescence in situ Hybridization (smFISH) in *Caenorhabditis elegans*. *Bio-Protoc.* **7**, e2357 (2017).
68. Lee, C., Sorensen, E. B., Lynch, T. R. & Kimble, J. C. elegans GLP-1/Notch activates transcription in a probability gradient across the germline stem cell pool. *eLife* **5**, e18370 (2016).
69. Jose, A. M., Smith, J. J. & Hunter, C. P. Export of RNA silencing from C. elegans tissues does not require the RNA channel SID-1. *Proc. Natl Acad. Sci. USA* **106**, 2283–2288 (2009).
70. Fire, A. et al. Potent and specific genetic interference by double-stranded RNA in Caenorhabditis elegans. *Nature* **391**, 806–811 (1998).

Acknowledgements

We thank Nathan Shugarts for most of the Sanger sequencing of *oxSi487*, referred to as *T* within the manuscript, presented in Supplementary Fig. 1a; members of the Jose laboratory, Norma Andrews, Karen Carleton, Steve Mount, and anonymous reviewers for comments on the manuscript; the *Caenorhabditis elegans* Genetic Stock Center, the Seydoux laboratory (Johns Hopkins University), the Cohen-Fix laboratory (National Institutes of Health), the Fire laboratory (Stanford University), the Bringmann laboratory (Max Planck Institute) and the Hunter laboratory (Harvard University) for worm strains. This work was supported in part by National Institutes of Health Grants R01GM111457 and R01GM124356 to A.M.J.

Author contributions

All authors contributed to experimental design and analysis. S.D., P.R., S.A., F.E., M.D., Y.L, Y.E.C, and M.C. performed experiments. S.D., P.R., M.C., and A.M.J. wrote the manuscript. All authors edited the manuscript.

Competing interests

The authors declare no competing interests.

Additional information

Supplementary information The online version contains supplementary material available at https://doi.org/10.1038/s41467-021-24053-4.

Correspondence and requests for materials should be addressed to A.M.J.

Peer review information *Nature Communications* thanks the anonymous reviewers for their contributions to the peer review of this work. Peer review reports are available.

Reprints and permission information is available at http://www.nature.com/reprints

Publisher's note Springer Nature remains neutral with regard to jurisdictional claims in published maps and institutional affiliations.

Open Access This article is licensed under a Creative Commons Attribution 4.0 International License, which permits use, sharing, adaptation, distribution and reproduction in any medium or format, as long as you give appropriate credit to the original author(s) and the source, provide a link to the Creative Commons license, and indicate if changes were made. The images or other third party material in this article are included in the article's Creative Commons license, unless indicated otherwise in a credit line to the material. If material is not included in the article's Creative Commons license and your intended use is not permitted by statutory regulation or exceeds the permitted use, you will need to obtain permission directly from the copyright holder. To view a copy of this license, visit http://creativecommons.org/licenses/by/4.0/.

© The Author(s) 2021

Mating can initiate stable RNA silencing that overcomes epigenetic recovery

Sindhuja Devanapally*, Pravrutha Raman*, Mary Chey, Samual Allgood, Farida Ettefa, Maïgane Diop, Yixin Lin, Yongyi E Cho, and Antony M Jose
*equal contribution

This supplement contains the following text, figures and tables.

Supplementary Discussion

Maintenance of silencing initiated by mating occurs through mechanisms that are reminiscent of paramutation/RNAe

Paramutation refers to meiotically heritable changes in gene expression transferred from one allele ("paramutagenic") to another allele ("paramutable") when they interact within a cell (reviewed in ref. 1). In addition to similar heritability, both paramutation[2-6] and mating-induced silencing rely on small RNAs to spread silencing from one locus to another homologous locus. However, there are some aspects of paramutation that were found to be different from mating-induced silencing when tested. First, a paramutagenic allele often requires associated repetitive sequences[7-9]. Second, how a paramutagenic allele first arises remains unclear[1]. Third, while some alleles are paramutable, others are not, for reasons that are unknown[2]. The reliability of initiating and also protecting from meiotically heritable silencing at a defined single-copy locus described in this study will be useful in discovering possible shared mechanisms that have remained unclear in the ~65 years since the original discovery of paramutation in maize[3].

The unpredictable silencing that occurs at some single-copy reporter transgenes within the *C. elegans* germline has been called RNA-induced epigenetic silencing or RNAe[10-15]. Some studies of RNAe[13,14,16], but not others (p.94 in ref. 12), report a requirement for PRG-1 only in the initiation of silencing during RNAe, which is similar to the requirement for maternal PRG-1 in mating-induced silencing (Fig. 2a,b). However, while *hrde-1/wago-9* was uniformly reported to be required for the maintenance of silencing, our results reveal a requirement for HRDE-1 in both the initiation and the maintenance of mating-induced silencing (Fig. 2a, Fig. 3c). Transgenes silenced through RNAe are associated with specific genome sequences or a differential subset of small RNAs compared to unsilenced transgenes[16-18] but it remains unclear whether these associated properties of the silenced genes are the cause or consequence of silencing. Nevertheless, a model proposing RNAe as a response to foreign or non-self DNA emerged[10-14]. This model is inadequate because the same target sequence (e.g. *mCherry*, *gfp*) can be either silenced or expressed within the germline (Figs. 1a, 6a and S2a; refs. 13,14,16,17) and endogenous genes are subjected to transgenerational silencing through similar PRG-1- and HRDE-1-dependent mechanisms[19-24]. Furthermore, the features of a transgene that trigger silencing are unknown. Tethering the Argonaute CSR-1 to the nascent transcript[11] or adding intronic sequences that are found in native germline-expressed genes[25] can increase the frequency of expression of a foreign sequence but does not itself determine whether a sequence is expressed. Thus, despite these efforts, the factors that enable stable expression or silencing of a gene across generations remain unclear.

Unlike RNAe, mating-induced silencing can be predictably initiated at the population level with stochastic differences in initiation at the individual level, which together provide a reliable assay for evaluating how organisms establish stable expression or silencing of a gene. Our analyses suggest that the decision to express paternal foreign sequences (*mCherry* and *gfp*) is re-evaluated in each generation based upon maternal mRNA (Fig. 2). Although mating-induced silencing is not a general property of genes (Supplementary Fig. 2a, b), a similar silencing phenomenon with dependence on maternal mRNA has been observed for the endogenous gene *fem-1*[26]. However, it is unknown whether *fem-1* silencing also shares the *trans* silencing properties and genetic requirements of mating-induced silencing.

Taken together, the mating-induced silencing documented in this study provides a reliable model for analyzing epigenetic mechanisms that dictate expression or silencing of a sequence in every generation in otherwise wild-type animals.

Supplementary Figures and Figure Legends

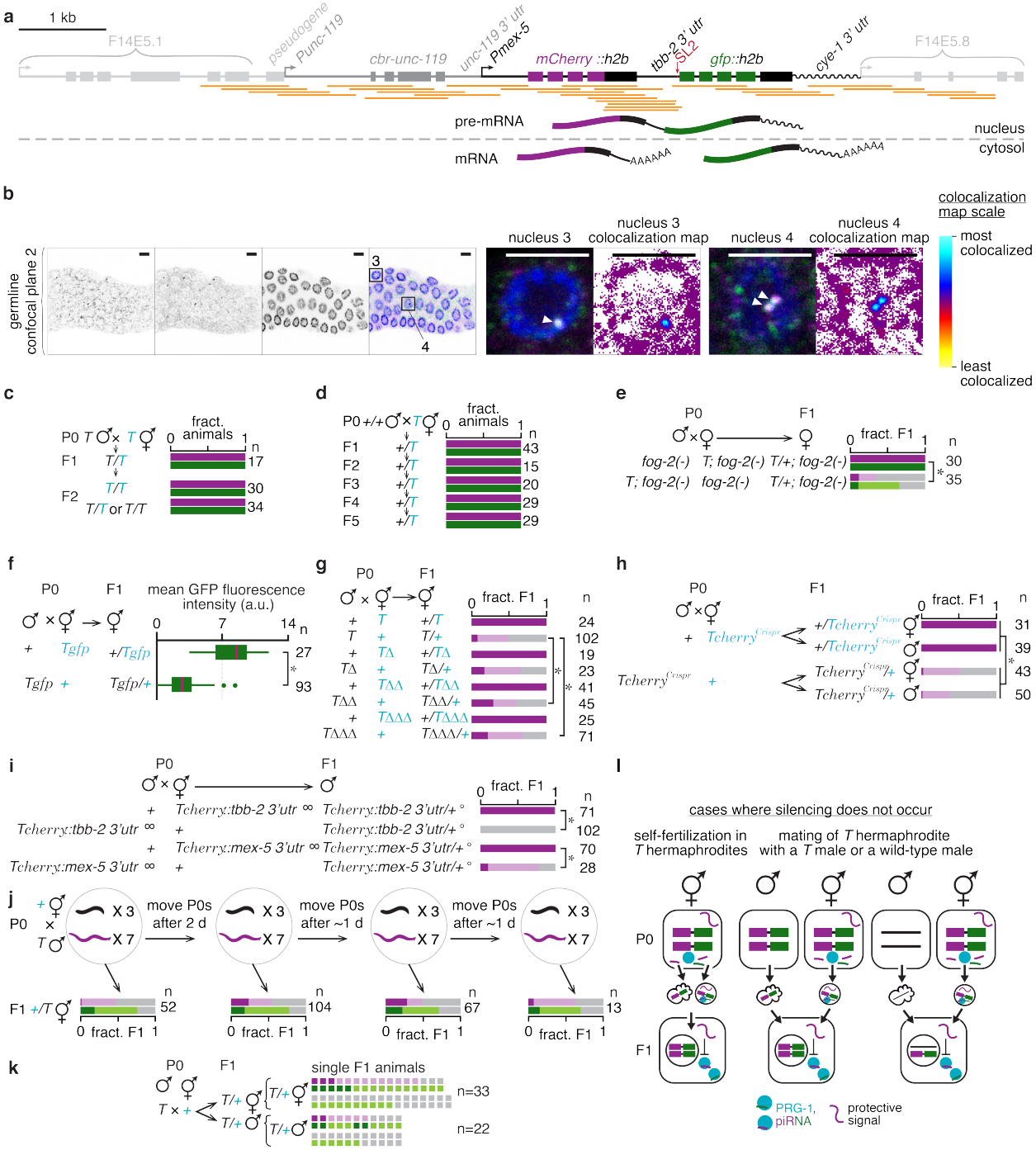

Supplementary Fig. 1. Mating-induced silencing can be robustly initiated despite modifications of the gene sequence.

a Schematic of *T* (*oxSi487*: *Pmex-5::mCherry::h2b::tbb-2 3' utr::gpd-2 operon::gfp::h2b::cye-1 3' utr*) within its genomic context where it is present as a single copy transgene as verified by PCR and Sanger sequencing. The transgene consists of *mCherry* and *gfp* genes tagged to *histone 2b* (*his-58* or *his-66*) arranged in an operon, and is presumably transcribed into one nascent transcript (pre-mRNA) with both *mCherry::h2b* and *gfp::h2b* present as two separate mature

transcripts (mRNA) in the cytosol. Orange lines correspond to sequence stretches verified by individual Sanger sequencing experiments. The genes surrounding the insertion site of *T* on chromosome II are shown.
b smFISH against *mCherry* and *gfp* in dissected gonads of animals expressing *T* reveals that *mCherry* RNA and *gfp* RNA colocalize as one or two spots (white arrowheads) within nuclei. A different confocal plane imaged from the same dissected gonad in Fig. 1b reveals different nuclei with colocalized *mCherry* and *gfp*. Colocalization heat map represents the extent of overlap between smFISH pixels corresponding to *mCherry* RNA and *gfp* RNA as indicated by the scale. *mCherry* RNA image was obtained by subtracting DAPI signal from images that contain combined pixels corresponding to mCherry::H2B protein (with which DAPI signal completely overlaps) and *mCherry* RNA fluorescence.
c Males and hermaphrodites expressing *T* were mated, and fluorescence was scored in cross progeny (F1) and self-fertilized grand-progeny (F2) that inherited only the grand-maternal allele or only the grand-paternal allele or both. F1 data shown here is the same as that in Fig. 1d.
d Wild-type males were mated with *T* hermaphrodites and hemizygous cross progeny (F1) as well as descendant hemizygous self-progeny (F2 through F5) were scored. In contrast to previous reports[27], we find that *T* is not subject to meiotic silencing by unpaired DNA[28].
e Mutation of *fog-2* feminizes the germline in 100% of hermaphrodites but has no effect in males[29]. Feminized mothers expressing *T* were used in a control cross and those without *T* were used in a cross to initiate mating-induced silencing.
f Germline GFP fluorescence from hemizygous *Tgfp*/+ cross progeny shown in Fig. 1e was quantified. Box plot characteristics are: red line, median; box limits, upper and lower quartiles; whiskers, 1.5x interquartile range; points, outliers.
g Animals expressing variants of *T* were mated with non-transgenic animals and cross progeny were scored.
h Animals expressing *Tcherry* inserted into the genome using CRISPR-Cas9 were mated with non-transgenic animals and cross progeny were scored.
i Animals expressing *Tcherry* with altered 3' UTR were mated to non-transgenic animals and cross progeny were scored. To reverse spontaneous transgene silencing[16,25] upon genome insertion, *hrde-1(-)* was introduced (∞) into P0 transgenic animals resulting in heterozygous *hrde-1(+/-)* cross progeny (°).
j *T* males and non-transgenic hermaphrodites were mated and cross progeny that were laid in the first 48 hours (2 days, 2 d) or in subsequent ~24 hour intervals (1 day, 1 d), were collected after moving the P0s to fresh plates. While silencing triggered by parental ingestion of dsRNA is less effective in later progeny[30,31], silencing triggered by mating can be equally effective in early and in late progeny.
k Cross progeny males and hermaphrodites that inherited *T* paternally were scored. Scoring data from the crosses in Fig. 1d is depicted as a coloured pair of boxes to show mCherry and GFP fluorescence in each individual.
l Schematics that depict possible explanations for lack of silencing: *left*, when homozygous *T* hermaphrodites self-fertilize using transgenic sperm carrying *T* and oocytes that express *T* and carry PRG-1-dependent piRNAs complementary to *T*, self-progeny remain unsilenced possibly due to a protective signal derived from *T* transmitted from the hermaphrodite parent through the oocyte into progeny; *middle*, when *T* males are mated with hermaphrodites expressing *T*, cross progeny remain unsilenced due to the protective signal transmitted from the hermaphrodite parent through the oocyte into progeny; *right*, when wild-type males are mated with

hermaphrodites expressing *T*, cross progeny inherit the protective signal through the oocyte that prevents initiation of mating-induced silencing.
Chromosomes with a *dpy* marker (blue font) and number of animals scored (n) are indicated. Scoring of silencing is as in Fig. 1. Asterisks indicate $P < 0.05$ using χ^2 test (e, g, h, i) or two-sided Student's t-test (f). Scale bars, 5 µm (b). Also see 'Genetic Crosses' under Supplementary Methods.

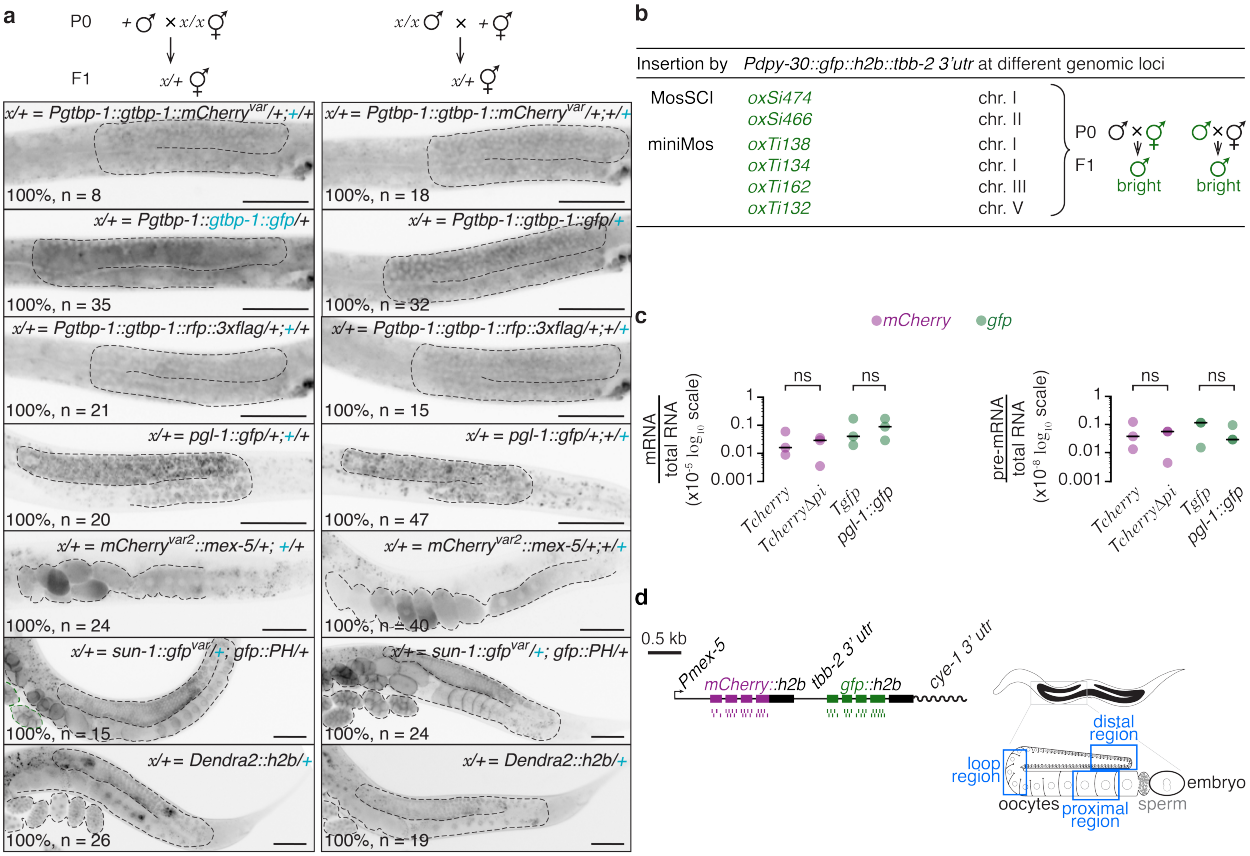

Supplementary Fig. 2. Mating-induced silencing does not occur with other germline genes and is not explained by changes in transcript abundance or localization in the germline.
a and b Endogenous genes tagged with reporter sequences (*gtbp-1::mCherry*^{var}, *gtbp-1::gfp*, *gtbp-1::rfp::3xflag*, *mCherry*^{var2}*::mex-5* and *pgl-1::gfp*) using CRISPR-Cas9-mediated genome

editing and transgenes made using miniMos[14] (*Pdpy-30::gfp::h2b::tbb-2 3' utr*), MosSCI (*Pdpy-30::gfp::h2b::tbb-2 3' utr*, *sun-1::gfp*^{var} and *Pmex-5::Dendra2::h2b::tbb-2 3' utr*), or bombardment (*Ppie-1::gfp::PH(PLCdelta1)*) were tested for susceptibility to mating-induced silencing. Germlines of representative cross progeny at L4 or adult stage are outlined and percentages of animals showing the expression depicted in the image are indicated in **a**.
c *mCherry* and *gfp* mRNA levels were measured by qRT-PCR between animals expressing *Tcherry* or *Tcherry*Δ*pi* and *Tgfp* or *pgl-1::gfp* respectively. The fold change of pre-mRNA:mRNA ratios between *Tcherry* and *Tcherry*Δ*pi* is ~0.5 and between *Tgfp* and *pgl-1::gfp* is ~2.2. ns indicate $P > 0.05$ using two-sided Student's t-test.
d smFISH probes that hybridize to *mCherry* or *gfp* exonic RNA (*left*) and schematics of germline regions imaged for smFISH or protein fluorescence using confocal microscopy (this figure, Fig. 1, Supplementary Fig. 1, Supplementary Fig. 4, and Supplementary Fig. 6) are indicated (*right*).
e Animals that express sequence variants of *mCherry* (*top*) or *gfp* (*bottom*) genes were subjected to smFISH against *mCherry* or *gfp* transcripts within dissected gonads. Genotypes of *gtbp-1::gfp* and *gtbp-1::mCherry*^{var} animals shown here are the same as those shown in **a**. Numbers within fluorescence images refer to number of RNAs per 100 μm^2 with standard error of the mean. Animals with median values of fluorescence or RNA signal in the distal region are represented along with the loop and proximal regions within the same animals. Pink arrowheads indicate the nucleus of the distal tip cell, when included in the imaging plane.
Chromosomes with a recessive marker (blue font) and numbers of animals scored or imaged (n) are indicated. Scale bars are 50 μm (a) or 10 μm (e).

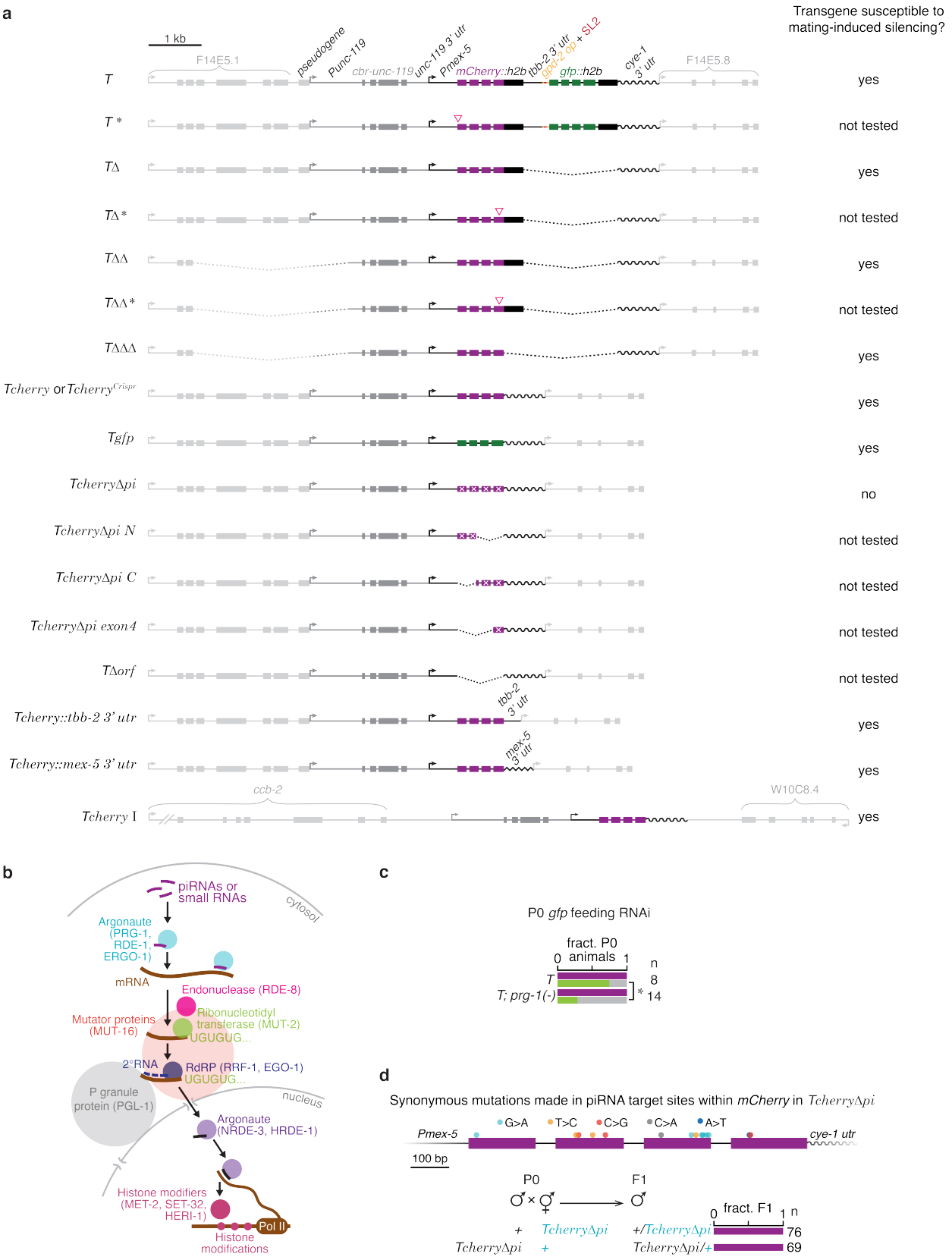

Supplementary Fig. 3. Schematics of key transgenes, schematic of the piRNA-mediated silencing pathway, and tests of its requirement for two forms of RNA silencing.

a Schematics of *T*, of serial deletions and/or indels of *T* and of minimal variants of *T* that were newly integrated into a naive genome. Successive deletions that remove *gfp* and *tbb-2 3' utr* (*T*Δ), a ~3 kb region upstream of the *unc-119(+)* coding region (*T*ΔΔ), and *h2b* (*T*ΔΔΔ) are depicted in their genomic context, along with variations that in addition contain small indels (*T**, *T*Δ*, *T*ΔΔ*). *Tcherry*, *Tcherry*^{Crispr}, *Tgfp*, *Tcherry*Δ*pi*, *Tcherry::tbb-2 3' utr*, *Tcherry::mex-5 3' utr* and *Tcherry* on chromosome I were integrated independently of each other. *Tcherry*Δ*pi N*, *Tcherry*Δ*pi C* and *Tcherry*Δ*pi exon4* were generated by independently editing animals carrying *Tcherry*Δ*pi*. *T*Δ*orf* was made by deleting *mCherry* in animals carrying *Tcherry.* The susceptibility of each variant to mating-induced silencing is indicated on the right. Certain variants were not tested for mating-induced silencing because they either contain a premature stop codon or do not contain a coding region. Also see Supplementary Table 5.
b Working model of RNA silencing mechanisms in *C. elegans* based on prior studies. Schematic depicting the described role of different components of the small RNA pathway that were examined for their requirement in initiation (Fig. 2) or maintenance (Fig. 3c) of mating-induced silencing[32-34]. Within the germline, secondary (2°) RNA production is not always correlated with gene silencing[32,35,36].
c Animals expressing *T* in a wild-type or *prg-1(-)* background were exposed to *gfp* RNAi or control RNAi for one generation (P0 RNAi) and scored.
d Schematic of synonymous changes in predicted piRNA sites within *mCherry* is depicted. Animals expressing *Tcherry* lacking piRNA binding sites (*Tcherry*Δ*pi*) were mated with non-transgenic animals, and cross progeny males were scored. Scoring of silencing (c and d) is as in Fig. 1c. Chromosomes with a *dpy* marker (blue font in d) and number of animals scored (n) are indicated. Asterisks indicate $P < 0.05$ using χ^2 test.

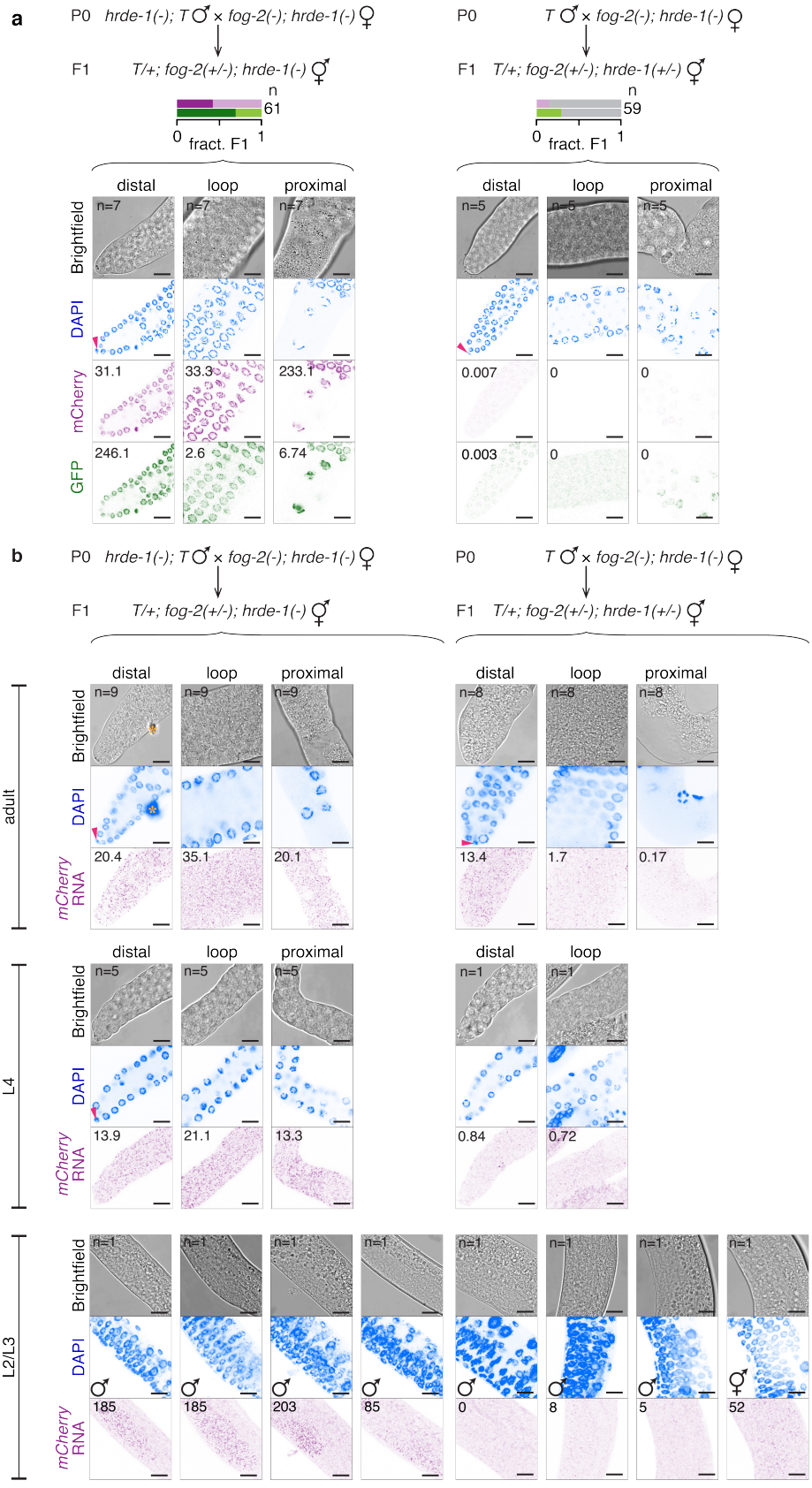
a
P0 hrde-1(-); T ♂ × fog-2(-); hrde-1(-) ♀
F1 T/+; fog-2(+/-); hrde-1(-) ♀
n
61
0
fract. F1
1
P0 T ♂ × fog-2(-); hrde-1(-) ♀
F1 T/+; fog-2(+/-); hrde-1(+/-) ♀
n
59
0
fract. F1
1
distal
loop
proximal
Brightfield
DAPI
mCherry
GFP
n=7
31.1
33.3
233.1
246.1
2.6
6.74
n=5
0.007
0
0
0.003
0
0
b
P0 hrde-1(-); T ♂ × fog-2(-); hrde-1(-) ♀
F1 T/+; fog-2(+/-); hrde-1(-) ♀
P0 T ♂ × fog-2(-); hrde-1(-) ♀
F1 T/+; fog-2(+/-); hrde-1(+/-) ♀
adult
L4
L2/L3
mCherry RNA
n=9
20.4
35.1
20.1
n=8
13.4
1.7
0.17
n=5
13.9
21.1
13.3
n=1
0.84
0.72
185
185
203
85
0
8
5
52

Supplementary Fig. 4. Mating-induced silencing results in quantitative reduction of *mCherry* and *gfp* transcripts and protein within the germline in cross progeny.
Initiation of mating-induced silencing was measured by protein fluorescence microscopy or smFISH against *mCherry* RNA in dissected gonads of cross progeny that were impaired for (*top*) or susceptible to (*bottom*) mating-induced silencing. While control cross progeny would ideally be derived from *T* hermaphrodites mated with wild-type males, we did not examine progeny from such a cross because maternally deposited transcripts from *T* would add to progeny transcripts detected. Instead, mating-induced silencing was attempted in the parental and zygotic absence of *hrde-1,* which is required for initiation of silencing (refer to Fig. 2a, b), thus allowing us to examine transcripts from *T* in the absence of silencing in cross progeny.
a *T* or *T; hrde-1(-)* males were mated with *hrde-1(-); fog-2(-)* females and fluorescence due to mCherry::H2B and GFP::H2B in cross progeny was scored by eye after imaging (*top*) or by quantifying confocal slices of indicated regions of dissected gonads (*bottom*). Scoring of silencing by eye and number of animals assayed are as in Fig. 1c. For confocal images of cross progeny in left panel (control cross), fluorescence intensity values (arbitrary units) ranged from 5.3 to 42.6 (mCherry, distal), 0.0006.4 to 246.1 (GFP, distal), 4.6 to 39.1 (mCherry, loop), 0.2 to 14.2 (GFP, loop), 0 to 250.5 with 5/7 animals >5.0 (mCherry, proximal), 0.002 to 7.9 with 4/7 animals ≥2.2 (GFP, proximal). For confocal images of cross progeny in right panel (mating-induced silencing cross), fluorescence intensity values (arbitrary units) ranged from 0.0005 to 24.5 (mCherry, distal), 0.001 to 0.6 (GFP, distal), 0 to 254 with 3/5 animals = 0 (mCherry, loop), 0.0007 to 254.8 with 4/5 animals ≤0.8 (GFP, loop), 0 to 6.5 with 4/5 animals = 0 (mCherry, proximal), 0.0007 to 2.9 with 4/5 animals ≤0.03 (GFP, proximal).
b smFISH of *mCherry* RNA in cross progeny adults obtained from a mating as in panel a. For confocal images of cross progeny in left panel (control cross), *mCherry* RNAs per 100 μm^2 ranged from 2.5 to 33.8 (adult, distal), 1.5 to 42.6 (adult, loop), 0.6 to 37 with 8/9 animals >15.8 (adult, proximal), 0.8 to 18.9 (L4, distal), 17.3 to 29.2 (L4, loop), 0.12 to 15.8 with 4/5 animals >6.9 (L4, proximal). For confocal images of cross progeny in right panel (mating-induced silencing cross), *mCherry* RNAs per 100 μm^2 ranged from 0.9 to 27.8 (adult, distal), 0 to 19 (adult, loop), 0 to 26.2 with 7/8 animals <9.6 (adult, proximal).
Pink arrowhead, nucleus of the distal tip cell and orange asterisk, non-specific signal. Numbers within fluorescence images refer to mean fluorescence intensity per unit area measured in arbitrary units (a) or number of RNAs per 100 μm^2 (b). Animals with median values of protein or RNA fluorescence signal in the distal region are represented along with the loop and proximal regions within the same animals. Scoring of silencing (a, *top*) is as in Fig. 1. Scale bars are 10 μm. Number (n) of animals scored (a) or imaged per region using confocal microscopy (a and b) is indicated.

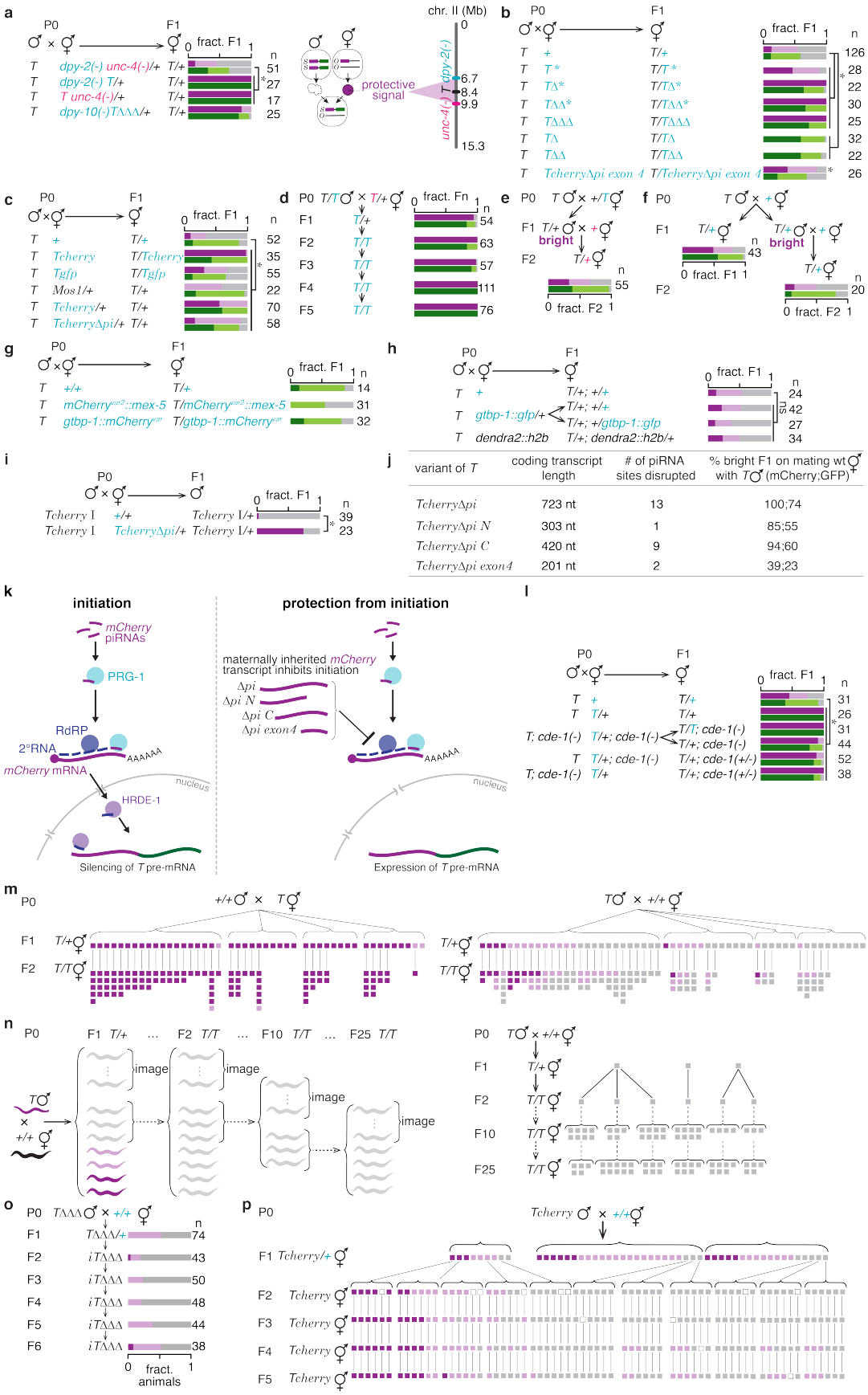
a
P0
F1
fract. F1
T dpy-2(-) unc-4(-)/+ T/+ 51
T dpy-2(-) T/+ T/+ 27
T T unc-4(-)/+ T/+ 17
T dpy-10(-)TΔΔΔ/+ T/+ 25
chr. II (Mb)
protective signal
dpy-2(-)
unc-4(-)
6.7
8.4
9.9
15.3
b
T + T/+ 126
T T* T/T* 28
TΔ* TΔ* 22
TΔΔ* TΔΔ* 30
TΔΔΔ TΔΔΔ 25
TΔ TΔ 32
TΔΔ TΔΔ 22
T TcherryΔpi exon 4 T/TcherryΔpi exon 4 26
c
T + T/+ 52
T Tcherry T/Tcherry 35
T Tgfp T/Tgfp 55
T Mos1/+ T/+ 22
T Tcherry/+ T/+ 70
T TcherryΔpi/+ T/+ 58
d
P0 T/T × T/+
F1 T/+ 54
F2 T/T 63
F3 T/T 57
F4 T/T 111
F5 T/T 76
fract. Fn
e
P0 T × +/T
F1 T/+ × + bright
F2 T/+ 55
fract. F2
f
P0 T × +
F1 T/+ 43 T/+ × + bright
F2 T/+ 20
fract. F2
g
T +/+ T/+ 14
T mCherry^eat2::mex-5 T/mCherry^eat2::mex-5 31
T gtbp-1::mCherry^ear T/gtbp-1::mCherry^ear 32
h
T + T/+; +/+ 24
T gtbp-1::gfp/+ T/+; +/+ 42
T dendra2::h2b T/+; +/gtbp-1::gfp 27
T dendra2::h2b/+ T/+; dendra2::h2b/+ 34
ns
i
Tcherry I +/+ Tcherry I/+ 39
Tcherry I TcherryΔpi/+ Tcherry I/+ 23
j
variant of T | coding transcript length | # of piRNA sites disrupted | % bright F1 on mating wt with T♂ (mCherry;GFP)
TcherryΔpi | 723 nt | 13 | 100;74
TcherryΔpi N | 303 nt | 1 | 85;55
TcherryΔpi C | 420 nt | 9 | 94;60
TcherryΔpi exon4 | 201 nt | 2 | 39;23
k
initiation
protection from initiation
mCherry piRNAs
PRG-1
RdRP
2°RNA
mCherry mRNA
AAAAAA
nucleus
HRDE-1
Silencing of T pre-mRNA
maternally inherited mCherry transcript inhibits initiation
Δpi
Δpi N
Δpi C
Δpi exon4
Expression of T pre-mRNA
l
T + T/+ 31
T T/+ T/+ 26
T; cde-1(-) T/+; cde-1(-) T/T; cde-1(-) 31
T/+; cde-1(-) 44
T T/+; cde-1(-) T/+; cde-1(+/-) 52
T; cde-1(-) T/+ T/+; cde-1(+/-) 38
m
P0 +/+ × T
F1 T/+
F2 T/T
T × +/+
T/+
T/T
n
P0 F1 T/+ … F2 T/T … F10 T/T … F25 T/T
image
T
+/+
P0 T × +/+
F1 T/+
F2 T/T
F10 T/T
F25 T/T
o
P0 TΔΔΔ × +/+ n
F1 TΔΔΔ/+ 74
F2 iTΔΔΔ 43
F3 iTΔΔΔ 50
F4 iTΔΔΔ 48
F5 iTΔΔΔ 44
F6 iTΔΔΔ 38
fract. animals
p
P0 Tcherry × +/+
F1 Tcherry/+
F2 Tcherry
F3 Tcherry
F4 Tcherry
F5 Tcherry

Supplementary Fig. 5. Protection and maintenance of mating-induced silencing.
a *T* males were mated with genetically marked hermaphrodites and animals with paternally inherited *T* were scored. Schematic: maternal presence of *T*ΔΔΔ protects paternally inherited *T* from mating-induced silencing, suggesting that the oocyte carries a separable protective signal derived from a ~3.2 Mb region between *dpy-2* and *unc-4*, which are linked to *T*.
b and c *T* males were mated with non-transgenic hermaphrodites or hermaphrodites expressing a variant of *T* or *Mos1* transposon in the same genomic position as *T* and paternally inherited *T* was scored in resulting cross progeny. Control cross progeny to compare with *T/Tcherry*Δ*pi exon 4* cross progeny in this panel are shown in Fig. 2e.
d Hemizygous *T*/+ hermaphrodites were mated with homozygous *T* males containing a recessive marker and hemizygous cross progeny (F1) as well as four generations of homozygous descendants (F2 through F5) were scored.
e and f Male progeny with bright mCherry fluorescence that were protected from initiation (e) or that escaped initiation of mating-induced silencing (f) were tested for mating-induced silencing.
g and h Males expressing *T* were mated with hermaphrodites expressing genes with homologous protein (g) or DNA (h) sequences, and fluorescence of GFP (g) or mCherry (h) from paternally inherited *T* was scored in cross progeny.
i Mating-induced silencing of *Tcherry* expressed from chromosome I could be protected by maternally expressed *Tcherry*Δ*pi* on chromosome II.
j Table indicating the length of coding regions and number of disrupted piRNA target sites[37] in *Tcherry*Δ*pi* or its derivatives, along with the percentage of bright cross progeny obtained upon mating hermaphrodites expressing one of these variants with *T* males. The percentages indicated here represent data from Fig. 2e and panel b in this figure.
k Model depicting one possible explanation for how protection from mating-induced silencing occurs in cross progeny. During initiation of mating-induced silencing, maternally inherited PRG-1 stabilizes complementary *mCherry* piRNAs which bind the *mCherry* mRNA made in progeny, resulting in recruitment of an RdRP to produce secondary small RNAs, which are then used by HRDE-1 to cause silencing of the pre-mRNA transcript comprising both *mCherry* and *gfp* in the nucleus (*left*). In protection from mating-induced silencing, it is possible that maternally inherited fragments of *mCherry* act as a sponge to soak up secondary RNAs, thus preventing the silencing of the pre-mRNA containing both *mCherry* and *gfp* transcript in the nucleus (*right*). Consistent with this model, the level of protection (i.e. the percentage of animals with bright mCherry and GFP fluorescence) is directly proportional to the length of the maternal transcript (see j). In other words, the longer the maternally inherited transcript, the more the capacity for it to soak up secondary small RNAs in progeny. See text for additional possibilities.
l Mutants of a CSR-1 pathway gene, *cde-1*, were used to test parental and zygotic requirement for protection.
m Animals expressing *T* were mated with wild-type animals in four independent crosses (brackets) and mCherry fluorescence was scored in hemizygous cross progeny and in homozygous grand progeny. Each box indicates fluorescence intensity of a single adult animal and lines indicate descent. Once initiated, mating-induced silencing persists despite passage of *T* through oocytes of hermaphrodites and is therefore unlike genomic imprinting[38,39], where passage of *T* through oocytes is expected to revive expression.
n F2 'off' progeny (from **m**) obtained after initiation of mating-induced silencing were propagated without further selection by self-fertilization for 23 generations as indicated by the passaging scheme. mCherry fluorescence intensity was measured in animals (boxes) at F1, F2,

F10 and F25 generations from three independent P0 crosses. At each generation indicated, siblings of the animals that were passaged were scored. Presence of the transgene was verified by genotyping in F1 and F2 generations.
o *T*ΔΔΔ males were mated with non-transgenic hermaphrodites and scoring was done in cross progeny (F1) and in descendants propagated blindly from 'off' F1 animals.
p *Tcherry* males were mated with non-transgenic hermaphrodites in three independent crosses and cross progeny belonging to each fluorescence level were singled out to give F2 animals. From F2 through F5, a single animal was blindly passaged and a single descendant was scored. Empty box indicates that the animal could not be scored because it was lost after being passaged on to a fresh plate, but only after having laid eggs, which enabled the continued scoring of its descendants.
Scoring of silencing is as in Fig. 1c. Chromosomes with a recessive marker (blue font in **o** and **p**) and numbers of animals scored (n) are indicated. Asterisks indicate $P < 0.05$ using χ^2 test.

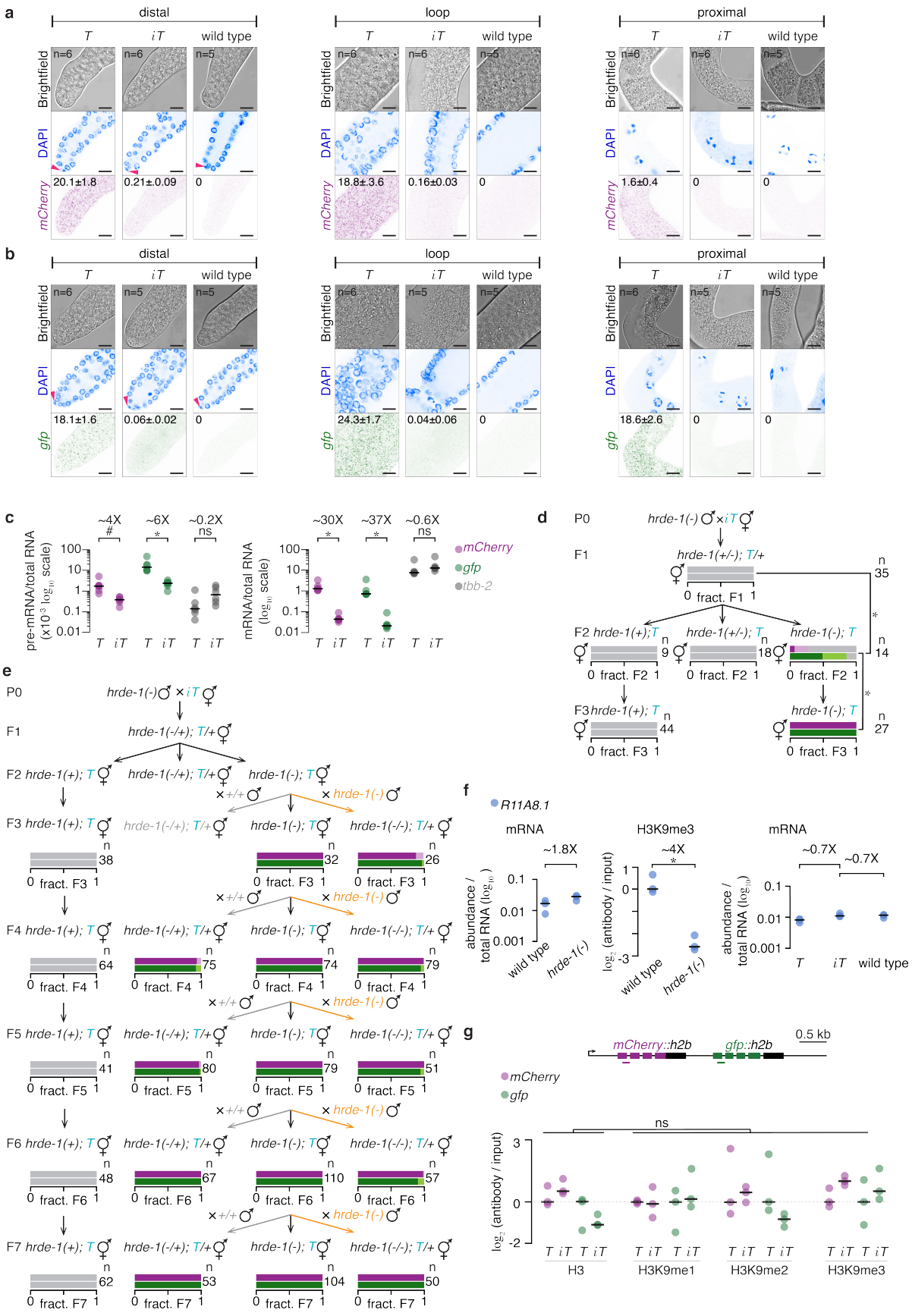
a
distal
loop
proximal
T
iT
wild type
Brightfield
DAPI
mCherry
n=6
n=5
20.1±1.8
0.21±0.09
0
18.8±3.6
0.16±0.03
1.6±0.4
b
gfp
18.1±1.6
0.06±0.02
24.3±1.7
0.04±0.06
18.6±2.6
c
~4X
~6X
~0.2X
~30X
~37X
~0.6X
pre-mRNA/total RNA (x10^-3 log10 scale)
mRNA/total RNA (log10 scale)
mCherry
gfp
tbb-2
d
P0
hrde-1(-) ♂ × iT ♀
F1
hrde-1(+/-); T/+
0 fract. F1 1
n 35
F2 hrde-1(+); T
hrde-1(+/-); T
hrde-1(-); T
n 9
n 18
n 14
0 fract. F2 1
F3 hrde-1(+); T
n 44
hrde-1(-); T
n 27
0 fract. F3 1
e
P0
hrde-1(-) ♂ × iT ♀
F1
hrde-1(-/+); T/+ ♂
F2 hrde-1(+); T ♀
hrde-1(-/+); T/+ ♀
hrde-1(-); T ♀
× +/+ ♂
× hrde-1(-) ♂
F3 hrde-1(+); T ♀
hrde-1(-/+); T/+ ♀
hrde-1(-); T ♀
hrde-1(-/-); T/+ ♀
n 38
n 32
n 26
0 fract. F3 1
F4 hrde-1(+); T ♀
hrde-1(-/+); T/+ ♀
hrde-1(-); T ♀
hrde-1(-/-); T/+ ♀
n 64
n 75
n 74
n 79
0 fract. F4 1
F5 hrde-1(+); T ♀
hrde-1(-/+); T/+ ♀
hrde-1(-); T ♀
hrde-1(-/-); T/+ ♀
n 41
n 80
n 79
n 51
0 fract. F5 1
F6 hrde-1(+); T ♀
hrde-1(-/+); T/+ ♀
hrde-1(-); T ♀
hrde-1(-/-); T/+ ♀
n 48
n 67
n 110
n 57
0 fract. F6 1
F7 hrde-1(+); T ♀
hrde-1(-/+); T/+ ♀
hrde-1(-); T ♀
hrde-1(-/-); T/+ ♀
n 62
n 53
n 104
n 50
0 fract. F7 1
f
R11A8.1
mRNA
~1.8X
abundance / total RNA (log10)
wild type
hrde-1(-)
H3K9me3
~4X
log2 (antibody / input)
mRNA
~0.7X
~0.7X
T
iT
wild type
g
mCherry::h2b
gfp::h2b
0.5 kb
mCherry
gfp
ns
log2 (antibody / input)
T iT T iT
H3
H3K9me1
H3K9me2
H3K9me3

Supplementary Fig. 6. Mating can trigger maintenance of transgenerational silencing by quantitative reduction of transcripts without detectable changes in H3K9me across generations.

a and b smFISH of *mCherry* (**a**) or *gfp* (**b**) exonic RNA was performed in indicated regions of dissected gonads of adult *T*, *iT* (silenced for ~320 generations in 100% of animals) or wild-type animals. Pink arrowheads indicate the nucleus of the distal tip cell. Numbers within images refer to number of RNAs per 100 μm^2 with standard error of the mean. Animals with median values of fluorescence or RNA signal in the distal region are shown in representative images along with the loop and proximal regions within the same animals. Number of animals imaged per region is indicated within the brightfield image. Positions of smFISH probes within the RNAs is shown in Supplementary Fig. 2d.

c *mCherry*, *gfp* and *tbb-2* pre-mRNA (*left*) or mRNA (*right*) levels were measured by qRT-PCR in animals that express *T* and in animals that showed loss of expression from *T* for >200 generations (*iT*).

d *hrde-1(-)* mutants were mated with *iT* silenced for 171 generations, and scoring was performed in cross progeny, in F2 and F3 descendants.

e Experiment depicting the test for whether *iT* that had been silenced in 100% of animals for 270 generations recovers expression upon removal of *hrde-1* (orange) can show silencing upon re-introduction of *hrde-1(+)* (grey) without re-initiating mating-induced silencing in the descending generations. F3 animals of the genotype *hrde-1(+/-); T/+* from F2 *hrde-1(-); T* hermaphrodites crossed with N2 males were not obtained due to experimental constraints (Supplementary Methods).

f qRT-PCR of mRNA and ChIP-qPCR of H3K9me3 levels of an *hrde-1* target gene[40,41], *R11A8.1*, were measured in wild-type, *hrde-1(-)*, *T* and *iT* animals. H3K9me3 measurements were normalized to wild-type levels. Similar to previous reports, we detected a decrease in H3K9me3 at the *R11A8.1* gene upon loss of HRDE-1, however, no significant change in mRNA was detected. mRNA levels of *R11A8.1* was not significantly altered between *T*, *iT* and wild-type animals and hence was used as a control gene for ChIP experiments. Each dot represents one biological replicate and black line indicates the median value. Each mRNA measurement is the median of five technical replicates.

g H3, H3K9me1, H3K9me2 and H3K9me3 levels were measured at genomic *mCherry* and *gfp* in *T* and *iT* animals. Measurements were normalized to levels at *R11A8.1* measured from each sample's respective input and then to *T*. Each circle represents one biological replicate, which is the median of five technical replicates and black line indicates the median value.

Scoring of silencing (d and e) is as in Fig. 1c. Chromosomes with a *dpy* marker (blue font), number of animals scored (n) and scale bar (10 µm) are indicated. Asterisks indicate $P < 0.05$ and 'ns' indicates $P > 0.05$ using χ^2 test (d) or two-sided Student's t-test (c, f and g). Hash symbol (c) indicates $P = 0.05$ using two-sided Student's t-test. Also see 'Genetic Crosses' in Methods.

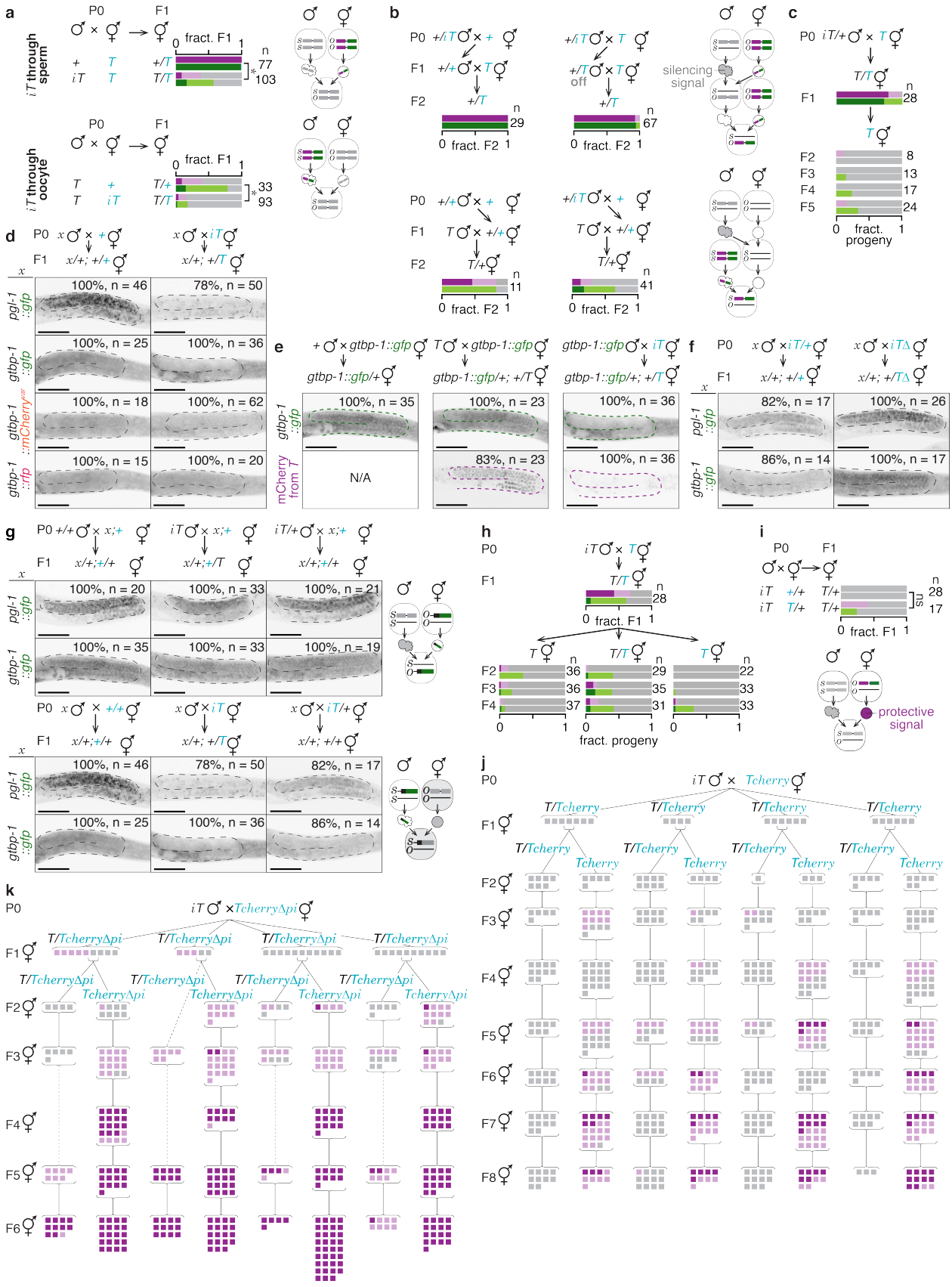
a
P0
F1
fract. F1
n
77
103
*
i T through sperm
+ T
i T T
+/T
T/T
i T through oocyte
T +
T i T
T/+
T/T
33
93
b
P0 +/i T ♂ × + ♀
F1 +/+ ♂ × T ♀
F2 +/T
n
29
0 fract. F2 1
+/i T ♂ × T ♀
+/T off ♂ × T ♀
+/T
67
silencing signal
P0 +/+ ♂ × + ♀
F1 T ♂ × +/+ ♀
F2 T/+ ♀
11
41
P0 +/i T ♂ × + ♀
c
P0 i T/+ ♂ × T ♀
T/T ♀
F1
28
T ♀
F2
F3
F4
F5
8
13
17
24
0 fract. progeny 1
d
P0 x ♂ × + ♀
x ♂ × i T ♀
F1 x/+; +/+ ♂
x/+; +/T ♂
pgl-1 ::gfp
gtbp-1 ::gfp
gtbp-1 ::mCherry var
gtbp-1 ::rfp
100%, n = 46
78%, n = 50
100%, n = 25
100%, n = 36
100%, n = 18
100%, n = 62
100%, n = 15
100%, n = 20
e
+ ♂ × gtbp-1::gfp ♀
T ♂ × gtbp-1::gfp ♀
gtbp-1::gfp ♂ × i T ♀
gtbp-1::gfp/+ ♀
gtbp-1::gfp/+; +/T ♀
gtbp-1 ::gfp
mCherry from T
100%, n = 35
100%, n = 23
100%, n = 36
N/A
83%, n = 23
f
P0 x ♂ × i T/+ ♀
x ♂ × i TΔ ♀
F1 x/+; +/+ ♂
x/+; +/TΔ ♂
pgl-1 ::gfp
gtbp-1 ::gfp
82%, n = 17
100%, n = 26
86%, n = 14
100%, n = 17
g
P0 +/+ ♂ × x;+ ♀
i T ♂ × x;+ ♀
i T/+ ♂ × x;+ ♀
F1 x/+;+/+ ♀
x/+;+/T ♀
x/+;+/+ ♀
pgl-1 ::gfp
gtbp-1 ::gfp
100%, n = 20
100%, n = 33
100%, n = 21
100%, n = 35
100%, n = 33
100%, n = 19
P0 x ♂ × +/+ ♀
x ♂ × i T ♂
x ♂ × i T/+ ♀
F1 x/+;+/+ ♂
x/+; +/T ♂
x/+; +/+ ♂
100%, n = 46
78%, n = 50
82%, n = 17
100%, n = 25
100%, n = 36
86%, n = 14
h
P0
i T ♂ × T ♀
F1
T/T ♀
n
28
0 fract. F1 1
T ♀
T/T ♂
T ♀
F2
F3
F4
36
36
37
29
35
31
22
33
33
0 1 0 1 0 1
fract. progeny
i
P0
F1
i T +/+ T/+
i T T/+ T/+
n
28
17
ns
0 fract. F1 1
protective signal
j
P0
i T ♂ × Tcherry ♀
T/Tcherry
F1 ♀
T/Tcherry
Tcherry
F2 ♀
F3 ♀
F4 ♀
F5 ♀
F6 ♀
F7 ♀
F8 ♀
k
P0
i T ♂ × TcherryΔpi ♀
T/TcherryΔpi
TcherryΔpi
F1 ♀
F2 ♀
F3 ♀
F4 ♀
F5 ♀
F6 ♀

Supplementary Fig. 7. Variants of *T* can recover from silencing by a heritable silencing signal acting in *trans*.

a Animals expressing *T* were mated with *iT* animals that remained silenced for many generations (*iT* gen. number indicated in Fig. 4b), and cross progeny were scored. The combined data from each cross in Fig. 4b is shown here.

b Crosses to test the transmission of the separable silencing signal across more than one generation.

c Silencing of *T* in *trans* by *iT* was assessed across generations. The remaining results of this cross showing the effect of separable silencing signal is shown in Fig. 4f.

d Males that express homologous (*gfp*) or non-homologous (*rfp* or synonymous *mCherry* variant) sequences fused to endogenous genes (*x = pgl-1* or *gtbp-1*) expressed in the germline (*pgl-1*) or expressed ubiquitously (*gtbp-1*) were mated with non-transgenic or *iT* hermaphrodites and fluorescence of PGL-1::GFP, GTBP-1::GFP, GTBP-1::mCherry^{var} or GTBP-1::RFP was imaged in cross progeny. Here, and in the panels below, percentages less than 100 report animals that are silenced as much as or more than the animals shown in the image.

e *gtbp-1::gfp* animals were mated with non-transgenic, *T* or *iT* animals and cross progeny were imaged. Expression level of *mCherry* from *T* is also indicated. N/A, not applicable.

f Males that express *pgl-1::gfp* or *gtbp-1::gfp* were mated with hemizygous *iT* or homozygous *iT*Δ hermaphrodites and GFP fluorescence from the tagged gene was scored in cross progeny that did not inherit *iT* or that inherit *T*Δ. Images from the left panels are also represented for a different comparison in panel **g**.

g Animals that express *pgl-1::gfp* or *gtbp-1::gfp* were mated with homozygous or hemizygous *iT* animals and GFP fluorescence from the tagged gene was scored in cross progeny. Schematics: Maternal (*bottom*) but not paternal (*top*) transmission of the silencing signal (grey filling) affects the expression of homologous genes (green box) in cross progeny, indicating that the hermaphrodite parent carrying *iT* transmits a different type or level of silencing signal (shaded P0 hermaphrodite) compared to the male parent[32,35,38,39].

h *iT* males (silenced upon mating for >250 generations) were mated with *T* hermaphrodites and resulting cross progeny and subsequent generations of descendants of indicated genotypes were scored for expression of mCherry and GFP.

i *Top*, *iT* males were mated with non-transgenic or hemizygous hermaphrodites and cross progeny inheriting only paternal *iT* were scored. *Bottom*, schematic representation of *iT* males mated with hemizygous hermaphrodites indicates the inheritance of both parental protective and silencing signals. The protective signal in this case aids in recovery of weak mCherry and GFP expression from *iT* that remained silenced for ~78 generations.

j and **k** *Tcherry* or *Tcherry*Δ*pi* hermaphrodites were mated with *iT* males and maternally inherited *mCherry* was scored in resulting cross progeny by examining cytoplasmic mCherry fluorescence (i.e. not the nuclear protein-encoding *mCherry::h2b* that is paternally inherited, albeit in a silenced state) in subsequent generations of descendants of indicated genotypes. GFP fluorescence from *iT* was off in all scored animals across generations (data not shown), and therefore independent of the level of mCherry fluorescence from *Tcherry* or *Tcherry*Δ*pi*.

Scoring of silencing is as in Fig. 1c. Chromosomes with a *dpy* marker (blue font), number of animals scored (n) and scale bar (50 μm) are indicated. Germlines of representative cross progeny at L4 stage are outlined and percentages of animals with the depicted expression are indicated (d to g). Asterisks indicate $P < 0.05$ and 'ns' indicates $P > 0.05$ using χ^2 test.

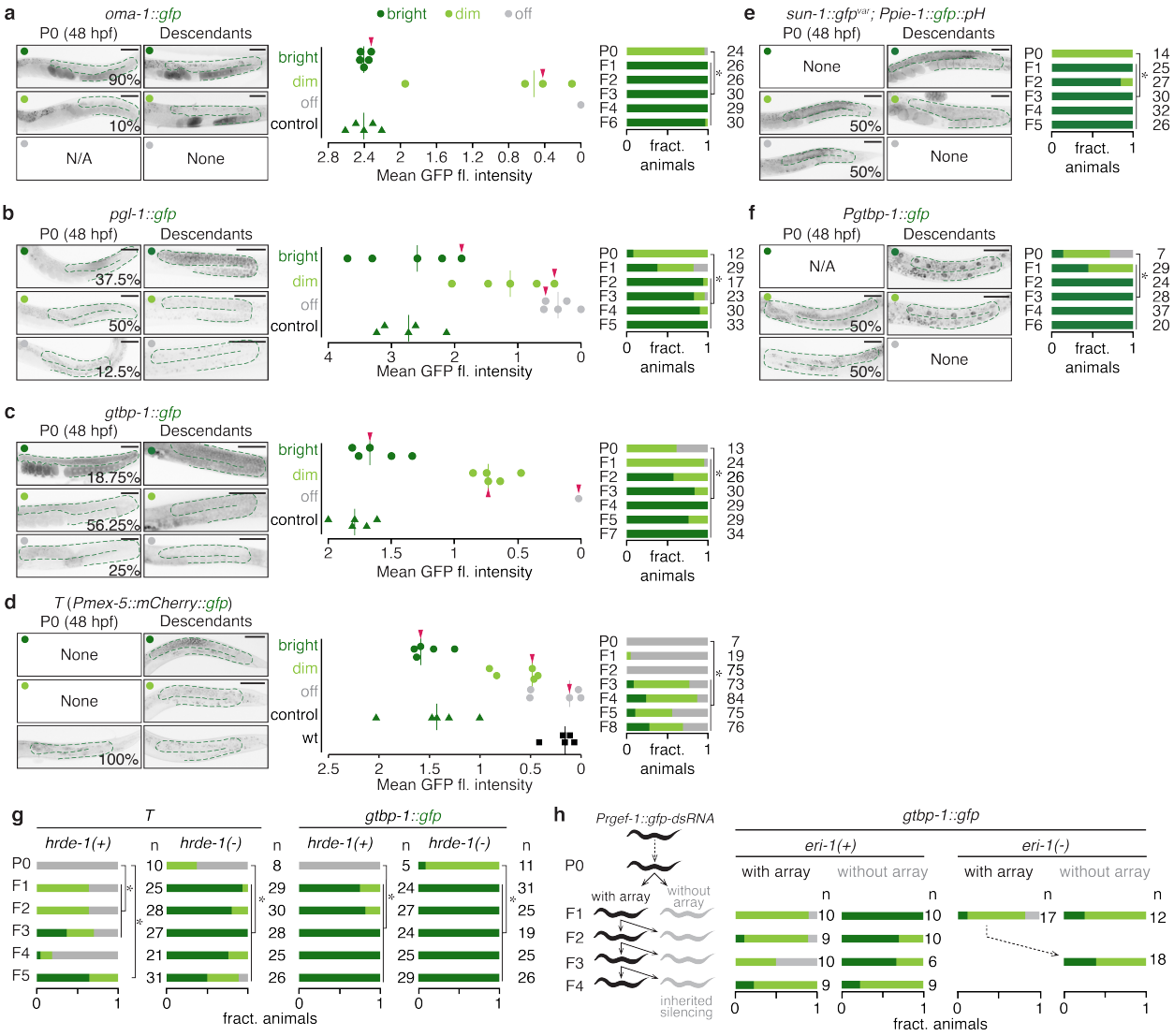

Supplementary Fig. 8. The same target sequence can show variability in transgenerational silencing within the germline upon feeding RNAi.

a to f Six target genes expressing *gfp* (green) were exposed to control RNAi or *gfp* RNAi. The target genes were low copy (*Ppie-1::gfp::pH*, *oma-1::gfp*, *T* (*Pmex-5::mCherry::gfp*)) transgenes or endogenous gene reporters (*gtbp-1::gfp*, *pgl-1::gfp*, *Pgtbp-1::gfp*). Representative images of the germline (*far left*) of P0 animals exposed to RNAi for 24 hours and imaged an additional 24 hours later (48 hours post feeding (hpf)) to eliminate any GFP protein perdurance, are shown. Images of (*middle left*) and the level of GFP expression in (*middle right*) representative descendant animals (F1-F8) categorized as bright, dim or off are shown. Average (green or grey vertical lines) GFP fluorescence intensity within the germline was calculated for descendants of animals exposed to *gfp*-dsRNA (circles, bright: dark green, dim: light green, off: grey) or control dsRNA (green triangles). One to five L4-staged hermaphrodites were quantified after scoring fluorescence from animals by eye within each category. Red arrowheads indicate fluorescence of animals shown in representative images on the left. P0 animals (24 hpf) and F1-F8 descendants were analysed for expression of GFP and categorized based on intensity of fluorescence (*far right*). The P0 to F7 data for *gtbp-1::gfp* (**c**) are the same as in

Fig. 6d. Asterisks indicate $P < 0.05$ using χ^2 test. Scale bar (50 μm) and numbers of animals scored (n) are indicated. N/A indicates not available. Percentages of animals that are silenced as much as or more than the animals shown in the image.
g Hermaphrodites expressing *T* or *gtbp-1::gfp* in a wild-type (*hrde-1(+)*) or *hrde-1(-)* background were exposed to *gfp* RNAi for 24 hours and descendants in subsequent generations (F1-F5) were scored.
h *gtbp-1::gfp* animals expressing neuronal dsRNA against *gfp* (*Prgef-1::gfp-dsRNA*, black) from a mitotically unstable array can have progeny with or without the array. Animals expressing dsRNA in a wild-type (*eri-1(+)*) or *eri-1(-)* background with or without the dsRNA array were scored for expression of GFP. Asterisks indicate $P < 0.05$ using χ^2 test. Numbers of animals scored (n) are indicated.

Supplementary Tables

Supplementary Table 1. Reports on heritability of RNA silencing suggest variable stability of induced RNA silencing.

Target	Genetic background	Generations of inherited silencing	Reference
dpy-11, mex-3, unc-22, lir-1, lin-15, unc-15, dpy-13, sqt-3, dpy-28, pos-1, par-1, dpy-11	*eri-1(-)*	1	42-51
Plet-858::gfp, Psur-5::sur-5::gfp, Pmyo-3::gfp, pes-10::gfp	wild type	1	43, 46, 51, 52
Pdpy-30::mcherry::gpd-2/3::gfp	wild type	1	53
mom-2, pos-1, sgg-1, unc-22, dpy-11	wild type	2	54, 55
Ppie-1::gfp::H2B	wild type	3	50
oma-1	*met-2(-); set-25(-); set-32(-)*	2-5	20, 42, 44, 50, 56-58
Ppie-1::gfp::H2B	wild type	1-9	12, 20, 42, 51, 58-60
Pcdk-1::gfp	wild type	> 10	16
Ppie-1::gfp::H2B	*eri-1(-)*	>20	61
Ppie-1::gfp::H2B	*heri-1(-)*	>23	56
gfp::his-58	wild type	>30	14
oma-1 *Pmex-5::gfp*	*met-2(-)*	>10 >30	57, 62
Pmex-5::mCherry::gfp	wild type	>25	63

Supplementary Table 2. Comparison of mating-induced silencing with related epigenetic phenomena.

Phenomenon	Reference(s) for the phenomenon	Similarity with mating-induced silencing	Difference from mating-induced silencing
Paramutation in plants, flies, or mice	1, 2, 4-9	Silencing is transgenerational. Silenced allele inherited through either gamete can silence homologous sequences.	Whether silencing will occur is not predictable at the population level. When a silenced allele induces meiotically heritable silencing of another allele, this allele also becomes a silencing allele.
RNA induced epigenetic silencing (RNAe)	12-14, 16, 19	Initiation requires PRG-1; maintenance requires HRDE-1. Silencing is transgenerational.	Silencing cannot be predictably initiated. The same DNA inserted into the same locus can show expression or silencing.

			Changes upon mating, if any, are unknown.
Multi-generational RNAe caused by meiotic silencing by unpaired DNA	27	Initiation requires PRG-1. oxSi487 (T in our study) introduced through the male parent showed silencing in cross progeny.	Effect of introducing oxSi487 through the hermaphrodite parent on silencing in cross progeny or its hemizygous descendants was not tested.
RNA-induced epigenetic gene activation (RNAa)	17, 18, 64	Extragenic signal can be inherited from male to control gene expression in progeny. Inheritance of an active transgene from hermaphrodite affects expression of paternally inherited transgene.	Extragenic signals inherited from sperm promote expression.
Meiotic silencing by unpaired DNA	28	Silencing occurs on hemizygous DNA.	DNA must be unpaired during meiosis for silencing.
Epigenetic licensing of *fem-1*	26	Maternal transcript of a gene is sufficient to enable expression of the paternal copy in the zygote.	Repeated crossing was required for increased severity of silencing.
Genomic imprinting and parent of origin effects	38, 39, 65	Silencing occurs when a gene is inherited through a specific gamete.	Expression is reset upon passage through the other gamete.
Transposon silencing in flies	6, 66	Inherited piRNAs silence a paternally inherited gene.	Maternal transcript does not prevent gene silencing.
Transvection in flies	67	Interaction between alleles on homologous chromosomes can result in changed expression.	Changes in gene expression are not heritable.
Licensing by DNA sequences	25	Not all transgenes are susceptible to germline silencing.	Initiation of silencing is independent of mating.

Supplementary Table 3. Strains used*.

Strain Name	Genotype
N2	wild type
AMJ471	*jamEx140* [*Prgef-1::gfp-dsRNA:: unc-54 3' utr & Pmyo-2::DsRed::unc-54 3' utr*]
AMJ501	*oxSi487* (*Pmex-5::mCherry::h2b::tbb-2 3'utr::gpd-2 operon::gfp::h2b::cye-1 3' utr + unc-119(+)*) II*; unc-119(ed3)* III?; *sid-1(qt9)* V
AMJ506	*prg-1(tm872)* I*; oxSi487* II; *unc-119(ed3)*? III
AMJ544	*oxSi487* II*; unc-119(ed3)?* III; *nrde-3(tm1116)* X
AMJ545	*oxSi487* II*; unc-119(ed3)* III?; *rde-1(ne219)* V
AMJ552	*oxSi487 dpy-2(jam33)* II; *unc-119(ed3)?* III [*iT*]
AMJ577	*hrde-1(tm1200)* III [4x]
AMJ581	*oxSi487 dpy-2(e8)* II
AMJ586	*oxSi487 dpy-2(e8)* II; *unc-119(ed3)?* III; *rde-1(ne219)* V
AMJ587	*rde-3/mut-2(jam9)* I
AMJ591	*jamSi25* [*Punc-119deletion *jamSi19*] II [*T*ΔΔ]
AMJ593	*oxSi487 dpy-2(e8)* II; *unc-119(ed3)?* III; *sid-1(qt9)* V
AMJ602	*oxSi487 dpy-2(e8)* II; *unc-119(ed3)? hrde-1(tm1200)* III
AMJ626	*rrf-1(ok589)* I; *oxSi487 dpy-2(e8)* II; *unc-119(ed3)?* III
AMJ646	*dpy-17(e164) unc-32(e189)* III; *rde-1(ne219)* V
AMJ647	*dpy-17(e164) unc-32(e189)* III; *sid-1(qt9)* V
AMJ667	*dpy-20(e1282) ax2053* [*gtbp-1::gfp*] IV
AMJ673	*rrf-1(ok589)* I; *dpy-2(e8) unc-4(e120)* II
AMJ675	*oxSi487* II; *unc-119(ed3)? hrde-1(tm1200)* III
AMJ683	*oxSi487 dpy-2(e8)* II; *unc-119(ed3)?* III*; nrde-3(tm1116)* X
AMJ685	*K08F4.2::gfp* [*Pgtbp-1::gtbp-1::gfp*] IV; *jamEx140*
AMJ689	*rrf-1(ok589)* I; *oxSi487* II; *unc-119(ed3)?* III
AMJ690	*dpy-2(e8) unc-4(e120)* II; *nrde-3(tm1116)* X
AMJ691	*dpy-2(e8) unc-4(e120)* II; *hrde-1(tm1200)* III
AMJ692	*oxSi487 dpy-2(e8)* II [*iT*]
AMJ693	*dpy-2(e8) unc-4(e120)* II; *Pmex-5::mCherry^{var2}::mex-5::mex-5 3' utr* IV
AMJ709	*dpy-10(jam21) jamSi25* [*Punc-119deletion *jamSi19*] II [*T*ΔΔ]
AMJ711	*prg-1(tm872)* I [1x]
AMJ712	*dpy-2(e8) unc-4(e120)* II; *Pgtbp-1::gtbp-1::RFP::linker::3xflag::gtbp-1 3'utr* IV
AMJ713	*dpy-2(e8) unc-4(e120)* II; *Ppgl-1::pgl-1::gfp::pgl-1 gfp 3' utr* IV
AMJ714	*oxSi487* II; *unc-119(ed3)? hrde-1(tm1200)* III
AMJ724	*oxSi487* II; *unc-119(ed3)?* III [*iT*]
AMJ725	*oxSi487* II; *unc-119(ed3)?* III
AMJ727	*dpy-2(e8) unc-4(e120)* II; *gtbp-1::mCherry^{var}* IV
AMJ753	*dpy-10(jam38) oxSi487* II; *unc-119(ed3)* III
AMJ763	*dpy-10(jam40) jamSi16* [*Pmex-5::mCherry::h2b::cye-1 3' utr *oxSi487*] II [*T*Δ]

AMJ765	*dpy-10(jam41) jamSi18* [*Pmex-5::mCherry::h2b::cye-1 3' utr *oxSi487*] II [*T*Δ]
AMJ766	*jamSi19* [*Pmex-5::mCherry::h2b::cye-1 3' utr *oxSi487*] II [*T*Δ]
AMJ767	*dpy-10(jam42) jamSi20* [*Pmex-5::mCherry::h2b::cye-1 3' utr *oxSi487*] II [*T*Δ]
AMJ768	*dpy-10(jam43) jamSi21* [*Pmex-5::mCherry::h2b::cye-1 3' utr *oxSi487*] II [*T*Δ]
AMJ769	*dpy-10(jam44) oxSi487* II; *unc-119(ed3)* III
AMJ774	*dpy-10(jam139) jamSi23* [*Pmex-5::mCherry (6 bp indel)::h2b::tbb-2 3' utr::gpd-2 operon::gfp::h2b::cye-1 3' utr *oxSi487*] II; *unc-119(ed3)* III [*T**]
AMJ777	*dpy-10(jam45)* II
AMJ792	*dpy-10(jam46)* II
AMJ819	*Pgtbp-1::gtbp-1::gfp eri-1(mg366)* IV
AMJ842	*Pgtbp-1::gtbp-1::gfp eri-1(mg366)* IV; *jamEx140*
AMJ844	*oxSi487 dpy-2(e8)* II [*iT*]
AMJ917	*dpy-10(jam47) jamSi20* [*Pmex-5::mCherry::h2b::cye-1 3' utr *oxSi487*] II; *unc-119(ed3)* III [*iT*Δ]
AMJ918	*dpy-10(jam140) jamSi32* [*Pmex-5::mCherry (3 bp indel)::h2b::cye-1 3' utr *jamSi19*] II; *unc-119(ed3)* III [*T*Δ*]
AMJ919	*dpy-10(jam141) jamSi33* [*Pmex-5::mCherry (2 bp indel)::h2b::cye-1 3' utr *jamSi25*] II; *unc-119(ed3)* III [*T*ΔΔ*]
AMJ922	*prg-1(tm872)* I [1x]; *dpy-2(e8) oxSi487* II; *unc-119(ed3)?* III
AMJ923	*prg-1(tm872)* I [1x]; *dpy-2(e8) unc-4(e120)* II
AMJ926	*dpy-10(jam39) jamSi27* [*Pmex-5::mCherry::cye-1 3' utr *jamSi25*] II [*T*ΔΔΔ]
AMJ928	*jamSi27* [*Pmex-5::mCherry::cye-1 3' utr *jamSi25*] II [*T*ΔΔΔ]
AMJ930	*dpy-10(jam68)* II
AMJ929	*oxSi487* II
AMJ1045	*oxSi487* II; *unc-119(ed3)? hrde-1(tm1200)* III
AMJ1100	*oxSi487 unc-4(e120)* II; *unc-119(ed3)?* III
AMJ1101	*oxSi487 unc-4(e120)* II; *unc-119(ed3)?* III
AMJ1102	*oxSi487 unc-4(e120)* II; *unc-119(ed3)?* III
AMJ1103	*oxSi487 unc-4(e120)* II; *unc-119(ed3)?* III
AMJ1116	*oxSi487 dpy-2(e8)* II; *unc-119(ed3)?* III; *met-2(n4256)* III
AMJ1117	*oxSi487 dpy-2(e8)* II; *unc-119(ed3)?* III; *met-2(n4256)* III
AMJ1118	*oxSi487 dpy-2(e8)* II; *unc-119(ed3)?* III; *met-2(n4256)* III
AMJ1126	*mut-16(pk710)* I; *oxSi487 dpy-2(e8)* II; *unc-119(ed3)?* III
AMJ1127	*mut-16(pk710)* I; *oxSi487 dpy-2(e8)* II; *unc-119(ed3)?* III
AMJ1128	*mut-16(pk710)* I; *oxSi487 dpy-2(e8)* II; *unc-119(ed3)?* III
AMJ1135	*rde-3/mut-2(jam9)* I; *oxSi487 dpy-2(e8)* II; *unc-119(ed3)?* III
AMJ1136	*rde-3/mut-2(jam9)* I; *oxSi487 dpy-2(e8)* II; *unc-119(ed3)?* III
AMJ1137	*met-2(n4256)* III; *Pgtbp-1::gtbp-1::gfp* IV
AMJ1138	*met-2(n4256)* III; *Pgtbp-1::gtbp-1::gfp* IV
AMJ1139	*met-2(n4256)* III; *Pgtbp-1::gtbp-1::gfp* IV
AMJ1142	*oxSi487 dpy-2(e8)* II; *unc-119(ed3)?* III; *pgl-1(ct131) him-3(e1147)* IV
AMJ1143	*oxSi487 dpy-2(e8)* II; *unc-119(ed3)?* III; *pgl-1(ct131) him-3(e1147)* IV

AMJ1157	*oxSi487 dpy-2(jam33)* II; *unc-119(ed3)?* III; *rde-8(jam75)* IV
AMJ1158	*oxSi487 dpy-10(jam82) dpy-2(jam33)* II; *unc-119(ed3)?* III; *rde-8(jam76)* IV
AMJ1162	*dpy-10(jam43) oxSi487* II; *unc-119(ed3)* III
AMJ1170	*jamSi37* [*Pmex-5::mCherry::cye-1 3'UTR + unc-119(+)*] II; *unc-119(ed3)* III
AMJ1174	*dpy-10(jam106) jamSi37 [Pmex-5::mCherry::cye-1 3'UTR]* II*; unc-119(ed3)* III
AMJ1176	*jamSi27* II*; Pgtbp-1::gtbp-1::gfp* IV
AMJ1186	*jamSi37* II*; unc-119(ed3)?* III
AMJ1190	*jamSi38* [*Pmex-5::mCherry::cye-1 3'utr*] II; *unc-119(ed3)* III [*Tcherry*^{Crispr}]
AMJ1191	*jamSi40* [*Pmex-5::mCherry::cye-1 3'utr*] II; *unc-119(ed3)* III [*Tcherry*^{Crispr}]
AMJ1192	*jamSi41* [*Pmex-5::mCherry::cye-1 3'utr*] II; *unc-119(ed3)* III [*Tcherry*^{Crispr}]
AMJ1195	*jamSi59* [*Pmex-5::gfp::cye-1 3'UTR + unc-119(+)*] II*; unc-119(ed3)* III [*Tgfp*]
AMJ1200	*jamSi60* [*Pmex-5::gfp::cye-1 3'UTR + unc-119(+)*] II*; unc-119(ed3)* III [*Tgfp*]
AMJ1206	*set-32(jam46)* I*; oxSi487 dpy-2(e8)* II*; unc-119(ed3)?* III
AMJ1207	*oxSi487 dpy-2(e8) heri-1(jam47)* II*; unc-119(ed3)?* III
AMJ1208	*jam197* [*Pmex-5::mCherry::mex-5::mex-5 3'UTR*] IV
AMJ1209	*jamSi39* [*Pmex-5::mCherry (without piRNA sites)::cye-1 3' utr*] II; *unc-119(ed3)* III [*TcherryΔpi*]
AMJ1210	*jamSi42* [*Pmex-5::mCherry (without piRNA sites)::cye-1 3' utr*] II; *unc-119(ed3)* III [*TcherryΔpi*]
AMJ1211	*jamSi43* [*Pmex-5::mCherry (without piRNA sites)::cye-1 3' utr*] II; *unc-119(ed3)* III [*TcherryΔpi*]
AMJ1212	*jamSi44* [*Pmex-5::mCherry (without piRNA sites)::cye-1 3' utr*] II; *unc-119(ed3)* III [*TcherryΔpi*]
AMJ1213	*dpy-10(jam73) jamSi39* II; *unc-119(ed3)* III [*TcherryΔpi*]
AMJ1214	*dpy-10(jam74) jamSi42* II; *unc-119(ed3)* III [*TcherryΔpi*]
AMJ1215	*dpy-10(jam84) jamSi43* II; *unc-119(ed3)* III [*TcherryΔpi*]
AMJ1216	*dpy-10(jam85) jamSi44* II; *unc-119(ed3)* III [*TcherryΔpi*]
AMJ1228	*mut-16(pk710)* I; *oxSi487* II; *unc-119(ed3)* III
AMJ1236	*jamSi37* II*; unc-119(ed3?)* III*; Pgtbp-1::gtbp-1::gfp* IV
AMJ1238	*dpy-10(jam106) jamSi37* II
AMJ1240	*dpy-10(jam106) jamSi37* II*; ccTi1594 [Pmex-5::gfp::gpr-1::smu-1 3'UTR + Cbr-unc-119(+)] unc-119(ed3?)* III
AMJ1245	*jamSi61 [Pmex-5::gfp::cye-1 3' utr + unc-119(+)]* II; *unc-119(ed3)* III [*Tgfp*]
AMJ1248	*dpy-10(jam142) jamSi51* [*Pmex-5::cye-1 3' utr *jamSi37*] II; *unc-119(ed3)* III [*TΔorf*]
AMJ1249	*dpy-10(jam143) jamSi49* [*Pmex-5::cye-1 3' utr *jamSi37*] II; *unc-119(ed3)* III [*TΔorf*]
AMJ1259	*hrde-1(tm1200)* III; *fog-2(q71)* V
AMJ1260	*hrde-1(tm1200)* III; *fog-2(q71)* V
AMJ1261	*hrde-1(tm1200)* III; *fog-2(q71)* V
AMJ1267	*dpy-10(jam106) jamSi37* II*; ccTi1594 unc-119(ed3?)* III
AMJ1268	*dpy-10(jam106) jamSi37* II*; ccTi1594 unc-119(ed3?)* III
AMJ1272	*jamSi45* [*unc-119(+) Pmex-5::mCherry::mex-5 3' utr*] II; *hrde-1(tm1200)* III [*Tcherry mex-5 3' utr*]

AMJ1273	*jamSi47* [*unc-119(+) Pmex-5::mCherry::mex-5 3' utr*] II; *hrde-1(tm1200)* III [*Tcherry mex-5 3' utr*]
AMJ1274	*jamSi46* [*unc-119(+) Pmex-5::mCherry::mex-5 3' utr*] II; *hrde-1(tm1200)* III [*Tcherry mex-5 3' utr*]
AMJ1275	*jamSi48* [*unc-119(+) Pmex-5::mCherry::mex-5 3' utr*] II; *hrde-1(tm1200)* III [*Tcherry mex-5 3' utr*]
AMJ1288	*dpy-10(jam144) jamsSi52* II; *unc-119(ed3)* III [*TcherryΔpi N*]
AMJ1290	*dpy-10(jam146) jamsSi54* II; *unc-119(ed3)* III [*TcherryΔpi C*]
AMJ1296	*unc-119(ed3) cde-1(jam111)* III
AMJ1307	*oxSi487* II*; unc-119(ed3) cde-1(jam110)* III
AMJ1308	*oxSi487 dpy-10(jam138)* II*; unc-119(ed3)? cde-1(jam111)* III
AMJ1320	*rrf-1(ok589) ego-1(jam93)* I
AMJ1321	*rrf-1(ok589) ego-1(jam93)* I
AMJ1336	*dpy-10(jam147) jamSi57* [*Pmex-5::mCherry(exon 4)::cye-1 3' utr *jamSi39*] II; *unc-119(ed3)* III [*TcherryΔpi exon 4*]
AMJ1337	*dpy-10(jam149) jamSi58* [*Pmex-5::mCherry(exon 4)::cye-1 3' utr *jamSi39*] II; *unc-119(ed3)* III [*TcherryΔpi exon 4*]
AMJ1338	*jamSi56* I; *unc-119(ed3)* III [*Tcherry* I]
AMJ1339	*jamSi63* [*unc-119(+) Pmex-5::mCherry::tbb-2 3' utr*] II; *hrde-1(tm1200)* III [*Tcherry tbb-2 3' utr*]
AMJ1340	*jamSi64* [*unc-119(+) Pmex-5::mCherry::tbb-2 3' utr*] II; *hrde-1(tm1200)* III [*Tcherry tbb-2 3' utr*]
AMJ1341	*jamSi65* [*unc-119(+) Pmex-5::mCherry::tbb-2 3' utr*] II; *hrde-1(tm1200)* III [*Tcherry tbb-2 3' utr*]
DR439	*unc-8(e49) dpy-20(e1282)* IV
EG4322	*ttTi5605* II; *unc-119(ed9)* III
EG6787	*oxSi487* II*; unc-119(ed3)* III
EG6771	*oxSi466* [*Pdpy-30::gfp::h2b::tbb-2 cb-unc-119(+)*] II; *unc-119(ed3)* III [gift from Christian Frøkjær-Jensen]
EG6779	*oxSi474* [*Pdpy-30::gfp::h2b::tbb-2 cb-unc-119(+)*] I; *unc-119(ed3)* III [gift from Christian Frøkjær-Jensen]
EG6808	*unc-119(ed3)* III; *oxTi132* [*Pdpy-30::gfp::h2b::tbb-2 cb-unc-119(+)*] V (*him-5* in background?) [gift from Christian Frøkjær-Jensen]
EG6810	*unc-119(ed3)* III; *oxTi134* [*Pdpy-30::gfp::h2b::tbb-2 cb-unc-119(+)*] I (*him-5* in background?) [gift from Christian Frøkjær-Jensen]
EG6814	*unc-119(ed3)* III; *oxTi138* [*Pdpy-30::gfp::h2b::tbb-2 cb-unc-119(+)*] I (*him-5* in background?) [gift from Christian Frøkjær-Jensen]
EG6838	*unc-119(ed3) oxTi162* [*Pdpy-30::gfp::h2b::tbb-2 cb-unc-119(+)*] III (*him-5* in background?) [gift from Christian Frøkjær-Jensen]
GE1708	*dpy-2(e8) unc-4(e120)* II
GR1373	*eri-1(mg366)* IV
HC196	*sid-1(qt9)* V
HC780	*rrf-1(ok589)* I
HT1593	*unc-119(ed3)* III
JH3197	*ax2053* (*Pgtbp-1::gtbp-1::gfp*) IV [gift from Geraldine Seydoux]

JH3270	*Ppgl-1::pgl-1::gfp::pgl-1 gfp 3' utr* IV [gift from Geraldine Seydoux]
JH3296	*Pmex-5::mCherry^{var2}::mex-5::mex-5 3' utr* IV [gift from Geraldine Seydoux]
JH3323	*Pgtbp-1::gtbp-1::mCherry::gtbp-1 3' utr* IV [*gtbp-1::mCherry^{var}*; gift from Geraldine Seydoux]
JH3337	*Pgtbp-1::gtbp-1::RFP::linker::3xflag::gtbp-1 3'utr* II [gift from Geraldine Seydoux]
JH4009	*Pgtbp-1::gfp::h2b::gtbp-1 3'utr* II [gift from Geraldine Seydoux]
MT13293	*met-2(n4256)* III
NL1810	*mut-16(pk710)* I
OCF62	*jfSi1* [*Psun-1::gfp cb-unc-119(+)*] II*; ltIs38* [*(pAA1) pie-1::GFP::PH(PLC1delta1) + unc-119(+)*] [*sun-1::gfp^{var}*; gift from Orna Cohen-Fix]
OCF69	*ocfSi1* [*Pmex-5::Dendra2::his-58::tbb-2 3' utr + unc-119(+)*] I*; unc-119(ed3)* III [gift from Orna Cohen-Fix]
PD1594	*ccTi1594 unc-119(ed3)* III (*gpr-1 oe*)
SP471	*dpy-17(e164) unc-32(e189)* III
SS2	*pgl-1(ct131) him-3(e1147)* IV
TX189	*unc-199(ed3)* III*; teIs1* [*(pRL475) oma-1p::oma-1::GFP + (pDPMM016) unc-119(+)*] IV
WM27	*rde-1(ne219)* V
WM156	*nrde-3(tm1116)* X
WM161	*prg-1(tm872)* I

*All strains with fluorescent reporters showed invariable expression of fluorescence, except as indicated throughout the manuscript and in OCF69, which showed suppression of expression in one of the 34 animals examined by imaging.

Supplementary Table 4. Oligonucleotides used*.

P1	ATAAGGAGTTCCACGCCCAG
P2	CTAGTGAGTCGTATTATAAGTG
P3	TGAAGACGACGAGCCACTTG
P4	ATCGTGGACGTGGTGGTTAC
P5	CTCATCAAGCCGCAGAAAGAG
P6	GGTTCTTGACAGTCCGAACG
P7	ACGGTGAGGAAGGAAAGGAG
P8	ACAAGAATTGGGACAACTCCAG
P9	AGTAACAGTTTCAAATGGCCG
P10	TCTTCACTGTACAATGTGACG
P11	CACTATTCACAAGCATTGGC
P12	CGGACAGAGGAAGAAATGC
P13	TGCCATCGCAGATAGTCC
P14	TGGAAGCAGCTAGGAACAG
P15	CCGTGACAACAGACATTCAATC
P16	ACGATCAGCGATGAAGGAG
P17	GGAGATCCATGATTAGTTGTGC
P18	GCAGGCATTGAGCTTGAC

P19	TCATCTCGGTACCTGTCGTTG
P20	AGAGGCGGATACGGAAGAAG
P21	CATAACCGTCGCTTGGCAC
P22	TCGAGTCGTGGTACAGATCG
P23	CATGCTCGTCGTAATGCTCG
P24	CGATCGTGCCAGAACAATCC
P25	ATGAAAGCCGAGCAACAACG
P26	AGAATGATGAGTCGCCACAGG
P27	CATGCACAACAAAGCCGACTAC
P28	TGAGAATACGGTCGCAGTTAGG
P29	ACGGATGCCTAGTTGCATTG
P30	CCTTCCCAGAGGGATTCAAGTG
P31	TCTGTTCCTATTCTGTCTGCAC
P32	CGCGGTTCGCAATAGGTTTC
P33	TCACCTAGTCTGTGCCATTTC
P34	TGCGGGTTTCTGTTAGCTTC
P35	GCACAGACTAGGTGAAAGAGAG
P36	ACCTCCCACAACGAGGATTAC
P37	TGGGCGTGGAACTCCTTATC
P38	GGCGAAGAGCAAAGCAGAG
P39	GGGCCGTTATCCTTTCAAATGC
P40	CATGGGCCACGGATTGTAAC
P41	ACGCATCTGTGCGGTATTTC
P42	ATTTAGGTGACACTATAGGATCAGGTAGTGGCCCACCAGTTTTAGAGCTA GAAATAGCAAG
P43	AAAAGCACCGACTCGGT
P44	ATGGTCTCCAAGGGAGAGGAG
P45	GAATCCTATTGCGGGTTATTTTAGCCACTACCTGATCCCTTG
P46	ATTTAGGTGACACTATAGGTGTAATCCTCGTTGTGGGGTTTTAGAGCTAGA AATAGCAAG
P47	CAAGGGATCAGGTAGTGGCTAAAATAACCCGCAATAGGATTC
P48	TAAGGAGTTCCACGCCCAG
P49	TTTCGCTGTCCTGTCACACTC
P50	CGATGATAAAAGAATCCTATTGCGGGTTATTTTTTGAGCCTGCTTTTTTGTA CAAACTTG
P51	CAAGTTTGTACAAAAAAGCAGGCTCAAAAAATAACCCGCAATAGGATTCT TT TATCATCG
P52	AGCTAACAGAAACCCGCATAC
P53	CCTGTCACACTCGCTAAAAACAC
P54	ACAGAAACCCGCATACTCG
P55	ATTTAGGTGACACTATAGATTCCTTGTTCGGTGCTTGGGTTTTAGAGCTAG AAATAGCAAG
P56	ATTCCATGATGGTAGCAAACTCACTTCGTGGGTTTTCACAACGGCAAAATA TCAGTTTTT

P57	ATTTAGGTGACACTATAGCTACCATAGGCACCACGAGGTTTTAGAGCTAG AA ATAGCAAG
P58	CACTTGAACTTCAATACGGCAAGATGAGAATGACTGGAAACCGTACCGCA TG CGGTGCCTATGGTAGCGGAGCTTCACATGGCTTCAGACCAACAGCCTA
P59	ATTTAGGTGACACTATAGACAAATGCCCGGGGGATCGGGTTTTAGAGCTA GAAATAGCAAG
P60	TGAGGTCAAGACCACCTACAAG
P61	GAATCCTATTGCGGGTTATTTTACTTGCTGGAAGTGTACTTGG
P62	CCAAGTACACTTCCAGCAAGTAAAATAACCCGCAATAGGATTC
P63	GACCACCTACAAGGCTAAGAAG
P64	ATTTAGGTGACACTATAGGGGAGAGGGAAGACCATACGGTTTTAGAGCTA GAAATAGCAAG
P65	GCAAAAATTCCCCGACTTTCCC
P66	GAAAAGTTCTTCTCCTTTACTCATTTTTGAGCCTGCTTTTTTGTAC
P67	GTACAAAAAAGCAGGCTCAAAAATGAGTAAAGGAGAAGAACTTTTC
P68	CCCATGGAACAGGTAGTTTTCC
P69	CGACTTTCCCCAAAATCCTGC
P70	ACAGGTAGTTTTCCAGTAGTGC
P71	AGAGGGATTCAAGTGGGAGAG
P72	TGGGTCTTACCGCGTATACC
P73	TGATCCCTTGTAAAGCTCATCC
P74	GTGTGTGCTGCTCGGTTAAG
P75	AATTCCACAGTTGCTCCGAC
P76	TCATCTCGCCCGATTCATTG
P77	CCGTTTCTTCCTGGTAATCC
P78	GGGTGAAGGTGATGCAACATAC
P79	GGGACAACCTGTGTGCATG
P80	AAGGTCCACATGGAGGGATC
P81	AAAGTAATTCTACAGTATTCCTGAGATG
P82	CGTCTCTTGATATTCCTTGC
P83	CCAAGCGAATGGAAGCTGAAAATT
P84	CAAGCGAATGGAAGTGGTCCT
P85	GTAGTGACAAGTGTTGGCCATGG
P86	TCACATACACATCTTCTGCACC
P87	TTGGTAGAAGCTGCATCACTTT
P88	CCAGACGGAACCTTCAAG
P89	TCCGTCTGAAAAAATTTAATTAATT
P90	GAGATTCAAGGTCCACATGGAGG
P91	ATGGAAGTGGTCCTCCCTTGG
P92	TCTTCGGCGCTAATCTTTTC
P93	CACGAGTTCGAGATCGAG
P94	GTCATCTCCGACGAGCAC
P95	TTCCGTTGTTGGCTTCGTTG
P96	TTCTGTCAGTGGAGAGGG
P97	GTGTTGGCTGAAAATTTAAATAAT

P98	GGTGATGTTAATGGGCAC
P99	TGTTGGCCATGGAACAGG
P100	ATTTAGGTGACACTATAGGATTACTCATAATGACATGGTTTTAGAGCTAGAAATAGCAAG
P101	GGACCACGTGGAGTTCCAGGACATCCAGGTTTTCCAGGTGACCCAGGAGAGTATGGAATT
P102	ATTTAGGTGACACTATAGCGTTGGTGATGGTGATGAGGTTTTAGAGCTAGAAATAGCAAG
P103	ATCTGATTATTATATTTCAGATTACTCATAATTAATGTATTCAATTTGTTAATATATTTC
P104	ATTTAGGTGACACTATAGTGCTTCGATAGATCTCGAGGTTTTAGAGCTAGAAATAGCAAG
P105	ATTTAGGTGACACTATAGTTCAGCTTACAATGGACTAGTTTTAGAGCTAGAAATAGCAAG
P106	TTAATTCTTAACAAAAAACTGTTTCCGCTCCTACGGATACAACTACATGAAAAATCATCT
P107	ATTTAGGTGACACTATAGAGTAGTTACTGATGAGCTGGTTTTAGAGCTAGAAATAGCAAG
P108	ATTTAGGTGACACTATAGTCGAGCTGTAGGCTCTTGGGTTTTAGAGCTAGAAATAGCAAG
P109	GAGAGATTCAAAAGAACAAAAAAGCCGCAGAGAGCCTACAGCTCGATCTGTAGAGTGTTT
P110	GCUACCAUAGGCACCACGAGGUUUUAGAGCUAUGCU
P111	AGCAUAGCAAGUUAAAAUAAGGCUAGUCCGUUAUCAACUUGAAAAAGUGGCACCGAGUCGGUGCUUU
P112	TGATGATAGCCATGTTATCC
P113	GTGGACCTTGAATCTCATGA
P114	CTCTCCCTCGATCTCGAACTCGTGTC
P115	CTTGGTGACCTTAAGCTTAG
P116	GATATCCCAAGCGAATGGAA
P117	CGTACATGAACTGTGGGGAA
P118	TGCTTGACGTAAGCCTTGGA
P119	GGTAATCTGGGATATCAGCT
P120	GAATCCCTCTGGGAAGGAAA
P121	ATCCTCGAAGTTCATGACTC
P122	GAATCCTGGGTGACGGTGAC
P123	ATGAACTCTCCATCCTGAAG
P124	TCCTCTAAGCTTGACCTTGT
P125	GTCCATCGGATGGGAAGTTG
P126	ATGGTCTTCTTCTGCATGAC
P127	TACATTCTCTCGGAGGAAGC
P128	CTTGATCTCTCCCTTAAGAG
P129	TCCATCCTTAAGCTTAAGTC
P130	TTGACCTCAGCATCGTAGTG
P131	CTTCTTAGCCTTGTAGGTGG

P132	TAAGCTCCTGGAAGCTGGAC
P133	ATCAAGCTTGATGTTGACGT
P134	TGTAATCCTCGTTGTGGGAG
P135	CTCTCGTACTGCTCGACGAT
P136	TTGTAAAGCTCATCCATTCC
P137	AAGTTCTTCTCCTTTACTCA
P138	GAATTGGGACAACTCCAGTG
P139	CCCATTAACATCACCATCTA
P140	CCTCTCCACTGACAGAAAAT
P141	GTAAGTTTTCCGTATGTTGC
P142	TGGAACAGGTAGTTTTCCAG
P143	GGTATCTCGAGAAGCATTGA
P144	TCATGCCGTTTCATATGATC
P145	GGGCATGGCACTCTTGAAAA
P146	TTCTTTCCTGTACATAACCT
P147	GTTCCCGTCATCTTTGAAAA
P148	CCTTCAAACTTGACTTCAGC
P149	ACCTTTTAACTCGATTCTAT
P150	GTGTCCAAGAATGTTTCCAT
P151	GTGAGTTATAGTTGTATTCC
P152	GTCTGCCATGATGTATACAT
P153	CTTTGATTCCATTCTTTTG
P154	CCATCTTCAATGTTGTGTCT
P155	ATGGTCTGCTAGTTGAACGC
P156	CGCCAATTGGAGTA TTTTGT
P157	GTCTGGTAAAAGGACAGGGC
P158	AAGGGCAGATTGTGTGGACA
P159	TCTTTTCGTTGGGATCTTTC
P160	TCAAGAAGGACCATGTGGTC
P161	AATCCCAGCAGCTG TTACAA
P162	TATAGTTCATCCATGCCATG
P163	ATTTAGGTGACACTATAGTCAACTTCTAATTTTAATTCGTTTTAGAGCTAG AAATAGCAAG
P164	AUUUAGGUGACACUAUAGGUGAUGAACUUCGAGGAUGGGUUUUAGAGC UAGAAAUAGCAAG
P165	AUUUAGGUGACACUAUAGCUUUACAAGGGAUCAGGUAGGUUUUAGAGC UAGAAAUAGCAAG
P166	AUUUAGGUGACACUAUAGAAAAAUGGUCUCCAAGGGAGGUUUUAGAGC UAGAAAUAGCAAG
P167	AUUUAGGUGACACUAUAGCCUUCCCAGAGGGAUUCAAGGUUUUAGAGC UAGAAAUAGCAAG
P168	TCTCCTTCCCAGAGGGATTCAAGTGGGAGAGAGTGTAAAATAACCCGCAA TAGGATTCTTT TATCATCGA
P169	CAGAGACAAGTTTGTACAAAAAAGCAGGCTCAAAAATGAACTTCGAGGAT GGAGGAGTCGTCACCGTCAC

P170	AUUUAGGUGACACUAUAGAAUGGUCUCCAAGGGAGAGGGUUUUAGAGC UAGAAAUAGCAAG
P171	AUUUAGGUGACACUAUAGCUUUACAAGGGAUCAGGUAGGUUUUAGAGC UAGAAAUAGCAAG
P172	CAGAGACAAGTTTGTACAAAAAAGCAGGCTCAAAAAATAACCCGCAATA GGATTCTTTTATCATCGAAAT
P173	AUUUAGGUGACACUAUAGAAAAAUGGUCUCCAAGGGAGGUUUUAGAGC UAGAAAUAGCAAG
P174	AUUUAGGUGACACUAUAGUAAUCUGAUUUAAAUUUUCAGUUUUAGAGC UAGAAAUAGCAAG
P175	AGACAAGTTTGTACAAAAAAGCAGGCTCAAAAATGGGACACTACGATGCT GAGGTCAAGACCACCTACAA
P176	GCACATACTTTCCGTCTGAAAAAAT
P177	CGTGGCACATACTTTCCGTTGTTG
P178	GAAAGTAGTGACAAGTGTTGGCTG
P179	GGAAGCTGAAAATTTAAATAATCAG
P180	UUUCAGACAGAGAAUGAAAG
P181	ATTAATTTTATCGATAATCAATTGAATGTTTCAGACAGAGAATGGTCT CCAAGGGAGAGG
P182	ACTGATCCTCCGGCCGACGAGACACTATTTGATGCCGCTTTGCCACTA CCTGATCCCTTG

*RNA oligonucleotides have U in their sequence and DNA oligonucleotides have T in their sequence.

Supplementary Table 5. Reagents used for Cas9-mediated genome editing.

Allele name	CRISPR edit	DNA template for sgRNA transcription or crRNA sequence	Homology repair dsDNA or ssDNA template	Length of homology repair template	Concentration in pmol/µl of 1st & 2nd sgRNA or crRNA; homology repair template; *dpy-10* sgRNA# or crRNA; *dpy-10* homology repair template
+	*dpy-10(-)* in wild type	P57 (FOR), P43 (REV)	P58 (ssDNA)	100 b	-; -; -; 3.05; 0.66
T	*dpy-10(-)* in *oxSi487*	P57 (FOR), P43 (REV)	P58 (ssDNA)	100 b	-; -; -; 3.05; 0.66
T *	*mCherry* mutation in *oxSi487*$	P64 (FOR), P43 (REV), P163 (FOR)	Left: P65 + P66, Right: P67 + P68, Fusion: P69 + P70	309 bp	1.6; 1.4; 0.12; 1.3; 0.66
*TΔ**	*mCherry* mutation in *jamSi19* (*TΔ*)	P46 (FOR), P43 (REV)	P50 (ssDNA)	60 b	6.05; -; 8.85; 3.05; -
*TΔΔ**	*mCherry* mutation in *jamSi25* (*TΔΔ*)	P46 (FOR), P43 (REV)	P50 (ssDNA)	60 b	6.05; -; 8.85; 3.05; -
TΔ	Deletion of *gfp* and *tbb-2* 3'	P59 (FOR), P43 (REV)	Left: P60 + P61,	1074 bp	2.96; -; 0.08; 3.05; 0.66

	utr from *oxSi487*		Right: P62 + P52, Fusion: P63 + P54		
TΔΔ	Deletion of *Punc-119* from *jamSi19* (*TΔ*)	P55 (FOR), P43 (REV)	P56 (ssDNA)	60 b	8.4; -; 1.53; 8.16; 1.52
TΔΔΔ	Deletion of *h2b* from *jamSi25* (*TΔΔ*)	P42 (FOR), P43 (REV)	Left: P44 + P45, Right: P47 + P48, Fusion: P80 + P81	1604 bp	11.16; 12.87; 0.31; 2.89; 0.62
TcherryΔpi N	Deletion of *mCherry* C-terminus (*TcherryΔpi*)	P164 (crRNA), P165 (crRNA)	P168 (ssDNA)	70 b	4.0; 4.0; 24; 2.4; 100
TcherryΔpi C	Deletion of *mCherry* N-terminus (*TcherryΔpi*)	P166 (crRNA), P167 (crRNA)	P169 (ssDNA)	70 b	18.6; 11.2; 24; 2.4; 100
TcherryΔpi exon4	Deletion of three *mCherry* exons from *jamSi39* (*TcherryΔpi*)	P173 (crRNA), P174 (crRNA)	P175 (ssDNA)	70 b	4.9; 4.9; 3.6; 2.4; 100
TΔorf	Deletion of *mCherry* ORF from *jamSi37* (*Tcherry*)	P170 (crRNA), P171 (crRNA)	P172 (ssDNA)	70 b	4.8; 4.8; 25; 2.4; 100
iT	*dpy-2(-)* repair in *iT dpy-2(-)*	P42 (FOR), P43 (REV)	P101 (ssDNA)	60 b	7.2; -; 0.6; -; -
rde-8(-)	*rde-8* mutation in *iT*	P100 (FOR), P43 (REV), P102 (FOR)	P103 (ssDNA)	60 b	8.1; 10.9; 13.5; 6.9; 6.5
set-32(-)	*set-32* mutation in *iT*	P104 (FOR), P43 (REV), P105 (FOR)	P106 (ssDNA)	60 b	3.9; 3.9; 7.5; 2.8; 7.5
heri-1(-)	*heri-1* mutation in *iT*	P107 (FOR), P43 (REV), P108 (FOR)	P109 (ssDNA)	60 b	3.7; 3.7; 7.5; 2.3 crRNA (P110), 2.7 tracrRNA (P111); 7.5
mcherry::mex-5	*mcherry* N-terminal fusion	P180 (crRNA)	P181 (FOR) P182 (REV)	958 b	4.2; -; 0.35; 2.7; 6.5

[$]refers to cases where the resulting edit was not the originally intended edit and therefore does not relate to the reagents injected.
[#]*dpy-10* sgRNA was transcribed in vitro using a DNA template generated using primers P57 (forward) and P43 (reverse).

Supplementary References

1. Hollick, J. B. Paramutation and related phenomena in diverse species. *Nat. Rev. Genet* **18**, 5–23 (2017).

2. de Vanssay, A., Bougé, A. L., Boivin, A., Hermant, C., Teysset, L., Delmarre, V., Antoniewski, C., & Ronsseray, S. Paramutation in Drosophila linked to emergence of a piRNA-producing locus. *Nature* **490**, 112–115 (2012).

3. Brink, R. A. A Genetic Change Associated with the *R* Locus in Maize Which Is Directed and Potentially Reversible. *Genetics* **41** 872–889 (1956).

4. Chandler, V. L., Eggleston, W. B., and Dorweiler, J. E. Paramutation in maize. *Plant Mol. Biol* **43**, 121-145 (2000).

5. Rassoulzadegan, M., Grandjean, V., Gounon, P., Vincent, S., Gillot, I., and Cuzin, F. RNA-mediated non-mendelian inheritance of an epigenetic change in the mouse. *Nature* **441**, 469–474 (2006).

6. Kidwell, M. G., Kidwell, J. F., and Sved, J. A. Hybrid Dysgenesis in *DROSOPHILA MELANOGASTER*: A Syndrome of Aberrant Traits Including Mutation, Sterility and Male Recombination. *Genetics* **86**, 813–833 (1977).

7. Kermicle, J. L., Eggleston, W. B., and Alleman, M. Organization of paramutagenicity in R-stippled maize. *Genetics* **141**, 361–372 (1995).

8. Stam, M., Belele, C., Dorweiler, J. E., and Chandler, V. L. Differential chromatin structure within a tandem array 100 kb upstream of the maize *b1* locus is associated with paramutation. *Genes Dev* **16**, 1906–1918 (2002).

9. Belele, C. L., Sidorenko, L., Stam, M., Bader, R., Arteaga-Vazquez, M. A., and Chandler, V. L. Specific tandem repeats are sufficient for paramutation-induced trans-generational silencing. *PLoS Genet* **9**, e1003773 (2013).

10. Diag, A., Schilling, M., Klironomos, F., Ayoub, S., & Rajewsky, N. Spatiotemporal m(i)RNA architecture and 3' UTR regulation in the C. elegans germline. *Dev Cell* **47**, 785-800 (2018).

11. Wedeles, C. J., Wu, M. Z., and Claycomb, J. M. Protection of germline gene expression by the *C. elegans* argonaute CSR-1. *Dev. Cell* **27**, 664–671 (2013).

12. Ashe, A., Sapetschnig, A., Weick, E. M., Mitchell, J., Bagijn, M. P., Cording, A. C., Doebley, A. L., Goldstein, L. D., Lehrbach, N. J., Le Pen, J., et al. piRNAs can trigger a multigenerational epigenetic memory in the germline of *C. elegans*. *Cell* **150**, 88–99 (2012).

13. Lee, H. C., Gu, W., Shirayama, M., Youngman, E., Conte Jr., D., Mello, C. C. *C. elegans* piRNAs mediate the genome-wide surveillance of germline transcripts. *Cell* **150**, 78–87 (2012).

14. Luteijn, M. J., van Bergeijk, P., Kaaij, L. J., Almeida, M. V., Roovers, E. F., Berezikov, E., and Ketting, R. F. Extremely stable Piwi-induced gene silencing in *Caenorhabditis elegans*. *EMBO J.* **31**, 3422–3430 (2012).

15. Ishidate, T., Ozturk, A. R., Durning, D. J., Sharma, R., Shen, E. Z., Chen, H., Seth, M., Shirayama, M., and Mello, C. C. ZNFX-1 functions within perinuclear nuage to balance epigenetic signals. *Mol. Cell* **70**, 639–649 (2018).

16. Shirayama, M., Seth, M., Lee, H. C., Gu, W., Ishidate, T., Conte Jr., D., and Mello, C. C. piRNAs initiate an epigenetic memory of nonself RNA in the *C. elegans* germline. *Cell* **150**, 65–77 (2012).

17. Seth, M., Shirayama, M., Gu, W. T., Ishidate, T., Conte Jr., D., and Mello, C. C. The *C. elegans* CSR-1 argonaute pathway counteracts epigenetic silencing to promote germline gene expression. *Dev. Cell* **27**, 656–663 (2013).

18. Seth, M., Shirayama, M., Tang, W., Shen, E. Z., Tu, S., Lee, H. C., Weng, Z., and Mello, C. C. The coding regions of germline mRNAs confer sensitivity to Argonaute regulation in *C. elegans*. *Cell Rep* **27**, 2254-2264 (2018).

19. Bagijn, M. P., Goldstein, L. D., Sapetschnig, A., Weick, E. M., Bouasker, S., Lehrbach, N. J., Simard, M. J., and Miska, E. A. Function, targets, and evolution of *Caenorhabditis elegans* piRNAs. *Science* **337**, 574–578 (2012).

20. Buckley, B. A., Burkhart, K. B., Gu, S. G., Spracklin, G., Kershner, A., Fritz, H., Kimble, J., Fire, A., and Kennedy, S. A nuclear Argonaute promotes multigenerational epigenetic inheritance and germline immortality. *Nature* **489**, 447-451 (2012).

21. Ni, J. Z., Kalinava, N., Chen, E., Huang, A., Trinh, T., and Gu, S. G. A transgenerational role of the germline nuclear RNAi pathway in repressing heat stress-induced transcriptional activation in *C. elegans*. *Epigenetics Chromatin* **9**, 3 (2016).

22. Batista, P. J, Ruby, J. G., Claycomb, J. M., Chiang, R., Fahlgren, N., Kasschau, K. D., Chaves, D. A., Gu, W., Vasale, J. J., Duan, S., et al. PRG-1 and 21U-RNAs interact to form the piRNA complex required for fertility in *C. elegans*. *Mol. Cell* 31, 67–78 (2008).

23. de Albuquerque, B. F., Placentino, M., and Ketting, R. F. Maternal piRNAs are essential for germline development following de novo establishment of endo-siRNAs in *Caenorhabditis elegans*. *Dev. Cell* **34**, 448–456 (2015).

24. Phillips, C. M., Brown, K. C., Montgomery, B. E., Ruvkun, G., & Montgomery, T. A. piRNAs and piRNA-Dependent siRNAs Protect Conserved and Essential C. elegans Genes from Misrouting into the RNAi Pathway. *Dev. Cell* **34**, 457–465 (2015).

25. Frøkjær-Jensen, C., Jain, N., Hansen, L., Davis, M. W., Li, Y., Zhao, D., Rebora, K., Millet, J.R.M., Liu, X., Kim, S. K., Dupuy, D., Jorgensen, E. M., and Fire, A. Z. An abundant class of

non-coding DNA can prevent stochastic gene silencing in the *C. elegans* germline. *Cell* **166**, 343–357 (2016).

26. Johnson, C. L., and Spence, A. M. Epigenetic licensing of germline gene expression by maternal RNA in *C. elegans*. *Science* **333**, 1311–1314 (2011).

27. Leopold, L. E., Heestand, B. N., Seong, S., Shtessel, L., Ahmed, S. Lack of pairing during meiosis triggers multigenerational transgene silencing in *Caenorhabditis elegans*. *Proc. Natl. Acad. Sci. USA* **112**, E2667–E2676 (2015).

28. Shiu, P. K., Raju, N. B., Zickler, D., and Metzenberg, R. L. Meiotic silencing by unpaired DNA. *Cell* **107**, 905-916 (2001).

29. Schedl, T., and Kimble, J. *fog-2*, a germ-line-specific sex determination gene required for hermaphrodite spermatogenesis in *Caenorhabditis elegans*. *Genetics* **119**, 43-61 (1988).

30. Marré, J., Traver, E. C., Jose and A. M. Extracellular RNA is transported from one generation to the next in *Caenorhabditis elegans*. *Proc. Natl. Acad. Sci. USA* **113**, 12496–12501 (2016).

31. Wang, E., and Hunter, C. P. SID-1 functions in multiple roles to support parental RNAi in *Caenorhabditis elegans*. *Genetics* **207**, 547–557 (2017).

32. Almeida, M. V., Andrade-Navarro, M. A., and Ketting, R. F. Function and evolution of nematode RNAi pathways. *Noncoding RNA* **5**, 8 (2019).

33. Shukla, A., Yan, J., Pagano, D. J., Dodson, A. E., Fei, Y., Gorham, J., Seidman, J. G., Wickens, M., and Kennedy, S. poly(UG)-tailed RNAs in genome protection and epigenetic inheritance. *Nature* **582**, 283–288 (2020).

34. Phillips, C. M., Montgomery, T. A., Breen, P. C., and Ruvkun, G. MUT-16 promotes formation of perinuclear mutator foci required for RNA silencing in the *C. elegans* germline. *Genes Dev.* **26**, 1433–1444 (2012).

35. Almeida, M. V., de Jesus Domingues, A. M., and Ketting, R. F. Maternal and zygotic gene regulatory effects of endogenous RNAi pathways. *PLoS Genet* **15**, e1007784 (2019).

36. Reed, K. J., Svendsen, J. M., Brown, K. C., Montgomery, B. E., Marks, T. N., Vijayasarathy, T., Parker, D. M., Nishimura, E. O., Updike, D. L., and Montgomery, T. A. Widespread roles for piRNAs and WAGO-class siRNAs in shaping the germline transcriptome of Caenorhabditis elegans. *Nucleic Acids Res* **48**, 1811-1827 (2020).

37. Zhang, D., Tu, S., Stubna, M., Wu, W. S., Huang, W. C., Weng, Z., and Lee, H. C. The piRNA targeting rules and the resistance to piRNA silencing in endogenous genes. *Science* **359**, 587-592 (2018).

38. Sha, K. and Fire, A. Imprinting capacity of gamete lineages in Caenorhabditis elegans. *Genetics* **170**, 1633–1652 (2005).

39. Hadchouel, M., Farza, H., Simon, D., Tiollais, P., and Pourcel, C. Maternal inhibition of hepatitis B surface antigen gene expression in transgenic mice correlates with de novo methylation. *Nature* **329**, 454–456 (1987).

40. Dodson, A. E., and Kennedy, S. Germ granules coordinate RNA-Based epigenetic inheritance pathways. *Dev. Cell* **50**, 704-715 (2019).

41. van der Graaf, A., Wardenaar, R., Neumann, D. A., Taudt, A., Shaw, R. G., Jansen, R. C., Schmitz, R. J., Colomé-Tatché, M., and Johannes, F. Rate, spectrum, and evolutionary dynamics of spontaneous epimutations. *Proc. Natl. Acad. Sci. USA* **112**, 6676-6681 (2015).

42. Spracklin, G., Fields, B., Wan, G., Becker, D., Wallig, A., Shukla, A., and Kennedy, S. The RNAi inheritance machinery of *Caenorhabditis elegans*. *Genetics* **206**, 1403-1416 (2017).

43. Fire, A., Xu, S., Montgomery, M. K., Kostas, S. A., Driver, S. E., and Mello, C. C. Potent and specific genetic interference by double-stranded RNA in Caenorhabditis elegans. *Nature* **391**, 806–811 (1998).

44. Burton, N.O., Burkhart, K.B., and Kennedy, S. Nuclear RNAi maintains heritable gene silencing in Caenorhabditis elegans. *Proc Natl Acad Sci USA* **108**, 19683–19688 (2011).

45. Burkhart, K.B., Guang, S., Buckley, B.A., Wong, L., Bochner, A.F., Kennedy S. A. pre-mRNA-associating factor links endogenous siRNAs to chromatin regulation. *PLoS Genet* **7**, e1002249 (2011).

46. Guang, S., Bochner, A.F., Burkhart, K.B., Burton, N., Pavelec, D.M., and Kennedy, S. Small regulatory RNAs inhibit RNA polymerase II during the elongation phase of transcription. *Nature* **465**, 1097–1101 (2010).

47. Tabara, H., Sarkissian, M., Kelly, W.G., Fleenor, J., Grishok, A., Timmons, L., Fire, A., and Mello, C.C. The *rde-1* gene, RNA interference, and transposon silencing in *C. elegans*. *Cell* **99**, 123–132 (1999).

48. Winston, W.M., Molodowitch, C., and Hunter, C.P. Systemic RNAi in C. elegans requires the putative transmembrane protein SID-1. *Science* **295**, 2456–2459 (2002).

49. Mao, H., Zhu, C., Zong, D., Weng, C., Yang, X., Huang, H., Liu, D., Feng, X., and Guang, S. The Nrde Pathway Mediates Small-RNA-Directed Histone H3 Lysine 27 Trimethylation in Caenorhabditis elegans. *Curr. Biol* **25**, 2398–2403 (2015).

50. Wan, G., Fields, B.D., Spracklin, G., Shukla, A., Phillips, C.M., and Kennedy, S. Spatiotemporal regulation of liquid-like condensates in epigenetic inheritance. *Nature* **557**, 679–683 (2018).

51. Xu, F., Feng, X., Chen, X., Weng, C., Yan, Q., Xu, T., Hong, M., and Guang, S. A Cytoplasmic Argonaute Protein Promotes the Inheritance of RNAi. *Cell Rep* **23**, 2482–2494 (2018).

52. Timmons, L., Tabara, H., Mello, C.C., and Fire, A.Z. Inducible systemic RNA silencing in *Caenorhabditis elegans*. *Mol. Biol. Cell* **14**, 2972–83 (2003).

53. Sapetschnig, A., Sarkies, P., Lehrbach, N. J., and Miska, E. A. Tertiary siRNAs mediate paramutation in *C. elegans*. *PLoS Genet* **11**, e1005078 (2015).

54. Ashe, A., Sarkies, P., Le Pen, J., Tanguy, M., and Miska, E.A. Antiviral RNA Interference against Orsay Virus Is neither Systemic nor Transgenerational in *Caenorhabditis elegans*. *J Virol* **89**, 12035–12046 (2015).

55. Grishok, A., Tabara, H., and Mello, C.C. Genetic requirements for inheritance of RNAi in *C. elegans*. *Science* **287**, 2494–2497 (2000).

56. Perales, R., Pagano, D., Wan, G., Fields, B. D., Saltzman, A. L., and Kennedy, S.G. Transgenerational epigenetic inheritance is negatively regulated by the HERI-1 chromodomain protein. *Genetics* **210**, 1287–1299 (2018).

57. Lev, I., Seroussi, U., Gingold, H., Bril, R., Anava, S., and Rechavi, O. MET-2-dependent H3K9 methylation suppresses transgenerational small RNA inheritance. *Curr. Biol* **27**, 1138–1147 (2017).

58. Houri-Ze'evi, L., Korem, Y., Sheftel, H., Faigenbloom, L., Toker, I.A., Dagan, Y., Awad, L., Degani, L., Alon, U., and Rechavi, O. A tunable mechanism determines the duration of the transgenerational small RNA inheritance in *C. elegans*. *Cell* **165**, 88-99 (2016).

59. Weiser, N.E., Yang, D.X., Feng, S., Kalinava, N., Brown, K.C., Khanikar, J., Freeberg, M.A., Snyder, M.J., Csankovszki, G., Chan, R.C., et al. MORC-1 integrates nuclear RNAi and transgenerational chromatin architecture to promote germline immortality. *Dev. Cell* **22**, 408–423 (2017).

60. Woodhouse, R.M., Buchmann, G., Hoe, M., Harney, D.J., Low, J.K.K., Larance, M., Boag, P.R., and Ashe, A. Chromatin modifiers SET-25 and SET-32 are required for establishment but not long-term maintenance of transgenerational epigenetic inheritance. *Cell Rep* **20**, 2259–2272 (2018).

61. Vastenhouw, N.L., Brunschwig, K., Okihara, K.L., Müller, F., Tijsterman, M., and Plasterk, R.H. Gene expression: long-term gene silencing by RNAi. *Nature* **442**, 882 (2006).

62. Lev, I., Gingold, H., and Rechavi, O. H3K9me3 is required for inheritance of small RNAs that target a unique subset of newly evolved genes. *eLife* **14**, e40448 (2019).

63. Devanapally, S., Ravikumar, S., Jose, A.M. Double-stranded RNA made in *C. elegans* neurons can enter the germline and cause transgenerational gene silencing. *Proc. Natl. Acad. Sci. USA* **112**, 2133–2138 (2015).

64. Conine, C. C., Moresco, J. J., Gu, W., Shirayama, M., Conte Jr., D., Yates, J. R., and Mello, C.C. Argonautes promote male fertility and provide a paternal memory of germline gene expression in *C. elegans*. *Cell* **155**, 1532-1544 (2013).

65. Bennett, S. T., Wilson, A. J., Esposito, L., Bouzekri, N., Undlien, D. E., Cucca, F., Nisticò, L., Buzzetti, R., Bosi, E., Pociot, F. et al. Insulin VNTR allele-specific effect in type 1 diabetes depends on identity of untransmitted paternal allele. The IMDIAB Group. *Nat. Genet* **17**, 350–352 (1997).

66. Brennecke, J., Malone, C. D., Aravin, A. A., Sachidanandam, R., Stark, A., and Hannon, G. J. An epigenetic role for maternally inherited piRNAs in transposon silencing. *Science* **322**, 1387–1392 (2008).

67. Duncan, I. W. Transvection effects in *Drosophila*. *Annu. Rev. Genet* **36**, 521–556 (2002).